ADA044325

# NAVAL POSTGRADUATE SCHOOL
## Monterey, California

# THESIS

INVESTIGATION OF A LINEAR, TWO-DEGREE-OF-FREEDOM
SIMULATION OF THE XR-3 CAPTURED AIR BUBBLE
(CAB) CRAFT IN THE FREQUENCY DOMAIN

by

Lewis Frank McIntyre

June 1977

Thesis Advisor:                    Alex Gerba, Jr.

Approved for public release; distribution unlimited.

D D C
SEP 20 1977
C

| REPORT DOCUMENTATION PAGE | | READ INSTRUCTIONS BEFORE COMPLETING FORM |
|---|---|---|
| 1. REPORT NUMBER | 2. GOVT ACCESSION NO. | 3. RECIPIENT'S CATALOG NUMBER |
| 4. TITLE (and Subtitle) Investigation of a Linear, Two-Degree-of-Freedom Simulation of the XR-3 Captured Air Bubble (CAB) Craft in the Frequency Domain | | 5. TYPE OF REPORT & PERIOD COVERED Master's Thesis June 1977 |
| | | 6. PERFORMING ORG. REPORT NUMBER |
| 7. AUTHOR(s) Lewis Frank McIntyre | | 8. CONTRACT OR GRANT NUMBER(s) |
| 9. PERFORMING ORGANIZATION NAME AND ADDRESS Naval Postgraduate School Monterey, California 93940 | | 10. PROGRAM ELEMENT, PROJECT, TASK AREA & WORK UNIT NUMBERS |
| 11. CONTROLLING OFFICE NAME AND ADDRESS Naval Postgraduate School Monterey, California 93940 | | 12. REPORT DATE June 1977 |
| | | 13. NUMBER OF PAGES 187 |
| 14. MONITORING AGENCY NAME & ADDRESS(If different from Controlling Office) | | 15. SECURITY CLASS. (of this report) Unclassified |
| | | 15a. DECLASSIFICATION/DOWNGRADING SCHEDULE |

16. DISTRIBUTION STATEMENT (of this Report)

Approved for public release; distribution unlimited.

17. DISTRIBUTION STATEMENT (of the abstract entered in Block 20, if different from Report)

18. SUPPLEMENTARY NOTES

19. KEY WORDS (Continue on reverse side if necessary and identify by block number)

XR-3    Linear Model    Frequency Response

20. ABSTRACT (Continue on reverse side if necessary and identify by block number)

A simplified two-degree-of-freedom simulation in heave and pitch of the XR-3 Captured Air Bubble (CAB) testcraft is developed first in a non-linear form and is subsequently linearized about the steady-state operating point. The model is validated against the six-degree-of-freedom XR-3 Loads and Motions program in the time domain; the linear system is then transformed into the frequency domain by complex matrix inversion. ⟶ next page

DD FORM 1473   EDITION OF 1 NOV 65 IS OBSOLETE
1 JAN 73
(Page 1)   S/N 0102-014-6601 |

20. (continued)

A comparison is made between the linear system frequency response predicted by the two-degree-of-freedom model and that of the Loads and Motions program, as well as actual testcraft data, reduced to the frequency domain by a Fast Fourier Transform (FFT) technique. This comparison of frequency response curves highlights a non-linear mode of CAB craft behavior of possible interest to habitability and seaworthiness studies.

DD Form 1473
1 Jan 73
S/N 0102-014-6601

INVESTIGATION OF A LINEAR, TWO-DEGREE-OF-FREEDOM
SIMULATION FOR THE XR-3 CAPTURED AIR BUBBLE (CAB) CRAFT IN
THE FREQUENCY DOMAIN

by

Lewis Frank McIntyre
Lieutenant
Bachelor of Science

Submitted in partial fulfillment of the
requirements for the degree of

MASTER OF SCIENCE IN AERONAUTICAL ENGINEERING

from the
NAVAL POSTGRADUATE SCHOOL
June 1977

Author: _____

Approved by: _____
                                    Thesis Advisor

            _____
                                    Second Reader

            _____
                      Chairman, Department of Aeronautics

            _____
                      Dean of Science and Engineering

3

# ABSTRACT

A simplified two-degree-of-freedom simulation in heave and pitch of the XR-3 Captured Air Bubble (CAB) testcraft is developed first in a non-linear form and is subsequently linearized about the steady-state operating point. The model is validated against the six-degree-of-freedom XR-3 Loads and Motions program in the time domain; the linear system is then transformed into the frequency domain by complex matrix inversion. A comparison is made between the linear system frequency response predicted by the two-degree-of-freedom model and that of the Loads and Motions program, as well as actual testcraft data, reduced to the frequency domain by a Fast Fourier Transform (FFT) technique. This comparison of frequency response curves highlights a non-linear mode of CAB craft behavior of possible interest to habitability and seaworthiness studies.

4

## TABLE OF CONTENTS

5

# LIST OF FIGURES

# LIST OF ABBREVIATIONS

## PHYSICAL CONSTANTS

1. <u>G</u>                     Gravitational Constant

   $(32.2 \text{ ft/sec}^2)$

2. <u>Gamma</u>               Ratio of Specific Heats of Air

   $(1.4, \text{Dimensionless})$

3. <u>Rho</u>                  Density of Water

   $(2.0 \text{ Slugs/ft}^3)$

4. <u>Rhoa</u>                 Density of Air

   $(.002378 \text{ Slugs/ft}^3)$

CRAFT PARAMETERS


1.  Ab                Plenum Upper Surface Area
                                           $(200 \text{ ft}^2)$


2.  Al                Leakage Area, Stern Seal
                                           $(.438 \text{ ft}^2)$


3.  As                Sidewall Area
                                           $(18.75 \text{ ft}^2)$


4.  Cf                Sidewall Skin Friction Coefficient
                                   (.95, Dimensionless)


5.  Iyy               Y-Axis Moment of Inertia
                                           $(9620 \text{ lbm-ft}^2)$


6.  L                 Craft Waterline Length
                                           (20.0 ft)


7.  N                 Number of Lift Fans
                                           (5)


8.  QIC               Static Fan Flow Rate
                                           $(35 \text{ ft}^3/\text{sec})$


9.  Ws                Sidewall Width
                                           (.9375 ft)


13

10. Width             Craft Beam Width

                                                   (10.0 ft)

11. $V_n$                Empty Plenum Volume

                                               $(383 \ ft^3)$

12. $Z_s$               Keel to Center of Gravity Height

                                               (2.5 ft)

13. $M$               Mass of Craft

                                               (lbm)

14. $M_f C$             Residual Moment about Y-Axis

                                             (ft-lbf)

15. $X_{cg}$             Location  of Center of Gravity from Craft Geometric Center

                                               (ft)

16. $X_{cp}$             Location   of   Craft   Center   of Pressure   from   Craft   Geometric Center

                                               (ft)

# SEA-STATE VARIABLES

1. $\underline{C}$             Absolute Wave Velocity      (ft/sec)

2. $\underline{Lambda}$      Incident Wavelength        (ft)

3. $\underline{w_e}$           Wave Encounter Frequency    (rad/sec)

4. $\underline{w_i}$           Incident Wave Frequency     (rad/sec)

5. $\underline{Wvht}$        Wave Height               (ft)

15

STATE VARIABLES


1.  <u>Mb</u>                    Plenum Air Mass
                                                    (lbm)


2.  <u>Alfa</u>                  Angular Acceleration of Craft about
                                 Y-Axis
                                                    $(rad/sec^2)$


3.  <u>Mbdot</u>                 Mass Flow Rate into/out of Plenum
                                                    (lbm/sec)


4.  <u>Omega</u>                 Radial   Velocity  of  Craft  about
                                 Y-Axis
                                                    (rad/sec)


5.  <u>Pbbar</u>                 Plenum Gauge Pressure
                                                    $(lbf/ft^2)$


6.  <u>Theta</u>                 Pitch Angle about Y-Axis
                                                    (rad/sec)


7.  <u>Zdot</u>                  Vertical   Velocity  of  Center  of
                                 Gravity
                                                    (ft/sec)


8.  <u>Z2dot</u>                 Vertical Acceleration of Center of
                                 Gravity
                                                    $(ft/sec^2)$


9.  <u>Z</u>                     Vertical  Displacement of Center of
                                 Gravity above Water Line
                                                    (ft)


16

## SYSTEM VARIABLES

1.  <u>Aseal1</u>                    Wetted Area of Bowseal
                                                                    $(ft^2)$

2.  <u>Aseal2</u>                    Wetted Area of Sternseal
                                                                    $(ft)^2$

3.  <u>Hbuoy</u>                     Total Buoyant Force
                                                                    (lbf)

4.  <u>Hbuoy1</u>                    Buoyant Force due to Immersed Area
                                     forward of Center of Gravity
                                                                    (lbf)

5.  <u>Hbuoy2</u>                    Buoyant Force due to Immersed Area
                                     aft of Center of Gravity
                                                                    (lbf)

6.  <u>Hbuoyw</u>                    Additional Force due to Wave
                                     Buoyancy
                                                                    (lbf)

7.  <u>Hdamp</u>                     Total Viscous Damping Force
                                                                    (lbf)

8.  <u>Hdamp1</u>                    Damping Force due to Viscous
                                     Damping forward of Center of
                                     Gravity
                                                                    (lbf)

9.  <u>Hdamp2</u>                    Damping Force due to Viscous
                                     Damping aft of Center of Gravity
                                                                    (lbf)

17

10. **Hplan**   Vertical Planing Force due to Hydrodynamic Lift

         (lbf)

11. **Hpres**   Vertical Pressure Force, acting at Center of Pressure

         (lbf)

12. **Hseal1**   Vertical Force due to Bowseal

         (lbf)

13. **Hseal2**   Vertical Force due to Sternseal

         (lbf)

14. **Ld**   Draft , measured at Center of Gravity

         (ft)

15. **Ld1**   Draft, measured at bow

         (ft)

16. **Ld2**   Draft, measured at stern

         (ft)

17. **Ldbar1**   Average Draft forward of Center of Gravity

         (ft)

18. **Ldbar2**   Average Draft aft of Center of Gravity

         (ft)

19. **Pbpa0**   Initial Plenum Pressure Ratio

         (dimensionless)

20. **Pbuoy**   Total Buoyant Pitch Moment

         (ft-lbf)

21. **Pbuoyw**   Buoyant Pitch Moment due to Waves

         (ft-lbf)

22. Pbuoy1
Buoyant Pitch Moment due to Immersed Area forward of Center of Gravity
(ft-lbf)

23. Pbuoy2
Buoyant Pitch Moment due to Immersed Area aft of Center of Gravity
(ft-lbf)

24. Pdamp
Total Viscous Pitch Damping Moment
(ft-lbf)

25. Pdamp1
Viscous Pitch Damping Moment due to Area forward of Center of Gravity
(ft-lbf)

26. Pdamp2
Viscous Pitch Damping Moment due to Area aft of Center of Gravity
(ft-lbf)

27. Pplan
Planing Moment due to Hydrodynamic Lift
(ft-lbf)

28. Ppres
Pitch Pressure Moment
(ft-lbf)

29. Pseal1
Pitch moment due to Bowseal
(ft-lbf)

30. Pseal2
Pitch moment due to Sternseal
(ft-lbf)

31. Qout
Volume Flow out of Plenum
$(ft^3/sec)$

32. Qin
Volume Flow into the Plenum
$(ft^3/sec)$

33. <u>Vb</u>                    Net Plenum Volume

$$(ft^3)$$

34. <u>Vbar1</u>         Average Vertical Velocity forward of Center of Gravity

                                      (ft/sec)

35. <u>Vbar2</u>         Average Vertical Velocity aft of Center of Gravity

                                      (ft/sec)

36. <u>Xseal</u>        Length of Bowseal in Contact with the Water Surface

                                      (ft)

# INFLUENCE COEFFICIENTS

1. <u>Dhbth</u>    Partial derivative of vertical buoyant force with respect to Theta
(lbf)

2. <u>Dhbz</u>    Partial derivative of vertical buoyant force with respect to z
(lbf/ft)

3. <u>Dhplth</u>    Partial derivative of vertical force due to planing with respect to Theta
(lbf)

4. <u>Dhpth</u>    Partial derivative of vertical pressure force with respect to Theta
(lbf)

5. <u>Dhpmb</u>    Partial derivative of vertical pressure force with respect to Mb
(lbf/lbm)

6. <u>Dhpz</u>    Partial derivative of vertical pressure force with respect to z
(lbf/ft)

7. <u>Dhsz1</u>    Partial derivative of Bowseal vertical force with respect to z
(lbf/ft)

8. <u>Dhsth1</u>    Partial derivative of Bowseal vertical force with respect to Theta
(lbf)

9. <u>Dhsmb</u>    Partial derivative of Bowseal vertical force with respect to Mb  
(lbf/lbm)

10. <u>Dhsz2</u>    Partial derivative of Sternseal vertical force with respect to z  
( lbf/ft)

11. <u>Dhsth2</u>    Partial derivative of Sternseal vertical force with respect to Theta  
(lbf)

12. <u>Dhsz</u>    Sum of Dhsz1 and Dhsz2  
(lbf/ft)

13. <u>Dhsth</u>    Sum of Dhsth1 and Dhsth2  
(lbf)

14. <u>Dmbmb</u>    Partial derivative of Plenum Air Mass Flow Rate with respect to Mb  
$(sec)^{-1}$

15. <u>Dmbth</u>    Partial derivative of Plenum Air Mass Flow Rate with respect to Theta  
( lbm/sec)

16. <u>Dmbz</u>    Partial derivative of Plenum Air Mass Flow Rate with respect to z  
(lbm/ft-sec)

17. <u>Dpbmb</u>    Partial derivative of Pbbar with respect to Plenum Air Mass, Mb  
$( lbf/lbm-ft)^{2}$

18. <u>Dpbth</u>    Partial derivative of Pbbar with respect to Theta  
$(lbf/ft)^{2}$

19. __Dpbz__                  Partial derivative of Pbbar with
                              respect to z

                                                  $(lbf/ft^3)$

20. __Dpbyth__                Partial derivative of buoyant pitch
                              moment with respect to Theta
                                                  (ft-lbf)

21. __Dpbyz__                 Partial derivative of buoyant pitch
                              moment with respect to z
                                                  (lbf)

22. __Dpplth__                Partial derivative of Planing pitch
                              moment with respect to Theta
                                                  (ft-lbf)

23. __Dppmb__                 Partial   derivative   of   pressure
                              pitch moment with respect to Mb
                                                  (ft-lbf/lbm)

24. __Dppth__                 Partial   derivative   of   pressure
                              pitch moment with respect to Theta
                                                  (ft-lbf)

25. __Dppz__                  Partial   derivative   of   pressure
                              pitch moment with respect to z
                                                  (lbf)

26. __Dpsmb__                 Partial derivative of Bowseal pitch
                              moment with respect to Mb
                                                  ( ft-lbf/lbm)

27. __Dpsth1__                Partial derivative of Bowseal pitch
                              moment with respect to Theta
                                                  ( ft-lbf)

28. __Dpsth2__                Partial   derivative  of   Sternseal
                              pitch moment with respect to Theta
                                                  (ft-lbf)

29. __Dpsz1__                 Partial derivative of Bowseal pitch
                              moment with respect to z
                                                  ( lbf)

30. Dpsz2        Partial derivative of Sternseal
                 pitch moment with respect to z
                                                    (lbf)

31. Dpmb         Partial derivative of pitch
                 acceleration with respect to Mb
                                                $( 1/(lbm\text{-}sec)^2)$

32. Dpth         Partial derivative of pitch
                 acceleration with respect to Theta
                                                $( sec)^{-2}$

33. Dpz          Partial derivative of pitch
                 acceleration with respect to z
                                                $( 1/(ft\text{-}sec)^2)$

34. Dzmb         Partial derivative of vertical
                 acceleration with respect to Mb
                                                $( ft/lbm\text{-}sec)^2$

35. Dzth         Partial derivative of of vertical
                 acceleration with respect to Theta
                                                $(ft/sec)^2$

36. Dzz          Partial derivative of vertical
                 acceleration with respect to z
                                                $( sec)^{-2}$

24

ACKNOWLEDGEMENTS

26

# I.  INTRODUCTION


The  frequency  domain provides a useful method of study
for systems such as the Captured Air Bubble (CAB) type
surface effect ship, which are excited by forces whose
statistics of amplitude and frequency may be well-known, but
whose  time  domain  phase  relationships  are  quite
indeterminant.  In addition, the frequency response of such
high-speed  ships  should be closely examined for resonances
near wave encounter frequencies  most  likely  to  be
experienced.  Due  to its relatively shallow draft, the CAB
craft can easily be excited into  a  non-linear region of
operation  in  which  sidewall  gapping or wave/plenum upper
surface contact may occur; these non-linearities may excite
modes  of operation which are of importance to habitability,
and may limit the craft's speed during sea-state operation.


Booth  in  ref[1] analyzed the frequency domain response
of the XR-3 CAB craft utilizing the Loads and Motion program
developed by Oceanics,Inc., for the Bell 100B CAB and
modified extensively by Leo and Boncal (ref [2]) and Menzel
(ref[3]), for the XR-3.  However,  the Loads and Motion
program is an extremely inefficient tool to utilize for
Fourier series analysis; not only are waves numerically
integrated along the hull utilizing a table look-up, once
for  each  frequency component, and four times for each time
step, but the higher frequency components also drive the
variable-step integrators to extremely small step sizes.
The net effect of this technique is the exorbitant
utilization  of CPU time in a computer simulation of
sea-state conditions.  In addition, the time constants of
the craft response are relatively long in some modes,

26

particularly pitch; therefore still further CPU time is wasted attaining steady-state conditions. This inefficiency of CPU time has been noted by Mitchell in ref [4], who documented over 40 percent of CPU time utilized by the XR-3 Loads and Motion program to the WAVES subroutine. Accordingly, one is reduced to performing a point-by-point frequency analysis with a single wave frequency at a time. Since, under these conditions, the system is approximately linear, and superposition is valid for sufficiently small wave amplitudes, the utilization of a linearized, albeit highly simplified, program presents itself as a most desirable alternative. The effect of non-linearities may be added to the linear model with a describing function, and the system investigated in the complex plane utilizing the modified Nyquist criteria. Finally, a simplified model provides a starting point for the investigation of sensitivity of craft operation to the variation of assorted parameters through the technique of root locus plotting, and can be the heart of the development of any automatic control system, optimal or classical.

Gerba and Thaler, in ref [5], initiated the development of the linearized XR-3 model in heave only. In this work, that model is further developed to include the pitch mode, first in a non-linear form, from which a linearized version is derived. The wave forcing functions acting along the hull of the XR-3 are developed in the form of a quasi-linear B vector in state-space, and the linear system is then transformed into the frequency domain by complex matrix inversion, with significant savings in CPU time. This linear frequency response is then compared with ref [1] to provide additional insights into the XR-3 system behavior not readily apparent in the more complex Loads and Motions program.

A technique utilizing a mini-computer and spectral

27

analyzer is developed for the fast and efficient reduction of recorded XR-3 data from the time domain to the frequency domain utilizing a Fast Fourier Transform (FFT). Actual craft data is compared with the predicted linear system frequency response.

## II. NON-LINEAR XR-3 HEAVE-PITCH EQUATIONS OF MOTION

This chapter develops the non-linear equations of motions of the XR-3 in heave and pitch, following the approach utilized by Gerba and Thaler in the development of the simplified heave-only model in ref [5].

### A. ASSUMPTIONS

As in ref [5], the following assumptions are made:

1. constant leakage area;

2. equilibrium speed conditions;

3. plenum pressure and volume related through an adiabatic process;

The following assumptions and limiting conditions were removed:

4. vertically coincident geometric center, center of pressure and center of gravity;

5. negligible pitch changes;

6. negligible wave action;

7. negligible added mass effects;

and the following assumptions are added:

8. negligible wave action within plenum;

9. wave action due to head-on or following seas (negligible roll or yaw);

In addition some simplifying assumptions regarding the craft geometry were made. Fig 1 shows the simplified geometry of the craft assumed in this model. Note that Center of Gravity(C.G.) and Center of Pressure (C.P.) are arbitrarily located and not to scale.


B. COORDINATE SYSTEM


Fig 1 shows the coordinate system used in this model. Specifically, the coordinate system is attached to the geometric center of the craft at the calm waterline, and oriented in a right-hand system such that x is positive forward, y is positive to the right, and z is positive down. Angles are measured such that a roll to the right, a pitch up and a yaw right are positive. Note, however, that translations in the y direction and roll and yaw are not included in this model.


Draft, the distance of the keel below the calm water line, is the distance of the C.G. above the calm water line, z, plus the distance of the keel below the C.G., Zs, or:

Ld          $= z + Zs$


(II-1)



C. SIDEWALL GEOMETRY


30

The constant sidewall area as used by Gerba and Thaler yields a good approximation to craft motion in the heave and pressure modes. However ,it is a source of strong coupling between draft and pitch, and a more detailed modeling is necessary to achieve good agreement with the Loads and Motion Program, as well as known craft behavior in pitch.

Fig 1 shows the cross-sectional detail of assumed sidewall geometry. The fore and aft sections are identical with the exception of deadrise angle, that angle being 60° at the bow and 80° at the stern. The actual sidewall width used for computation of buoyancy forces is the effective sidewall width; this is the average value of the waterline sidewall width and the keel-line width,Ws10 or Ws20 (fore or aft section). This is one-half the draft averaged from the C.G. to the bow and stern respectively, divided by the tangent of the appropriate deadrise angle plus the keel-line width Ws10 or Ws20. This value is constrained between zero and Ws, the maximum sidewall width. Thus:

Ldbar1 = Ld - (L/2 - Xcg) * Theta

(II-2)

Ws1 = Ldbar1 / (2*tan(Dr1)) + Ws10

IF (Ws1.GT.Ws) Ws1=Ws

IF (Ws1.LT.0.0) Ws1=0.0

(II-3)

and for the stern section:

31

Ldbar2          $= Ld + (L/2 + Xcg) * Theta$

$$(II-4)$$

Ws2          $= Ldbar2/(2*tan(dr2)) + Ws20$

　　　　　IF(Ws2.GT.Ws) Ws2=Ws

　　　　　IF(Ws2.LT.0) Ws2=0.0

$$(II-5)$$

D.  SYSTEM DYNAMICS

The equations of the system dynamics are developed in this section and are an extension of the model of ref [5], modified as necessary; the remaining equations are derived from first principles.

1.  Plenum Pressure and Mass Flow Rate

Plenum pressure and plenum air mass are calculated using the adiabatic law. Using $Ld_1$ as the draft at the bow, and $Ld_2$ as the draft at the stern, the average draft overall becomes:

Ldbar          $= (Ld_1 + Ld_2)/2$

　　　　　$= (Ld - (L/2 - Xcg) * tan(Theta)$

$$+Ld+(L/2+Xcg)*\tan(Theta))/2$$

$$=Ld+Xcg*\tan(Theta)$$

(II-6)

which, when multiplied by the Plenum area, yields the submerged Plenum volume. Subtracting this from Plenum nominal volume yields the net Plenum volume, or:

$$Vb \qquad =Vn-Ab*(Ld+Xcg*\tan(theta))$$

(II-7)

The adiabatic relationship between pressure and volume yields:

$$Pb \qquad =Pa*(Mb/(Vb*Rhoa))^{Gamma}$$

(II-8)

and

$$Pbbar \qquad =Pb-Pa$$

(II-9)

Volume flow into the Plenum is, assuming a constant fan map:

$$Qin \qquad =N*(QIO-Pbbar)$$

(II-10)

and flow out is:

$$Qout \qquad =Cn*Al*(2*Pbbar/Rhoa)^{1/2}$$

(II-11)

thus the net mass flow rate within the plenum is:

33

$$\frac{d}{dt} (Mb) = Rhoa*(Qin-Qout)$$

$$(II-12)$$

## 2. Sum of Forces

Fig 2 shows the forces and their respective moment arms acting on the XR-3. The sum of vertical forces yields the vertical C.G. acceleration:

$$\frac{d^2}{dt^2} (z) = (Hpres+Hbuoy+Hseal+Hdamp+Hplan+W)/M$$

$$(II-13)$$

The individual force contributions may be calculated separately and their total contributions summed.

### a. Pressure Forces

The plenum pressure acting on the roof of the plenum produces a pressure force acting at the C.P.:

$$Hpres = -Ab*Pbbar$$

$$(II-14)$$

### b. Buoyant Forces

For purposes of calculating buoyant moments in the subsequent calculations, it is convenient to dissociate the buoyant force into two components, Hbuoy1 and Hbuoy2, the

34

bucyant forces generated by the submerged volume fore and aft of the C.G. Buoyant force is proportional to submerged volume multiplied by the density of the fluid and the gravitational constant. This term must be doubled to account for both sidewalls. The average draft forward of the C.G. is:

$$Ldbar1 = (Ld+Ld1)/2$$

$$= Ld - (L/2 - Xcg) * tan(Theta)/2$$

$$(II-15)$$

Thus the forward buoyant force is:

$$Hbuoy1 = -2*Rho*G*length*draft*sidewall\ width$$

$$= -2*Rho*G*(L/2-Xcg)*Ldbar1*Ws1$$

$$(II-16)$$

The aft average draft is:

$$Ldbar2 = Ld+(L/2+Xcg)*tan(Theta)/2$$

$$(II-17)$$

and the aft buoyant force is:

$$Hbuoy2 = -2*Rho*G*(L/2+Xcg)*Ldbar2*Ws2$$

$$(II-18)$$

and:

$$Hbuoy = Hbuoy1+Hbuoy2$$

$$(II-19)$$

c. Bow and Sternseal Forces

35

Fig 3 shows the detail of the assumed bowseal and sternseal geometry and water surface interactions. The seal is assumed to trail from the upper hinge point at a constant angle of 31.6° until it contacts the waterline. From that point on it is assumed to lie tangent to the waterline. The length of bowseal in contact with the water may be seen to be:

$$Xseal1 \quad = Ld1/\cos(31.6°)$$

$$= 1.65*(Ld-(L/2-Xcg)*\tan(Theta))$$

$$(II-20)$$

Pbbar exerts a force upon this wetted area which is resisted by an upward reaction from the water surface. This reaction is transmitted to the craft as:

$$Hseal1 \quad = -Pbbar*Width*Xseal1$$

$$(II-21)$$

As may be seen from Fig 3, the sternseal geometry is basically identical to that of the bowseal; however, the mechanism for force generation is different in that the sternseal rides atop an exhausting jet of plenum air. Therefore, the pressure differential is not that of Plenum pressure over atmospheric, but over the reduced pressure of the high-velocity jet. This is a complicated function of leakage area and other factors, but may be assumed approximately constant. This model assumes approximately 2.0 $lbf/ft^2$ differential pressure between the sternseal and plenum pressure.

The length of sternseal in contact with the water may be seen to be:

Xseal2        =Ld2/cos(31.6⁰)

              =1.65*(Ld+(L/2+Xcg)*tan(Theta))

$$(II-22)$$

the sternseal force is then the differential pressure,Sealp, times the sternseal area ,or:

Hseal2        =-Sealp*Width*Xseal2

$$(II-23)$$

d.  Damping Forces

Damping forces are developed for information only, as Taylor's series expansion of these forces about the zero-rate equilibrium point causes these equations to vanish in the linear model.

A body at motion within a fluid experiences a frictional force:

$F_f$              $=-C*(Rho/2)*V*|V|*S$

where $C_f$ is a non-dimensional friction coefficient based upon shape, roughness, and Reynold's Number.  Consistent with the six-degree-of-freedom Loads and Motion program, $C_f$ is taken to be .9.  The vertical velocity is taken to be the vertical velocity of the C.G., Zdot, plus the tangential velocity of the angular velocity, which varies along the hull as:

37

V(x)           $= Zdot + (Xcg-x) * Omega$

(II-24)

The differential surface wetted area also is a function of
x, as the depth of immersion varies along the hull, so that:

dS             $= Ws * (Ld - (x - Xcg) * tan(Theta))$

(II-25)

When multiplied by the absolute value of velocity, times
itself, times the differential wetted area, the resulting
expression may be integrated numerically along the hull.
However, this is most wasteful of CPU time, and the absolute
value term renders this expression intractable to closed
analytical solution.. In addition, the term is quite small,
and in fact must be, if pitch angles are to remain within
the small angle assumptions, and no sidewall gapping occur.
Therefore, this term is approximated by computing the
average velocity fore and aft of the center of gravity, and
the average wetted surface fore and aft, previously computed
as Ws1*Ldbar1 and Ws2*Ldbar2. For purposes of pitch
calculations to be discussed subsequently, these two forces
are assumed to act at two-thirds the length fore and aft the
C.G.; this yields closer agreement to the numerical
solution by weighting the higher velocities which occur at
the bow and stern. Vbar1 and Vbar2 may now be defined:

Vbar1          $= Zdot - (L/2 - Xcg) * Omega/2$

(II-26)

Vbar2          $= Zdot + (L/2 + Xcg) * Omega/2$

(II-27)

Since there are four surfaces forward and aft of the center

38

of gravity the damping terms evaluate as:

$$Hdamp1 = -2C_f * Rho * Vbar1 * |Vbar1| * Ldbar1 * (L/2 - Xcg) * Ws1$$

(II-28)

$$Hdamp2 = -2C_f * Rho * Vbar2 * |Vbar2| * Ldbar2 * (L/2 + Xcg) * Ws2$$

(II-29)

e.  Planing Forces

Initial time domain validation studies conducted with the model developed from the equations of this chapter, and the Loads and Motions program, disclosed a serious discrepancy between the two models in natural pitch frequency. Specifically, the Loads and Motions program predicted a natural pitch frequency of 3.2 rad/sec at 10 kts, and 5.4 rad/sec at 20 kts, compared with a constant pitch frequency of 3.3 rad/sec for the linear model. This was taken to indicate the presence of a velocity-dependent source of theta feedback. Examination of ref [2] disclosed that Leo and Boncal had indeed utilized an added mass effect which had the effect of a planing force, in their modifications of the Loads and Motions program.

A body in motion in a fluid experiences a lifting force proportional to the square of the velocity and directly proportional to the angle of attack, or:

$$Hplan_{la} = -C * Theta * Rho * V^2 * S/2$$

(II-30)

where S is the surface area of the body, or:

39

$$S \qquad = (Ws1 + Ws2) * L/2$$

<div align="right">(II-31)</div>

and $C_{la}$ is the lift-curve slope. This term is not directly available, and is a complex function of the sidewall geometry. A value of 1.5 gave good agreement with the natural frequency of the Loads and Motions program, but a less empirical approach to this value is recommended for future studies.

The planing force is assumed to act at the aft quarter-length point.

### 3. Sum of Moments

The forces described above are multiplied by their respective moment arms as shown in Fig 2 to yield the pitching moments about the center of gravity. The angular acceleration about the C.G. is then:

$$Alfa \qquad = (Ppres + Pbuoy + Pseal + Pdamp + Pplan)/Iyy$$

<div align="right">(II-32)</div>

### a. Pressure Moment

The pressure exerts a moment about the center of gravity, equal to:

<div align="center">40</div>

Ppres          $= -Hpres*(Xcp-Xcg)$

$$(II-33)$$


b.  Buoyant Moments


The  buoyant  forces due to the immersed volumes
fore and aft of the  center  of  gravity  exert  a  pitching
moment along their moment arms, which are approximately (for
small angles) the centroid of the rectangle from the  center
of gravity to the bow and stern:

Pbuoy1          $= -.5*(L/2-Xcg)*Hbuoy1$

$$(II-34)$$


Pbuoy2          $= .5*(L/2+Xcg)*Hbuoy2$

$$(II-35)$$


c.  Bow and Sternseal Moments


The  bowseal  acts  along  a  moment arm that is
formed by the distance from the C.G. to the centroid of  the
wetted area Aseal, or:

Pseal1          $= -Hseal1*(L/2-Xcg-Xseal1/2)$

$$(II-36)$$


The sternseal force acts on a moment arm that is
formed by the distance from the C.G. to the centroid of  the
sternseal wetted area, or:

Pseal2        $= Hseal2*(L/2+Xcg+Xseal/2)$

$$(II-37)$$


### d. Damping Moments

The damping moments in pitch are the damping forces in heave multiplied by their respective moment arms, two-thirds the distance from the C.G. to the bow and stern respectively:

Pdamp1        $=-(2/3)*(L/2-Xcg)*Hdamp1$

$$(II-38)$$


Pdamp2        $=(2/3)*(L/2+Xcg)*Hdamp2$

$$(II-39)$$


### e. Planing Moments

The planing moment is the planing force acting at the aft quarter-length point, or:

Pplan        $=(L/4+Xcg)*Hplan$

$$(II-40)$$


### E. INITIAL CONDITIONS

As in the Loads and Motion program, initial conditions must be carefully selected to ensure steady state conditions

42

at the beginning of a run. Since speed does not enter into this program, one of the major problems of the Loads and Motions program is obviated. However, the craft in this model is particularly sensitive to pitch, and once excited in this mode, is very lightly damped.

Selection of initial conditions proceeds as follows:

1. pitch rate and vertical velocity are defined as zero;

2. a value of Pbbar is selected such that plenum air mass flow rate is set to zero;

3. a value of draft is calculated such that weight and pressure forces are balanced by buoyant and planing forces;

4. a value of Theta is calculated such that pressure moments are balanced by buoyant and planing moments;

5. given the Plenum volume defined by the equilibrium values of draft and Theta, and the equilibrium value of Pbbar, the Plenum air mass may be calculated adiabatically.

More detail on the exact procedures for the selection of equilibrium conditions may be found in subsequent chapters dealing with the computer simulation of this model.

43
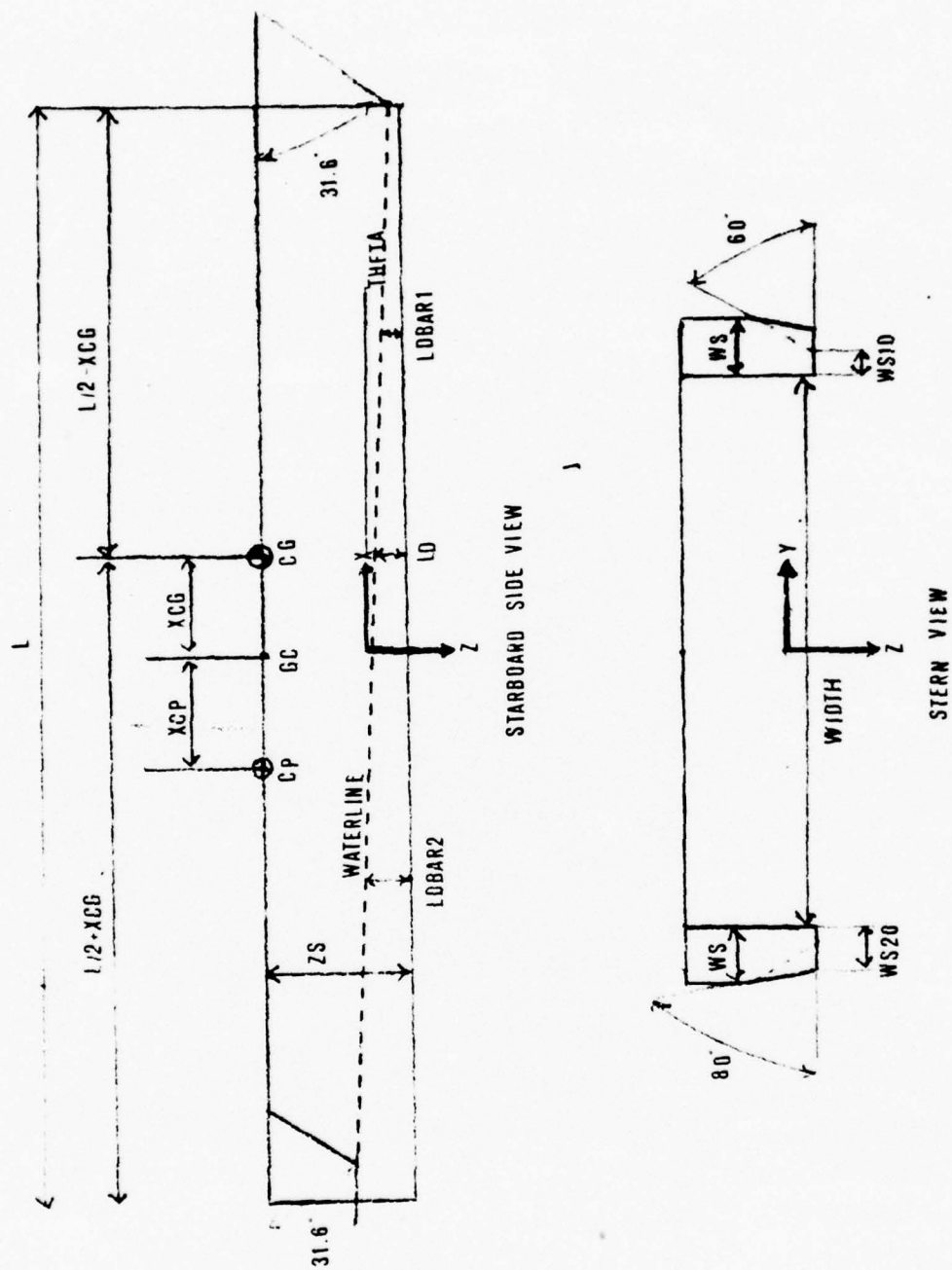
Figure 1 - ASSUMED GEOMETRY OF SIMPLIFIED XR-3

Figure 2 — FORCES AND MOMENTS ON XR-3

45
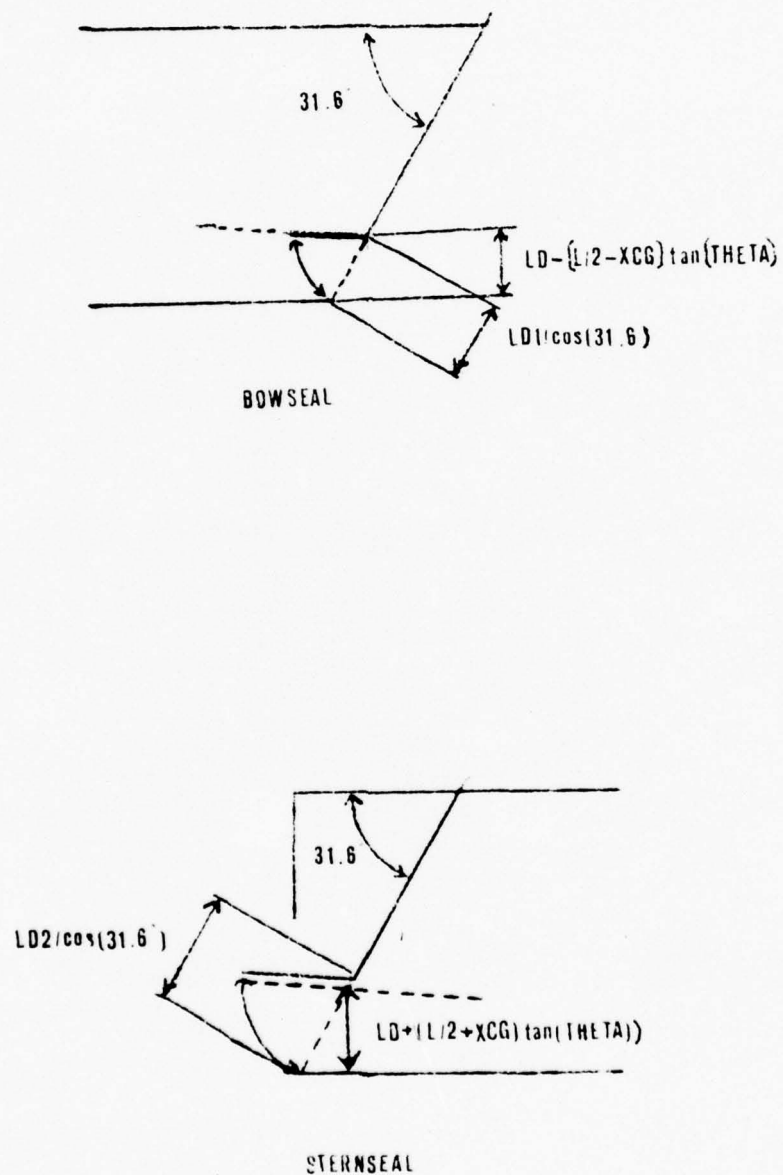
Figure 3 - DETAIL OF BOW AND STERNSEAL

46

## III. LINEAR HEAVE-PITCH MODEL

The non-linear equations of motion developed in the preceding chapter form the basis of a linearized heave-pitch model, valid for disturbances about its equilibrium point, defined as that point about which all rates are zero. The linear model permits the use of a variety of powerful techniques for parametric analysis, such as root locus; it furthermore simplifies the design of an automatic control system, which could serve to further limit excursions about the operating point.

## A. TAYLOR'S SERIES EXPANSION

For small excursions about an operating point, the non-linear relationships:

$$f = F(x,y)$$

$$g = G(x,y)$$

are approximately:

$$f + df_0 = F(x,y) + (dF/dx)_0 * Dx + (dF/dy)_0 * Dy$$

$$g_0 + dg = G(x_0, y_0) + (dG/dx) * Dx + (dG/dy) * Dy$$

where the derivatives of F and G with respect to x and y are evaluated at the operating point, $x_0$ and $y_0$. Cancelling the equilibrium point from both sides and dividing through by time yields:

47

$$\frac{d}{dt} (f) = (dF/dx) * \frac{d}{dt} (x) + (dF/dy) * \frac{d}{dt} (y)$$

$$\frac{d}{dt} (g) = (dG/dx) * \frac{d}{dt} (x) + (dG/dy) * \frac{d}{dt} (y)$$

Applying these principles to the non-linear model of the preceding chapter, the steady state operating point is defined as before for the equilibrium values of the state variables.


B. PLENUM GAUGE PRESSURE DERIVATIVES


Plenum gauge pressure has been been defined as:

Pbbar       = Pb-Pa

(II-9)

and since Pa is a constant:

dPbbar      = dPb

Pb, the plenum total pressure, has been defined as:

$$Pb(0) = Pa*(Mb(0)/(Rhoa*Vb(0)))^{Gamma}$$

(II-8)

Therefore expanding around the equilibrium values of Vb(0) and Mb(0):

$$Pb(0)+dPb = Pa*(Mb(0)/(Rhoa*Vb(0)))^{Gamma}$$

$$+ (Gamma/Mb(0))*Pa*(Mb(0)/(Rhoa*Vb(0))^{Gamma}*dMb$$

$$- (Gamma/Vb(0))*Pa*(Mb(0)/(Rhoa*Vb(0))^{Gamma}*dVb$$

<div align="right">(III-1)</div>

or, after substituting the definition of Pb(0) and cancelling the equilibrium values from both sides:

$$dPb = Gamma*(Pb(0)/Mb(0))*dMb$$

$$-Gamma*(Pb(0)/Vb(0))*dVb$$

<div align="right">(III-2)</div>

Vb(0) may be further expanded, since it has been defined in the preceding chapter as the empty plenum volume less the net submerged volume, following the definition of ref [5]:

$$Vb(0) = Vn-Ab*(z(0)+Zs+Xcg*Theta(0))$$

<div align="right">(II-7)</div>

and

$$dVb = -Ab*dz-Ab*Xcg*dTheta$$

<div align="right">(III-3)</div>

Substituting the expansion of incremental volume, Equation (III-3), into the expansion for incremental pressure, Equation (III-2), and dividing by differential time yields:

$$\frac{d}{dt}(Pbbar) = Gamma*(Pb(0)/Mb(0))*\frac{d}{dt}(Mb)$$

<div align="center">49</div>

$$+Gamma*Ab*(Pb(0)/Vb(0))*\frac{d}{dt}(z)$$

$$+Gamma*Ab*Xcg*(pb(0)/Vb(0))*\frac{d}{dt}(Theta)$$

$$(III-4)$$

For more compact notation the following influence coefficients are defined such that:

$$Dpbz=Gamma*Ab*(Pb(0)/Vb(0));$$

$$(III-5)$$

$$Dpbth=Gamma*Ab*Xcg*(Pb(0)/Vb(0));$$

$$(III-6)$$

$$Dpbmb=Gamma*(Pb(0)/Ab(0));$$

$$(III-7)$$

and the pressure differential equation becomes:

$$\frac{d}{dt}(Pbbar)=Dpbz*\frac{d}{dt}(z)$$

$$+Dpbth*\frac{d}{dt}(Theta)$$

$$+Dpbmb*\frac{d}{dt}(Mb)$$

$$(III-8)$$

C. PLENUM AIR MASS FLOW RATE DERIVATIVES

50

The plenum air mass flow rate has been defined in the preceding chapter as:

$$\frac{d}{dt}(Mb(0)) = Rhoa*(Qin(0) - Qout(0))$$

(II-12)

and

$$d(\frac{d}{dt}(Mb)) = Rhca*dQin - Rhoa*dQout$$

(III-9)

Qin has been defined as:

$$Qin(0) = N*(Qi0 - Pbbar(0))$$

(II-10)

so that

$$dQin = -N*dP.bbar$$

(III-10)

and Qout has been defined as:

$$Qout(0) = Cn*Al*(2*Pbbar(0)/Rhoa)^{1/2}$$

(II-11)

and

$$dQout = (Cn*Al/Rhoa)*(2*Pbbar(0)/Rhoa)^{-1/2}*dPbbar$$

(III-11)

Combining the two expressions for incremental volumetric flow into and out of the plenum, Equations (III-10,11), with

51

the expression for for incremental mass flow rate, Equation (III-9), and dividing by differential time yields:

$$\frac{d}{dt}^2 (Mb) = -(N*Rhoa+Cn*Al*(2*Pbbar(0)/Rhoa))^{-1/2} * \frac{d}{dt} (Pbbar)$$

(III-12)

The influence coefficients may be defined by substituting Equation (III-8) into Equation (III-12) and equating terms:

$$Dmbz = -(N*Rhoa+Cn*Al*(2*Pbbar(0)/Rhoa))^{-1/2}*dpbz$$

(III-13)

$$Dmbth = -(N*Rhoa+Cn*Al*(2*Pbbar(0)/Rhoa))^{-1/2}*dpbth$$

(III-14)

$$Dmbmb = -(N*Rhoa+Cn*Al*(2*Pbbar(0)/Rhoa))^{-1/2}*dpbmb$$

(III-15)

Thus the linearized differential equation for plenum mass flow rate may be written:

$$\frac{d}{dt}^2 (Mb) = Dmbz* \frac{d}{dt} (z)$$

$$+Dmbth* \frac{d}{dt} (Theta)$$

$$+Dmbmb* \frac{d}{dt} (Mb)$$

(III-16)

52

## D. HEAVE DERIVATIVES

The heave equation has been defined as:

$$\frac{d^2}{dt^2}(z) = (Hpres+Hbuoy+Hseal+Hdamp+Hplan+W)/M$$

(II-13)

Damping forces are neglected in the linear model. We shall consider the various components of heave force separately, and superimpose the components upon completion of all derivations.

### 1. Heave Force Due To Pressure

The heave force due to pressure has been defined as:

Hpres $=-Ab*Pbbar$

(II-14)

By inspection, its influence coefficients become:

$$Dhpz=-Ab*Dpbz$$

(III-17)

$$Dhpth=-Ab*Dpbth$$

(III-18)

$$Dhpmb=-Ab*Dpbmb$$

(III-19)

## 2. Heave Forces Due To Buoyancy

The buoyant heave force equation from the preceding chapter has been defined as:

Hbuoy          =Hbuoy1+Hbuoy2

=-2*Rho*G*Ws1*(L/2-Xcg)*(Ld-(L/2-Xcg)*Theta/2)

-2*Rho*G*Ws2*(L/2+Xcg)*(Ld+(L/2+Xcg)*Tneta/2)

(II-15,16,17,18)

which may be rearranged:

Hbuoy=

-2*Rho*G*(Ws1*(L/2-Xcg)+ws2*(L/2+Xcg))*(z(0)+Zs)

$+2*Rho*G*(Ws1*(L/2-Xcg)^2-Ws2*(L/2+Xcg)^2)*Theta/2$

and the influence coefficients may be written by inspection:

Dhbz          =-2*Rho*G*(Ws1*(L/2-Xcg)+Ws2*(L/2+Xcg))

(III-20)

$Dhbth          =Rho*G*(Ws1*(L/2-Xcg)^2-Ws2*(L/2+Xcg)^2)$

(III-21)

## 3. Heave Force due to Bow and Sternseal

54

The expression for the bowseal heave force has been defined as:

$$Hseal1(0) = -Width*Xseal1(0)*Pbbar(0)$$

$$(II-21)$$

which for small perturbations in Xseal1 and Pbbar becomes

$$dHseal1 = -Width*Pbbar(0)*dXseal1$$
$$-Width*Xseal1(0)*dPbbar$$

$$(III-22)$$

The expression for Xseal1 has been defined:

$$Xseal1(0) = 1.65*(z(0)+Zs-(L/2-Xcg)*Theta)$$

$$(II-20)$$

which for small perturbations around z(0) and Theta(0) is approximately

$$dXseal1 = 1.65*dz-1.65*(L/2-Xcg)*dTheta$$

$$(III-23)$$

Substituting these relations along with the relations for small perturbations in Pbbar due to z,Theta and Mb from Equations (III-5,6,7) yields:

$$dHseal1 = -Width*(1.65*Pbbar(0)+Xseal1(0)*Dpbz)*dz$$
$$-Width*(-1.65*(L/2-Xcg)*Pbbar(0)$$
$$+Xseal1(0)*Dpbth)*dTheta$$

55

$$-Width*Xseal1(0)*Dpbmb*dMb$$

$$(III-24)$$

The influence coefficients then become:

Dhsz1 $\quad$ =-Width*(1.65*Pbbar(0)+Xseal1(0)*Dpbz)

$$(III-25)$$

Dhsth1 $\quad$ =-Width*(-1.65*(L/2-Xcg)*Pbbar(0)

$$+Xseal1(0)*Dpbth)$$

$$(III-26)$$

Dhsmb $\quad$ =-Width*Xseal1(0)*Dpbmb

$$(III-27)$$

The expression for the stern seal has been defined:

Hseal2 $\quad$ =-Sealp*Width*Xseal2(0)

$$(II-23)$$

Xseal2(0) $\quad$ =1.65*(Ld(0)+(L/2+Xcg)*tan(Theta(0)))

$$(II-22)$$

Thus for small perturbations in draft and Theta:

dHseal2 $\quad$ =-1.65*sealp*Width*dz

$$-1.65*(L/2+Xcg)*Sealp*Width*dTheta$$

$$(III-28)$$

Thus the sternseal influence coefficients become:

Dhsz2        =-1.65*Sealp*Width

$$(III-29)$$

Dhsth2        =-1.65*(L/2+Xcg)*Sealp*Width

$$(III-30)$$

### 4. Heave Force due to Planing

The planing force is linear in Theta , or:

Hplan        $=-C_{la}*Rho*V^{2}*(Ws1+Ws2)*L*Theta$

$$(II-30,31)$$

and the influence coefficient may be written by inspection:

Dhplth        $=-C_{la}*Rho*V^{2}*(Ws1+Ws2)*L$

$$(III-31)$$

### 5. Sum Of Forces

The forces previously derived may be superimposed so that:

$$\frac{d^{2}}{dt^{2}}(z(0))+d(\frac{d^{2}}{dt^{2}}(z))=$$

57

$$(Hpres(0) + Hbuoy(0) + Hseal(0) + Hplan(0))/M$$

$$+ (Dhpz + Dhbz + Dhsz) * dz/M$$

$$+ (Dhpth + Dhbth + Dhsth + Dhplth) * dTheta/M$$

$$+ (Dhpmb + Dhsmb) * dMb/M$$

$$(III-32)$$

The influence coefficients may now be defined:

$$Dzz = (Dhpz + Dhbz + Dhsz)/M$$

$$(III-33)$$

$$Dzth = (Dhpth + Dhbth + Dhsth + Dhplth)/M$$

$$(III-34)$$

$$Dzmb = (Dhpmb + Dhsmb)/M$$

$$(III-35)$$

Removing the equilibrium values and dividing through by differential time yield the differential equation of motion in the z-direction:

$$\frac{d^3}{dt^3}(z) = Dzz * \frac{d}{dt}(z)$$

$$+ Dzth * \frac{d}{dt}(Theta)$$

$$+ Dzmb * \frac{d}{dt}(Mb)$$

$$(III-36)$$

E.  PITCHING MOMENT DERIVATIVES

58

The pitching moment equation is

$$\frac{d^2}{dt^2}(\text{Theta}) = (\text{Ppres} + \text{Pbuoy} + \text{Pseal} + \text{Pdamp} + \text{Pplan})/\text{Iyy}$$

(II-32)

As in the previous case of heave forces, damping moments are neglected in the linear model; the various moments are considered separately and superimposed after derivation.


1.   Pitch Moment due to Pressure


The pressure moment has been defined as

Ppres          =(Xcg-Xcp)*Hpres

(II-33)

The influence coefficients may be written by inspection:

$$\text{Dppz} = (\text{Xcg} - \text{Xcp}) * \text{Dhpz}$$

(III-37)

$$\text{Dppth} = (\text{Xcg} - \text{Xcp}) * \text{Dhpth}$$

(III-38)

$$\text{Dppmb} = (\text{Xcg} - \text{Xcg}) * \text{Dhpmb}$$

(III-39)


2.   Buoyant Moments


The buoyant moment has been defined:

59

$$Pbuoy \quad =Pbuoy1+Pbuoy2$$

$$=-(L/2-Xcg)*Hbuoy1/2+(L/2+Xcg)*Hbuoy2/2$$

$$=Rho*g*(Ws1*(L/2-Xcg)^2*(Ld-(L/2-Xcg)*Theta/2)$$

$$-Ws2*(L/2+Xcg)^2*(Ld+(Ld+(L/2+Xcg)*Theta/2)))$$

$$(II-34,35)$$

and the influence coefficients may be defined:

$$Dpbyz \quad =Rho*G*(Ws1*(L/2-Xcg)^2-Ws2*(L/2+Xcg)^2)$$

$$(III-40)$$

$$Dpbyth \quad =-Rho*G*(Ws1*(L/2-Xcg)^3+Ws2*(L/2+Xcg)^3)/2$$

$$(III-41)$$

### 3. Bow and Sternseal Moments

The bowseal contributes a moment

$$Pseal1 \quad =-Hseal1*(L/2-Xseal1/2-Xcg)$$

$$(II-36)$$

which for small disturbances , is approximately

$$dPseal1 \quad =-(L/2-Xseal1(0)/2-Xcg)*dHseal1$$

60

$$+ \text{Hseal1}(0) * \text{dXseal1}/2$$

$$(III-42)$$

Substituting the definition of dXseal1, Equation (III-23), and the influence coefficients of Hseal1, Equations (III-25,26,27) yields:

$$\text{dPseal1} = (- (L/2 - \text{Xseal1}(0)/2 - \text{Xcg}) * \text{Dhsz1}$$

$$+ 1.65 * \text{Hseal1}(0)/2) * dz$$

$$+ (- (L/2 - \text{Xseal1}(0)/2 - \text{Xcg}) * \text{Dhsth1}$$

$$- 1.65 (L/2 - \text{Xcg}) * \text{Hseal1}(0)/2) * \text{dTheta}$$

$$- (L/2 - \text{Xseal1}(0)/2 - \text{Xcg}) * \text{Dhsmb} * \text{dMb}$$

$$(III-43)$$

The influence coefficients may now be defined:

$$\text{Dpsz1} = - (L/2 - \text{Xseal1}(0)/2 - \text{Xcg}) * \text{Dhsz1}$$
$$+ 1.65 * \text{Xseal1}(0)/2$$

$$(III-44)$$

$$\text{Dpsth1} = - (L/2 - \text{Xseal1}(0)/2 - \text{Xcg}) * \text{Dhsth1}$$

$$- 1.65 * (L/2 - \text{Xcg}) * \text{Hseal1}(0)/2$$

$$(III-45)$$

$$\text{Dpsmb} = - (L/2 - \text{Xseal1}(0)/2 - \text{Xcg}) * \text{Dhsmb}$$

$$(III-46)$$

The sternseal contributes a moment:

$$Pseal2(0) \qquad =Hseal2*(L/2+Xseal2(0)/2+Xcg)$$

<div align="right">(II-37)</div>

which for small disturbances is approximately:

$$dPseal2 \qquad =(L/2+Xseal2(0)/2+Xcg)*dHseal2$$

$$+Hseal2(0)*dXseal2/2$$

<div align="right">(III-47)</div>

and substitution from the sternseal force influence coefficients, Equations (III-29,30), yields:

$$dPseal2 \qquad =((L/2+Xseal2(0)/2+Xcg)*Dhsz2$$

$$+1.65*Hseal2(0)/2)*dz$$

$$+((L/2+Xseal2(0)/2+Xcg)*Dhsth2$$

$$+1.65*(L/2+Xcg)*Hseal2(0)/2)*dTheta$$

<div align="right">(III-48)</div>

and the stern seal pitch influence coefficients may be defined:

$$Dpsz2=(L/2+Xseal2(0)/2+Xcg)*Dhsz2$$

$$+1.65*Hseal2(0)/2$$

<div align="right">(III-49)</div>

$$Dpsth2=(L/2+Xseal2(0)/2+Xcg)*Dhsth2$$

$$+1.65*(L/2+Xcg)*Hseal2(0)/2$$

<div align="right">(III-50)</div>

### 4. Pitch Moment due to Planing

The planing moment is linear in Theta:

Pplan        =(L/4+Xcg)*Hplan

$$(II-40)$$

and the influence coefficient is:

Dpplth        =(L/4+Xcg)*Dhplth

$$(III-51)$$

### 5.  <u>Sum Cf Moments</u>

The individual moment contributions may now be summed:

Alfa(0)+dAlfa=(Ppres(0)+Pbuoy(0)+Pseal(0)+Pplan(0))/Iyy

                    +(Dppz+Dpbyz+Dpsz)*dz/Iyy

                    +(Dppth+Dpbyth+Dpsth+Dpplth)*DTheta/Iyy

                    +(Dppmb+Dpsmb)*dMb/Iyy

$$(III-52)$$

The influence coefficients may now be defined

                Dpz=(Dppz+Dpbyz+Dpsmb)/Iyy

$$(III-53)$$

                Dpth=(Dppth+Dpbyth+Dpsth+Dpplth)/Iyy

$$(III-54)$$

63

$$Dpmb=(Dppmb+Dpsmb)/Iyy$$

(III-55)

and the differential equations of motion for angular rate of acceleration may be written, after dividing through by differential time and cancelling the equilibrium values:

$$\frac{d^3}{dt^3}(Theta)=Dpz*\frac{d}{dt}(z)$$

$$+Dpth*\frac{d}{dt}(Theta)$$

$$+Dpmb*\frac{d}{dt}(Mb)$$

(III-56)

## F.   STATE SPACE REPRESENTATION

Fig 4 is the linear model as derived in this chapter presented in matrix form as:

$$\dot{x}=A*x$$

Examination of the eigenvalues of the 9-by-9 matrix shows four eigenvalues at the origin (0±0j) which represent the integrated output equations for z, Theta, Mb, and Pbbar; the remaining eigenvalues consist of a complex pair, located in the vicinity of -30±30j, and a real eigenvalue in the vicinity of -.5, as in ref [5], and an additional complex pair near 0±4j, representing the very lightly-damped pitch response.

STATE VECTOR

$$
\begin{bmatrix} X_1 \\ X_2 \\ X_3 \\ X_4 \\ X_5 \\ X_6 \\ X_7 \\ X_8 \\ X_9 \end{bmatrix}
=
\begin{bmatrix} Z \\ ZDOT \\ ZDDOT \\ THETA \\ OMEGA \\ ALFA \\ PBBAR \\ \psi B \\ MBDOT \end{bmatrix}
$$

STATE EQUATION

$$
\begin{bmatrix} \dot{X}_1 \\ \dot{X}_2 \\ \dot{X}_3 \\ \dot{X}_4 \\ \dot{X}_5 \\ \dot{X}_6 \\ \dot{X}_7 \\ \dot{X}_8 \\ \dot{X}_9 \end{bmatrix}
=
\begin{bmatrix}
0 & 1 & 0 & 0 & 0 & 0 & 0 & 0 & 0 \\
0 & 0 & 1 & 0 & 0 & 0 & 0 & 0 & 0 \\
0 & DZZ & 0 & DZTH & 0 & 0 & 0 & 0 & DZMB \\
0 & 0 & 1 & 1 & 0 & 0 & 0 & 0 & 0 \\
0 & 0 & 0 & 0 & 1 & 0 & 0 & 0 & 0 \\
0 & DTHZ & 0 & DTHTH & 0 & 0 & 0 & 0 & DTHMB \\
0 & DPBZ & 0 & DPBTH & 0 & 0 & 0 & 0 & DPBMB \\
0 & 0 & 0 & 0 & 0 & 0 & 0 & 0 & 1 \\
0 & DMBZ & 0 & DMBTH & 0 & 0 & 0 & 0 & DMBMB
\end{bmatrix}
\begin{bmatrix} X_1 \\ X_2 \\ X_3 \\ X_4 \\ X_5 \\ X_6 \\ X_7 \\ X_8 \\ X_9 \end{bmatrix}
$$

Figure 4 –   STATE SPACE REPRESENTATION OF THE LINEAR SYSTEM

# IV. TIME DOMAIN VALIDATION

The linear heave-pitch XR-3 model was validated against the modified Oceanics XR-3 Loads and Motions Program of ref [3] prior to investigations in the frequency domain. The linearized program, which appears at the end of the text, was simulated using the Continuous System Modeling Program, version III. This is basically a FORTRAN language with extremely powerful variable-step integrators and versatile output structure. Readers familiar with FORTRAN should find little difficulty following the CSMP III programs developed for this simulation; for details of this simulation language, see ref [6].

The Time Domain Program consists of three sections:

1. Initial Conditions; this subsection identifies the equilibrium operating point for a given set of craft physical parameters.

2. Linearization; the partial derivatives of the non-linear state equations derived in the preceding chapter are evaluated at this particular operating point.

3. Dynamics; the weight and C.G. acceleration are perturbed at time zero by a step weight change, and the resultant linear state trajectories in time are computed. Note that the linear model is not self-starting; an initial C.G. acceleration must also be applied.

66

## A.  INITIAL CONDITIONS

.

Initial conditions involve the solution of the non-linear system equations of Chapter II for the equilibrium operating point defined at the end of the chapter.


### 1.  Plenum Pressure

A value of plenum pressure is selected so that plenum mass flow rate is set to zero, or, from Equations (II-10,11):

Qin          =Qout

$$Qi0-Pbbar \qquad =(Cn*Al/N)*(2*Pbbar/Rhoa)^{1/2}$$

(IV-1)

which is a quadratic in Pbbar:

$$Pbbar^2-(2*Qi0+(Cn*Al/N)^2/Rhoa)*Pbbar+Qi0^2=0$$

(IV-2)

The larger solution of this quadratic, corresponding to the physically unrealizable condition of reverse flow through the fans, is rejected.


### 2.  Draft and Pitch Angle

The solution for equilibrium values of draft and pitch, given the previously-computed value of Pbbar, requires an iterative technique, due to their close

67

coupling. An initial value of draft is first computed assuming zero pitch and no bow or stern seal contribution. The non-linear state equations are then solved for residual forces and moments due to all sources. A very small perturbation in draft and pitch angle of one percent with a minimum default magnitude of .001 is applied and the differential change in residual forces and moments with respect to draft and Theta are computed. Bairstow's method for the zeroes of functions of two variables, as described in ref [7], is used to drive the residuals to zero. This particular problem is somewhat slow to converge; convergence is enhanced by amplifying the computed changes in draft and pitch by 1.9, but after two hundred iterations residuals on the order of ten lbf and ten ft-lbf may still be observed. These residual forces and moments are applied to the initial values of Z2dot and Alfa.

### 3. Plenum Air Mass

The equilibrium values of draft and pitch angle define a unique plenum volume:

Vb          =Vn-Ab*(Ld+Xcg*tan(Theta))

(II-7)

which, when combined with the equilibrium pressure, yields a unique adiabatic plenum air mass, from Equation (II-8):

MbO          =Rhoa*Vb*(Pbbar/Pa)$^{1/Gamma}$

(IV-3)

The solutions to these equations define the equilibrium values of Pb(0), Ld(0), Theta(0), and Mb(0)

68

about which the partial differential equations of the preceding chapter may be evaluated.


B. LOADS AND MOTIONS PROGRAM OPERATING CONDITIONS


The XR-3 Loads and Motion program was run at 6500 lb weight, C.G. 9.825 ft. ahead of the aft transom at 20 kts. Simulation time was 30.0 sec. for the purpose of obtaining reasonably quiescent values of pitch angle, draft, and Plenum pressure. In order to obtain identical operating conditions, it was necessary to adjust various constants in the linear model until agreement was reached with the steady-state operating conditions of the Loads and Motion program. Specifically, these parameters were:

1. seal leakage area, Al, adjusted until the two programs agreed in Plenum pressure

2. Planing lift-curve slope coefficient, $C_{l\alpha}$, adjusted until the two programs agreed in natural pitch frequency;

3. minimum sidewall width, Ws0, adjusted until the two programs agreed in draft;

4. Residual pitching moment ,Mf0, adjusted until the two programs agreed in steady-state pitch angle.


The results of these trial-and-error iterations yielded the following table of values:

TABLE OF OPERATING PARAMETERS

| LINEAR SYSTEM | | | LOADS AND MOTIONS |
|---|---|---|---|
| PARAMETER | AFFECTED VARIABLE | STEADY-STATE VALUE | STEADY-STATE VALUE |
| Al=.390 | Pkbar | 24.85 lbf/ft$^2$ | 24.84 lbf/ft$^2$ |
| C=1.5 la | $\dot{w}_p$ | 5.02 rad/sec | 5.46 rad/sec |
| Ws0=.27 | Ld | 8.497 in. | 8.55 in. |
| Mf0=-1875 | Theta | 1.21 deg | 1.199 deg |

C.  COMPARISON OF RESULTS


The  Loads and Motions program was run 3.0 secs with the
initial conditions as obtained above, but with a  weight  of
6400  lbs.   The  linear model was simultaneously run with a
100 lb step  weight  reduction; data  from  the  Loads  and
Motions  program  was subsequently entered into the CSMP III
linear program in tabular form,  for  simultaneous  plotting
and error computation. For the purposes of comparison, error
was defined as the difference between the data from the  two
programs,  divided  by  the  average value of the two.  This
procedure  significantly  reduced  the  probability  of
inadvertent  division  by zero, as compared with normalizing
the difference with respect to one system or the other.


1.  Plenum Pressure


Plenum pressure and Plenum pressure error  (percent)

70

plotted vs. time appear in Figs 5 and 6. The two curves are in quite good general agreement, with the magnitude of error being on the order of several parts per thousand. The linear model exhibits a greater pressure reduction in the initial pressure transient, than does the Loads and Motion results, and this transient is more heavily damped in the linear model. One explanation for this difference would appear to be the variable leakage area of the Loads and Motion program. Pitch appears to couple more strongly into pressure in the linear model; however, the magnitude of pitch is significantly greater in the linear model due to the absence of significant damping terms. Finally, the pressure in the Loads and Motion program is tending toward a slightly higher value, further supporting the supposition that leakage area has decreased in the Loads and motion program.

### 2. C.G. Acceleration

Figs 7 and 8 show C.G. acceleration and C.G. acceleration error vs. time. They generally exhibit similar characteristics, but due to the larger initial pressure reduction of the linear model, there is a more pronounced overshoot in C.G. acceleration in the linear model. In addition, the stronger pitch-pressure coupling in the linear model also translates as stronger pitch-C.G. acceleration coupling. The errors appear as relatively large percentages; however, these are the differences of two very small numbers, and should be regarded cautiously.

### 3. Draft

Draft and draft error vs. time appear in Figs 9 and 10. As has been previously verifed by the Gerba/Thaler

model, draft is very well approximated by a linear model. For this particular disturbance, it appears to be slightly less damped and tending toward a lower steady-state value in the linear model. Little evidence of pitch coupling is apparent, and errors are on the order of parts per thousand.

### 4. Pitch Rate

Pitch rate and pitch rate error are shown plotted vs. time in Figs 11 and 12. The linear model exhibits a pitch rate of approximately twice the magnitude of the Loads and Motion program; this may ostensibly be attributed to the sharper pressure transient previously observed; with the center of pressure forward of the C.G. in both models, this would induce a higher initial angular acceleration in the linear model. In addition, the linear model is significantly less damped in pitch; therefore this larger magnitude angular acceleration would build to a larger angular velocity, and persist for a longer period of time in the linear model. The frequencies compare favorably, 5.04 rad/sec for the linear model and 5.28 for the Loads and Motion program.

### 5. Pitch Angle

Figs 13 and 14 display pitch angle in degrees and pitch angle error vs. time. Both show basically identical characteristics; i.e., an initial pitch down induced by the pressure drop, and an exponential decay to a lower pitch angle induced by the draft change. The magnitude of pitch angle change reflects the larger angular velocity of the linear model, and the difference between the damping of the Loads and Motion program and the linear model is quite dramatic. The magnitude of error, however, is on the order

of parts per hundred.
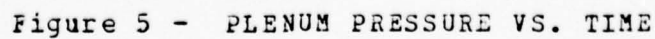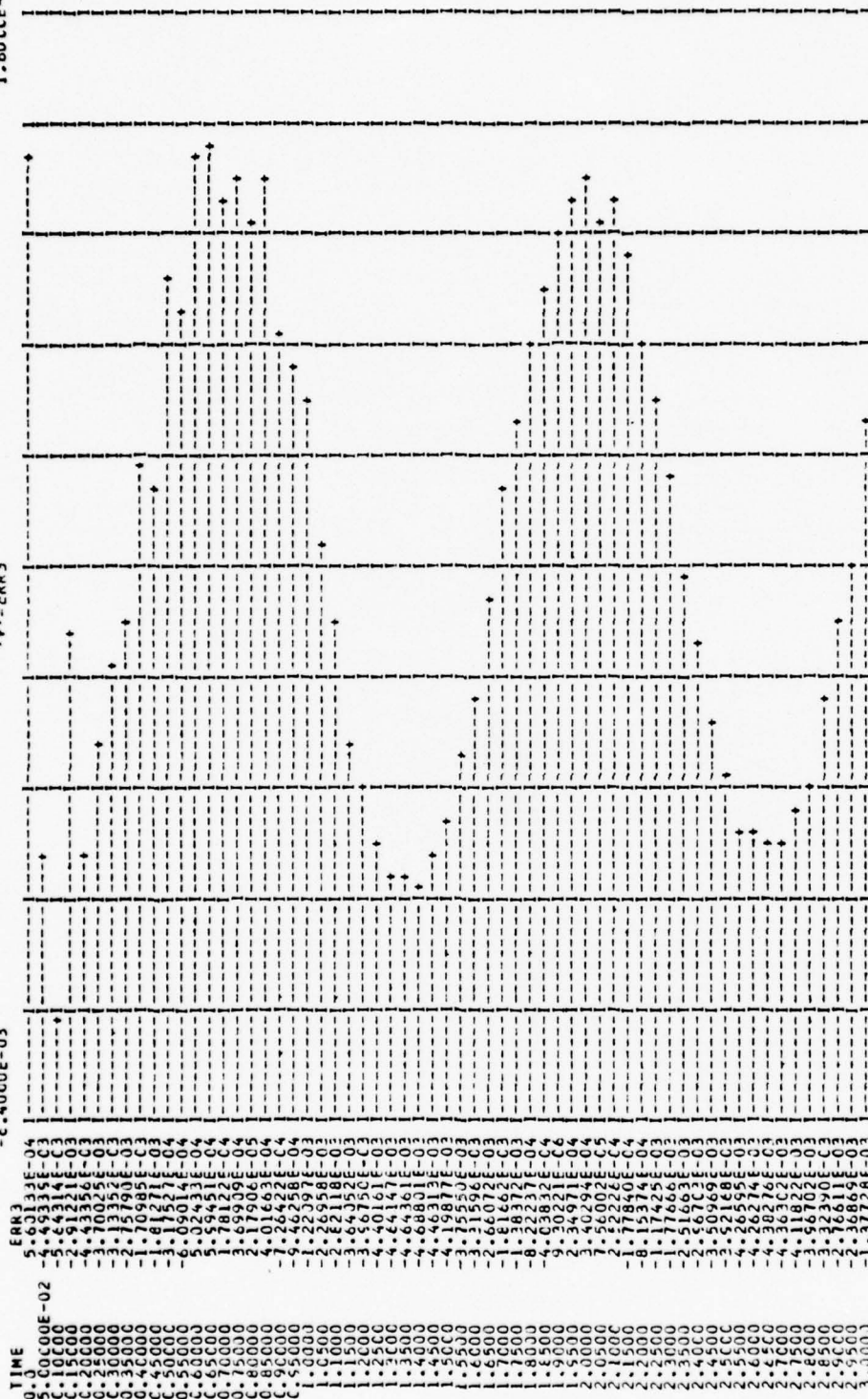
Figure 5 - PLENUM PRESSURE VS. TIME

Figure 6 - PLENUM PRESSURE ERROR VS. TIME

SPALL-TIGNAL XR-3 MODEL 100 LB WT STEP,6500 LB WT,20 KTS
CG VERT ACCEL, FT/SEC**2 VS TIME

*=Z2LM, LOADS AND MOTION DATA
+=Z2DCT, LINEAR SYSTEM DATA

Figure 7 -  C.G. ACCELERATION VS. TIME

SMALL-SIGNAL XR-3 MODEL 100 LB WT STEP,6500 LB WT,20 KTS
PERCENT ACCELERATION ERROR VS. TIME

-15.00                    '+'=ERR4                    10.00

Figure 8 -   C.G. ACCELERATION ERROR VS. TIME

Figure 9 -  DRAFT,INCHES VS. TIME

78
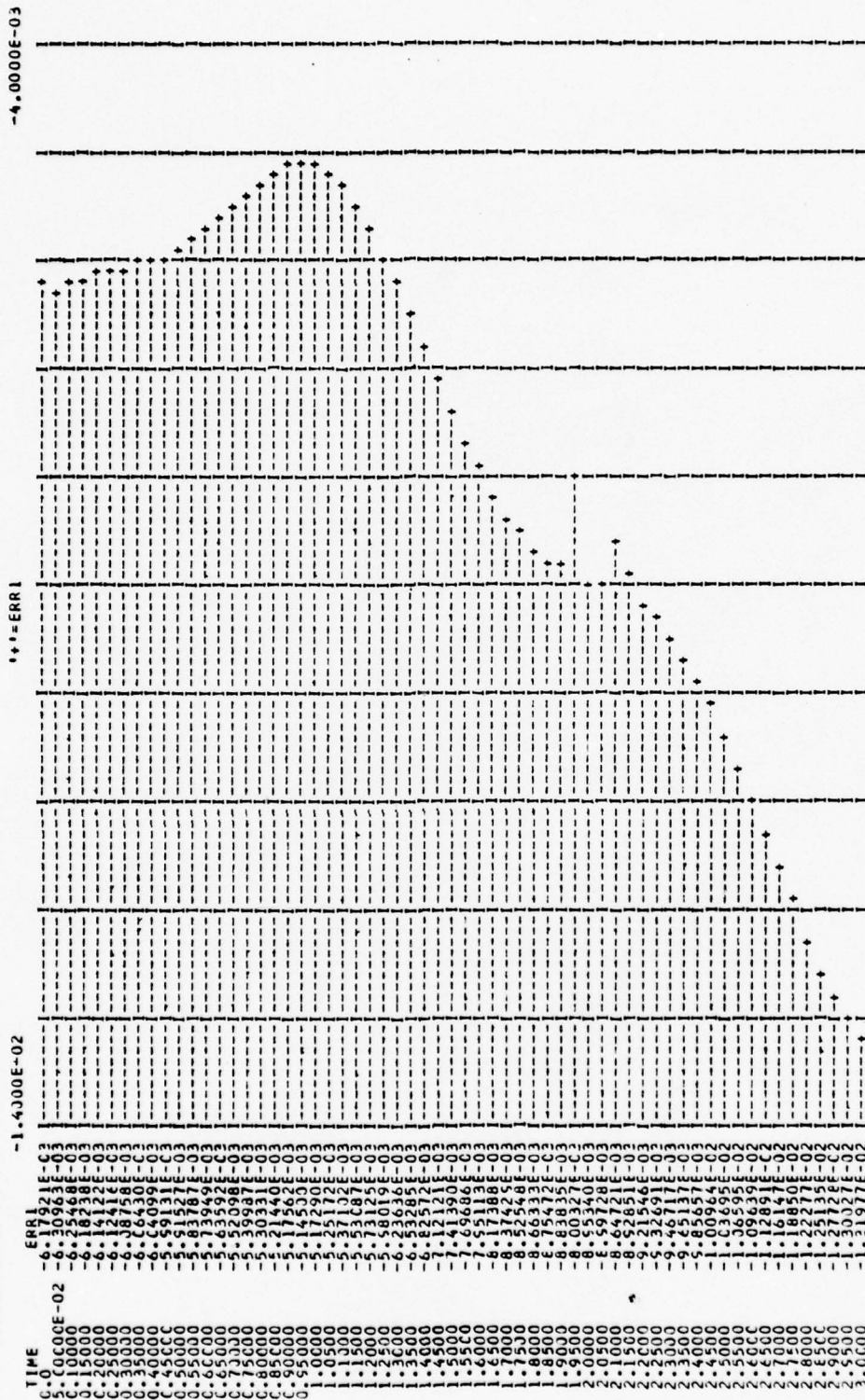
Figure 10 - DRAFT ERROR VS. TIME
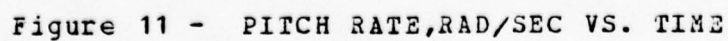
79

Figure 11 - PITCH RATE, RAD/SEC VS. TIME

SMALL-SIGNAL XH-3 MODEL 100 LB WT STEP,6500 LB WT,20 KTS
ANG VELOCITY PCT ERROR VS TIME

-3200.                          '+'=ERRS                          800.0

Figure 12 -   PITCH RATE ERROR VS. TIME

Figure 13 - PITCH ANGLE, DEGREES VS. TIME
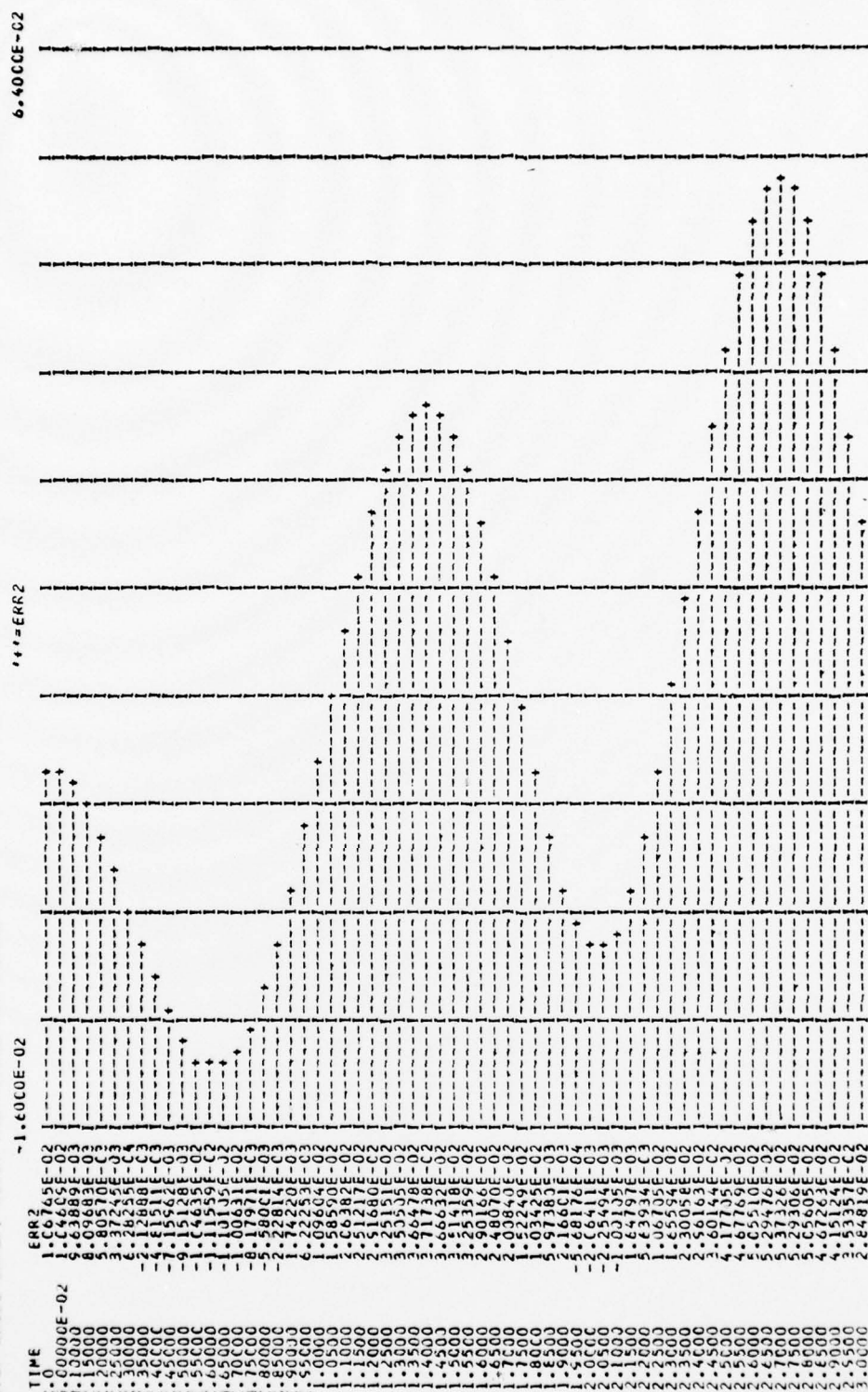
Figure 14 - PITCH ERROR VS. TIME

## V.   FREQUENCY DOMAIN DEVELOPMENT


This chapter develops the techniques for frequency
response of a general linear system by complex matrix
inversion.  The ocean wave equations utilized by Booth are
reviewed and summarized, and the forcing functions of wave
action on the linearized XR-3 model are developed in pitch
and heave.  Portions of Booth's work are repeated utilizing
the linearized model, and the results contrasted and
compared.


## A.   LINEAR SYSTEM FREQUENCY RESPONSE


The development of a linear system permits the
utilization of various techniques for the development of
frequency response characteristics which are vastly superior
in CPU time in simulation, than the methods to which one is
limited in non-linear models.  The definition of the state
matrix of the previous chapter defines the state transfer
matrix:

$$H(s) = |sI-A|^{-1} * B(s)$$

(V-1)


and if the system is forced by a sinusoid, s tends toward jw
as the transients decay and:

$$H(jw) \qquad = |jwI-A|^{-1}*B(jw)$$

$$(V-2)$$

yielding the magnitude and phase relationships:

$$G(w) \qquad = 10*\log_{10}*|H(jw)/H(0)|$$

$$(V-3)$$

$$\varphi(w) \qquad = \tan^{-1}|imag(H(jw)/real(H(jw)|$$

$$(V-4)$$

where $G(w)$ is the gain, in decibels, with respect to some arbitrary reference $H(0)$ , and $\varphi(w)$ is the phase angle in the complex plane. Thus the frequency response of a linear system to a given sinusoidal forcing function may be obtained by complex matrix inversion. While this is not in itself a particularly economical use of CPU time, it is still vastly superior to a Fourier transform. This is particularly true if the range of frequencies is wide and variable-step integrators driven to small step sizes which are not required for most of the array integration. Finally, it is not necessary to allow the system to attain steady-state AC conditions prior to computing the frequency response. This is particularly important in any model of the XR-3, which exhibits very light pitch damping.

B. WAVE CHARACTERISTICS

Booth in ref [1] provides an excellent discussion on the characteristics of gravity-free surface waves with straight, infinitely long, parallel, equally-spaced wave crests, and

85

constant wave height. Such a wave advances with a velocity C which is often referred to as celerity, in order to emphasize the fact that it is the wave front which advances, not the water particles.

The regular wave may thus be modeled:

$$C = G/w_i$$

$$(V-5)$$

$$Lambda = 2*Pi*C/w_i$$

$$= 2*Pi*G/w_i^2$$

$$(V-6)$$

where $w_i$ is the incident wave frequency, Lambda is the wavelength, and G is the gravitational acceleration. The wave surface is:

$$A(x,t) = A_0*cos(2*Pi*x/Lambda+w_i*t)$$

$$= A_0*(cos(w_i*x/C)*sin(w_i*t)+sin(w_i*x/C)*cos(w_i*t))$$

$$(V-7)$$

after substitution of Equations (V-5,6), and the appropriate trigonometric identities. The frequency experienced by the craft, however, is the encounter frequency:

$$w_e = w_i * (C - V*\cos(\text{Beta}))/C$$

$$= w_i - w_i^2 * V * \cos(\text{Beta})/G$$

<div align="right">(V-8)</div>

where V is the craft velocity and Beta is the angle of craft heading with respect to the advancing wave front, Beta=0 degrees corresponding to the craft and wave front travelling in the same direction (following seas).


C.  WAVE FORCING FUNCTIONS


Wave action introduces a vertical force in heave and a moment about the center of gravity in pitch.

It is assumed that:

1.  wave generated forces and moments are due solely to the net additional hull volume submerged by the wave;

2.  that the wave does not exist within the plenum.

These assumptions appear justified due to the small magnitude of waves considered, the large inertia of the craft, and the filtering action of the bowseal.

The waveheight as a function of the x-location along the hull and time t may be described by:

$$Wvht(x,t) = Wvht * \sin(w_e*t + 2*Pi*x/Lambda)$$

$$= Wvht * \left[ \sin(w_e*t) * \cos(x*w_i/C) \right.$$

<div align="center">87</div>

$$+\cos_e(w*t)*\sin(X*w_i/C)\Big]$$

<div align="right">( V- 9)</div>

after substitution from equations (V-5) and (V-6) and the appropriate trigoncmetric identities. As shown by Fig 15, the differential volume of both sidewalls immersed by the incident wave at time t is:

$$dV(x,t) = (1/2)*Wvht(x,t)*2*Ws*dx$$

<div align="right">( V-10)</div>

and the differential heave force at time t is:

$$dHbuoyw(x,t) = -Rho*G*dV(x,t)$$

<div align="right">( V-11)</div>

which may, after appropriate substitution from Equations (V-9,10), be integrated analytically from stern to bow as:

$$Hbuoyw(t) = -2*Rho*G*(C/w_i)*Wvht*\sin(w_i*L/(2*C))*\sin_e(w*t)$$

$$= HBUOYW*\sin_e(w*t)$$

<div align="right">( V-12)</div>

The differential moment due to the differential volume submerged by the incident wave at time t is:

$$dPbuoyw(x,t) = Rho*G*(x-Xcg)*dV(x,t)$$

$$= Rho*G*(x-Xcg)*Wvht(x,t)*Ws*dx$$

<div align="right">( V-13)</div>

which integrates from stern to bow as:

$$Pbuoyw(t) = 2*Rho*Ws*G*Wvht*\cos(w_e*t)*$$

$$((C/w_i)^2*\sin(w_i*L/(2*C))$$

$$- (C*L/(2*w_i))*\cos(w_i*L/(2*C)))$$

$$+Xcg*Hbuoyw(t)$$

$$=PBUOYW*\cos(w_e*t)+Xcg*HBUOYW*\sin(w_e*t)$$

$$( V-14)$$

A particular note of caution should be introduced at this point with regard to the integrals for wetted area and wetted moments along the hull; the integrals of these functions vanish for certain $w_i$. Specifically, for heave, Equation (V-12) vanishes for all time t when:

$$w_i^2*L/(2*G) = n*Pi$$

$$w_i = (2*n*Pi*G/L)^{1/2}, n=1,2,3,...$$

$$( V-15)$$

The pitch integral will likewise vanish for all time t if, for a value of n such that equation (V-12) is zero, the transcendental equation obtained by substitution of equation (V-15) into equation (V-14), and equating the latter to zero:

$$\tan((n*Pi*G*L/(2*C))^{2\ 1/2}) = (2*n*Pi*G/(L*C))^{2\ 1/2}$$

$$( V-16)$$

is also satisfied. Thus the frequency response of the craft should exhibit a certain ripple effect as these critical frequencies are passed.

The two previously-defined wave integrals HBUOYW and PBUOYW make up a two-dimensional B vector which couples the wave force onto the C.G. acceleration and pitch acceleration state variables, from the two forcing functions, $U_1 = \sin(w_e t)$ and $U_2 = \cos(w_e t)$. However, it is convenient to redefine this relationship in terms of a single forcing function since the sine and the cosine are related through the derivative. In order to facilitate this relationship, the state matrix is augmented with a dummy state variable:

$$\dot{x}_{10} = \frac{d}{dt}(U_2) = -w_e * (PBUOYW/Iyy) * U_1$$

$$( V-17)$$

Thus the new state $x_{10}$ represents, after integration, the control $U_2$, multiplied by the appropriate $B(w_e)$ vector terms of PBUOYW/Iyy. Note that if a time domain solution of wave forcing action were desired, a new initial condition would be required, representing the initial wave buoyant moment; however, that does not enter into the solution in the frequency domain. The resulting state equations are shown in Fig 16. As has been previously discussed, the frequency response may now be computed for any frequency:

$$G(jw)_e = \left| \left| jw_e * I - A \right|^{-1} * B(w)_e \right|$$

$$( V-18)$$

where $G(jw_e)$ is the column vector of gains for each state variable.


D.  FREQUENCY DOMAIN SOLUTION


The previously-defined state equations were solved in the frequency domain utilizing a CSMP III computer simulation which appears at the end of the text.  This simulation was based around the initialization portion of the time domain solution described in earlier chapters; however, rather than a call to integration in the Dynamic portion of the model, the CSMP III reserved variable TIME was used only as a stepping variable to generate 50 frequencies between $w_0$ and $w_{max}$, the specified minimum and maximum frequencies respectively, such that:

$$w_e = w_0 * e^{Delw*TIME}$$

$$(V-19)$$

where Delw was defined such that when TIME =1.0, $w_e = w_{max}$. The incident wave frequency then becomes, for ahead seas, the positive solution to the quadratic Equation (V-8), with cos(Beta)=-1.  The influence coefficients about the steady-state operating point from the initialization portion were copied onto a complex matrix Ajw, the $|jw_eI-A|$ matrix, and the B vector for that particular incident wave frequency computed. The International Mathematical and Statistical Libraries (IMSL) subroutine LEQT2C, complex linear simultaneous equation solution, was used to compute the

91

vector of gains:

$$G(jw)_e = |jwI-A|_e^{-1}*B(w)_e$$

$$(V-20)$$

and the resultant absolute values of $G(jw)_e$ were plotted against the encounter frequency $w_e$ as decibels with respect to the unit waveheight for heave, heave rate, and heave acceleration, and with respect to the waveslope, $w^2/G_i$, for pitch, pitch rate, and pitch acceleration. Note that this is a linear system; accordingly, variations in waveheight do not affect this model's response characteristics, as was true of the non-linear Loads and Motions program in ref |1|.


E.  COMPARISON WITH LOADS AND MOTIONS PROGRAM


    Booth in ref |1| studied the frequency response of the XR-3 Loads and Motion program in response to seas developed by the WAVES subroutine. It is of interest to compare the linear system developed in this study with the results of ref |1|. Duplicating his work, three runs were made representing ahead seas, cross seas and following seas at 10, 20 and 30 kts and a comparison made with his results. Merged plots of pitch and heave were obtained for each speed condition for encounter frequencies varying from 1 to 25 rad/sec. In addition, Cal-Comp plots of pitch and heave were obtained as functions of the ratio of craft length to wavelength. Initial conditions and craft parameters selected for initialization were identical to those selected

92

for the previous chapter with regard to time-domain validation.


1. Ahead Seas Run


Fig 17 to Fig 22 show plots of linear system response in heave and pitch for 10, 20 and 30 knot runs into ahead seas, alternating with plots reproduced from ref [1], representing identical runs done by Booth with the smallest wave amplitudes. These were selected as representing the most nearly-linear mode of operation of the Loads and Motion program in sea-state. One may observe the general similarity of the two simulations, with the speed-dependent resonant peak of heave in the linear model varying from an encounter frequency of 3.39 rad/sec at 10 knots , to 6.45 rad/sec at 30 kts, while the non-linear system varies from 4.0 to approximately 5.0 rad/sec. The frequency interval of the non-linear study was considerably coarser than that utilized in the linear model, 1 rad/sec vs. less than .1 rad/sec. The linear system is significantly less responsive than the Loads and Motions program, by 11 dB in heave and 6 dB in pitch. This is attributed to the absence of wave-plenum chamber interactions with the plenum pressure $Pb_{bar}$, and indicates that the presence or absence of significant wave action within the plenum chamber is an area of considerable impact on the response of the craft, and should be included in future studies.


The linear system is quite sharper in its resonant peak in pitch, as should be expected from the significantly reduced pitch damping previously demonstrated by the linear model in the time domain validation. This accounts in part for the tendency of the linear model to decrease in response slightly from an encounter frequency of 1 rad/sec, until just before the onset of resonance, unlike the Loads and

Motions data; the half-power points in the Loads and Motions frequency resonance are more widely separated than are those of the linear system, and this in part also accounts for this difference.

The linear system shows the distinctly periodic frequency response predicted, with a sharp null occurring at incident wave frequencies, $w_i$ of 3.14, 4.4, and 5.38 rad/sec. These frequencies correspond to a value of n, in eqn (V-15), of 1, 2 and 3. These nulls are quite sharp, and are not as well defined in the Loads and Motions studies due to the coarser frequency resolution, but are nonetheless visible in all runs.

The Loads and Motions studies also demonstrate an interesting form of non-linear response with regard to resonant pitch frequency. For small wave amplitudes, less than .1 ft, the Loads and Motions resonant pitch frequency varies with craft speed in nearly an identical manner with the linear system, with the slight exception of the 30 kt study; however, the only available data for that run was at a wave amplitude of .2 ft. For wave amplitudes greater than .1 ft, the resonant peak occurs at a frequency of 4 rad/sec, regardless of craft speed. A tentative explanation for this behavior is herein advanced: as the craft resonant frequency is approached, bowseal gapping commences for the larger wave amplitudes, with attendant loss of plenum airmass; the loss of seal force and plenum pressure cause the craft to settle back into the water, but a fixed amount of time must elapse before the fans can replenish the plenum airmass and restore normal system operation. Thus the 4 rad/sec period observed for larger wave amplitudes represents the fastest time (.66 sec) over which gapping can occur and the fans sufficiently replenish the airmass to

94

permit it to recur. This non-linear response is somewhat analogous to a relaxation oscillator, and represents an interesting area for future study, as such a non-linearity might easily be modeled in the Nyquist plane, utilizing the modified Nyquist stability criteria to predict this non-linear behavior.

a.  10 Kts Ahead Seas

Figs 17 and 18 show the superimposed heave and pitch response of the linear and Loads and Motions program, respectively, for an ahead-seas run at a craft velocity of 10 kts. The linear model represents the response of the craft in heave and pitch at 50 discrete frequencies ranging exponentially from 1.0 to 25.0 rad/sec. The non-linear data reproduced from ref [1] represents 8 discrete frequencies over that same range at 1.0, 2.0, 3.0, 4.0, 5.0, 6.0, 8.0, and 10.0 rad/sec, at a waveheight of .2 ft. Although this waveheight was the smallest used by Booth for runs at these speeds, it is still sufficiently large to excite the aforementioned non-linear response. This behavior makes itself manifest as the 4.0 rad/sec resonance in pitch, compared with 3.39 rad/sec for the linear model. The Loads and Motions program shows, for small weight disturbances at these speeds, a natural pitch period of 1.64 secs, or 3.7 rad/sec. As previously noted, the magnitude of the linear system pitch response agrees fairly well, within 3 dB, of the non-linear Loads and Motions data, with a sharper peak due to the lighter linear damping; the heave magnitudes differ considerably, by -15 dB, due to the absence of plenum waves in the linear system.

With the exception of the heave magnitude difference and the shift in resonance due to the non-linear behavior, the shape of the heave response curves of the two

95
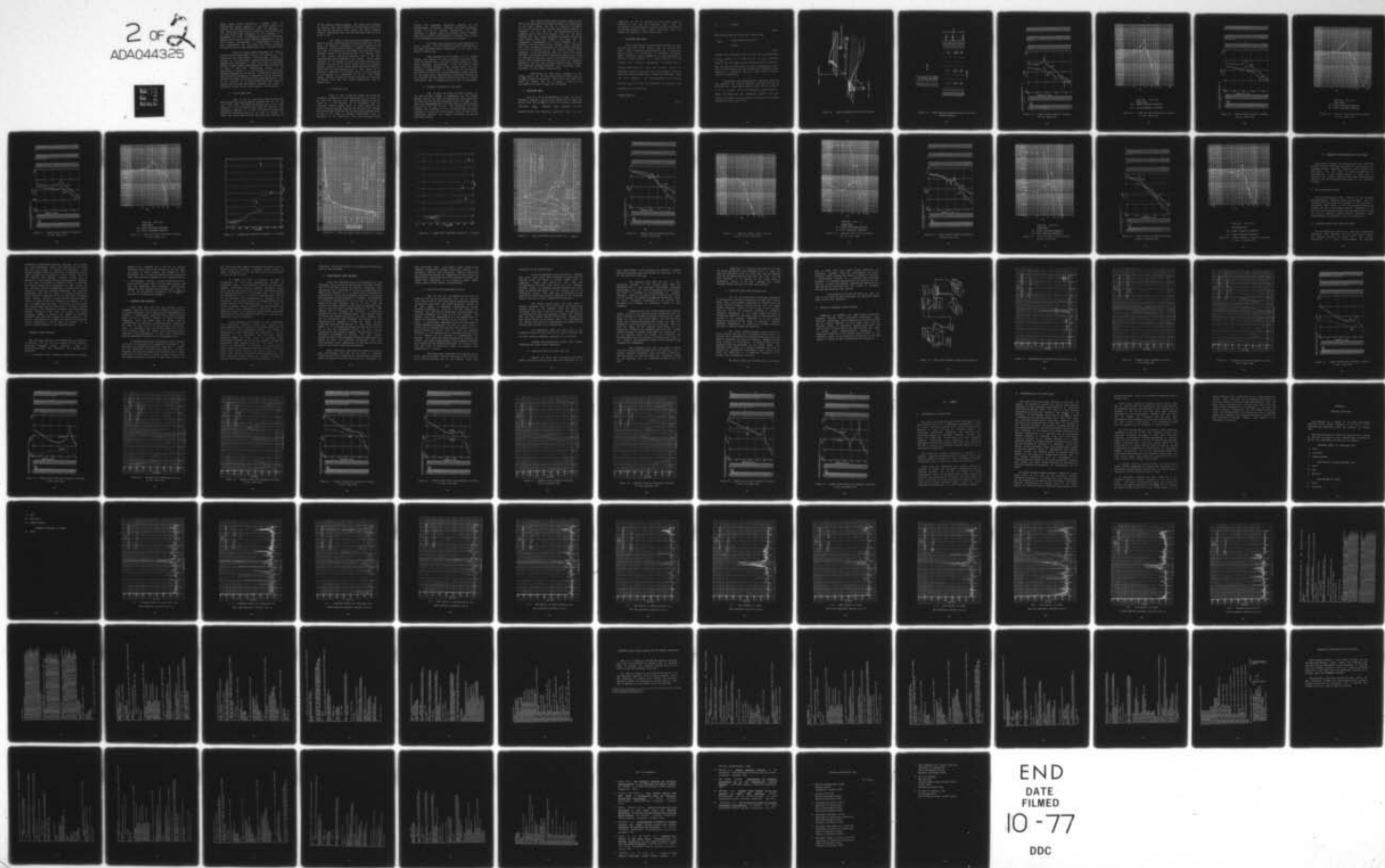
models compare quite favorably. A shallow null, of undetermined origin, appears in both heave curves at 3.0 rad/sec, just slightly before the onset of resonance. A very sharp null occurs at 8.36 rad/sec in both models; this is at an incident wave frequency of 3.15 rad/sec, or a wavelength of 20 ft. As predicted by Equations (V-15,16), further nulls occur at a wave incident frequency of 4.46 and 5.58 rad/sec, corresponding to wavelengths of 10 and 6.6 feet respectively, but the Loads and Motion encounter frequencies did not range sufficiently high to observe them.

Pitch also shows general agreement; but Booth's Loads and Motion data shows a null at 6.0 rad/sec, vs. 11.54 rad/sec for the linear system. This null may, however, be related to the non-linear response previously described, representing a frequency at which the phase relationship between plenum airmass replenishment and pitch buoyancy due to waves is such that cancellation occurs. It is suspiciously located at a 3/2 multiple of the non-linear response frequency of 4.0 rad/sec. In addition, Booth noted this identical discrepancy in comparison with the linearized Aerojet XR-3 model; the Aerojet model also predicted a null in the vicinity of 12 rad/sec, which Booth was unable to observe with the Loads and Motions program, but which is distinctly visible in the linear model at 11.54 rad/sec.

b. 20 Kts Ahead Seas

Figs 19 and 20 show the linear and Loads and Motions heave and pitch frequency response for a 20 kt run into ahead seas. The Loads and Motions data is for a wave height of .1 ft and is more nearly linear in behavior than previously observed at 10 kts. The range of frequencies spanned by the linear system is the same as before; the Loads and Motion data includes two additional points at 15

96

and 20 rad/sec in heave response. The linear pitch response
is smaller than that observed at 10 kts, being about 6 dB
less than the non-linear data, while the heave response
remains consistently less than the non-linear data by 12 dB
as at 10 kts.

The shape of the two sets of frequency response
data is in quite good agreement for these conditions, as the
Loads and Motions is apparently in a nearly-linear mode of
operation. The pitch data shows a distinct flattening at
the peak of resonance in both models, although this occurs
somewhat earlier in the non-linear data (4.0 rad/sec) than
in the linear data(4.68 rad/sec), due to the more
sharply-peaked pitch response of the latter. Both models
resonate at 5.0 rad/sec, and fall off above resonance with
identical roll-offs of 12 dB per octave, after the initially
steeper roll-off of the linear system from peak resonance.
Heave shows the characteristic null in both models at an
encounter frequency of 14 rad/sec; this is a wave frequency
of 3.15 rad/sec, or a wavelength of 20 ft. The linear
system predicts a pitch null at 20.0 rad/sec, but the Loads
and Motions data does not extend sufficiently high to
observe this.

c.   30 Kts Ahead Seas

Figs 21 and 22 show the linear and non-linear
frequency response for a 30 kt ahead-seas run. As in the 10
kt run, the smallest wave amplitude utilized in Booth's
study was .2 ft; however, it is considered that the
nose-down planing moment which is quite strong at high
speeds restrains bowseal gapping, and the Loads and Motions
data represents conditions for the non-linear response which
is just on the verge of becoming established. This is
supported by the observation that pitch resonance occurs

97

between the frequency previously observed as the characteristic non-linear response, and linear resonance, between 4.0 and 5.0 rad/sec; furthermore, the heave resonance is weakly peaked at a slightly higher frequency than pitch response, approximately 5.0 rad/sec, still closer to the predicted linear resonance at 6.46 rad/sec.

The linear model shows still lower magnitudes of pitch response, 6 to 8 dB below the Loads and Motion data. The heave magnitudes remain consistently 12 dB below the Loads and Motion data.

Pitch resonates at 6.46 rad/sec in the linear system, and between 4.0 and 5.0 rad/sec in the non-linear Loads and Motions data. Roll-off in pitch remains the same above resonance, approximately 12 dB per octave in both models, but heave response in both models falls off more shallowly, approximately 10 dB per octave in both models. The heave null due to the 20 ft wavelength is still apparent in the linear model, representing an encounter frequency of 20.0 rad/sec, but the Loads and Motions data did not extend sufficiently high in frequency for this null to be observed.

d.  Frequency Response vs. Wavelength

Figs 23 and 24 are plots of heave response, vs. the ratio of craft length to wavelength for the linear system, and vs. the ratio of wavelength to craft length for the Loads and Motion data reproduced from ref [1]. Both plots are superimposed with the data from all three velocity runs of 10, 20, and 30 kts. The difference in scale selected for plotting in the linearized model precludes crowding at the low end of the x-axis, since the bulk of the frequencies studied, 3.15 rad/sec and above, are shorter than craft length.

The linear system heave response shows distinct
nulls for waves which are integer multiples or submultiples
of the craft length, and may be observed at L/Lambda=
1/4,1.0,2.0, and 3.0; less distinct nodes may be observed at
L/Lambda= 3/2, 5/2, and 7/2. The corresponding nulls at
Lambda/L=4.0,1.0, and .5 are visible in Fig 24, but scale
crowding and the coarser frequency resolution utilized by
Booth render these less obvious. The sharp node at
L/Lambda=.3 corresponding to a wave frequency of 1.75
rad/sec is not the result of the periodic hull integrals;
this wave frequency corresponds to the encounter frequency
of 3.4 to 6.0 rad/sec, and is the craft's natural pitch
frequency. It may be observed, also as a node, in the pitch
response. The natural pitch frequency variation with speed
is obscured in this plot, since as the speed increases, the
natural pitch frequency increases; but this is an encounter
frequency, and the wave incident frequency which produces
this encounter frequency decreases with increasing speed.
Therefore, the two effects nearly cancel.

Figs 25 and 26 show pitch response for the
linear system and the non-linear loads and Motion data of
ref [1], plotted as was heave. Note that the nulls and
nodes are roughly 180° out of phase, a node in pitch
corresponding to null in heave and vice-versa.

2. Cross-seas Runs

Figs 27 to 31 are presentations of heave and pitch
frequency response of the linear system and the Loads and
Motions data from ref [1] at 20 and 30 kts under cross-seas
conditions $(w_e=w_i)$. Comments made regarding the the
ahead-seas runs are generally applicable here, but the

99

comparison of the two systems is in no manner nearly as striking as that for the ahead-seas runs. This is attributed to the significant effects of roll and yaw modes on the craft dynamics under these conditions, which are completely neglected in this linear model.

### 3.  Following Seas Runs

Booth acknowledged little agreement between his work with the Loads and Motion program and the Aerojet XR-3 linear model frequency response curves; this is apparently due to an error in calculating the encounter frequency. Higher frequency waves propagate at a slower velocity, so that for a craft traveling at a given velocity, as the incident wave frequency $w_i$ increases, a frequency will be attained above which the craft will actually outrun the following wave, and plow into such a wave bows-on. Thus the craft will actually experience an ahead-sea condition above that wave frequency. The $w_i$ corresponding to the maximum positive $w_e$ that the craft may experience for following seas (cos(Beta)=1.0) is given by:

$$d/dw_i(w_i-V*w_i^2/G)=0.0$$

(V-21)

100

$$w_i = G/(2*V)$$

<div align="right">(V-22)</div>

Substituting Equation (V-22) into (V-8) yields:

$$w_{emax} = G/(2*V) - (V/G)*(G/(2*V))^2$$

$$= G/(4*V)$$

<div align="right">(V-23)</div>

Incident wave frequencies above or below the $w_i$ corresponding to $w_{emax}$ result in a lower $w_e$, and if $w_i$ is increased sufficiently, past $w_i=G/V$, $w_e$ will become negative, indicating that the craft is overrunning the wave. Accordingly, a great deal of judiciousness must be utilized when interpreting the results of a following seas run, when plotted against encounter frequency $w_e$.

Accordingly, the following-seas frequency spectrum was generated in a manner different from that utilized on previous runs. $W_i$ was varied exponentially over the range of 1 to 25 rad/sec, and the corresponding $w_e$ was calculated. Hence, the results are not comparable directly with the results of Booth, but are presented in Fig 32 to Fig 33 for information only, at v=20 kts.

Figure 15 - WAVE DIFFERENTIAL FORCES AND MOMENTS

Figure 16 - STATE VARIABLE REPRESENTATION OF THE WAVE
FORCING FUNCTION

103

Figure 17 - LINEAR SYSTEM FREQUENCY RESPONSE, 10 KTS, AHEAD SEAS

V=10 kts,    A=0.2 ft,
Ahead Seas

⊡ =   Heave Frequency Response

⊙ =   Pitch Frequency Response

Figure 18 -   LOADS AND MOTION FREQUENCY RESPONSE,
10 KTS, AHEAD SEAS

Figure 19 -  LINEAR SYSTEM FREQUENCY RESPONSE,
20 KTS, AHEAD SEAS
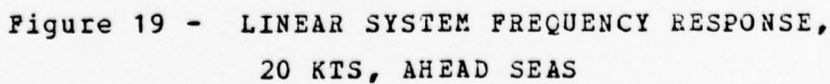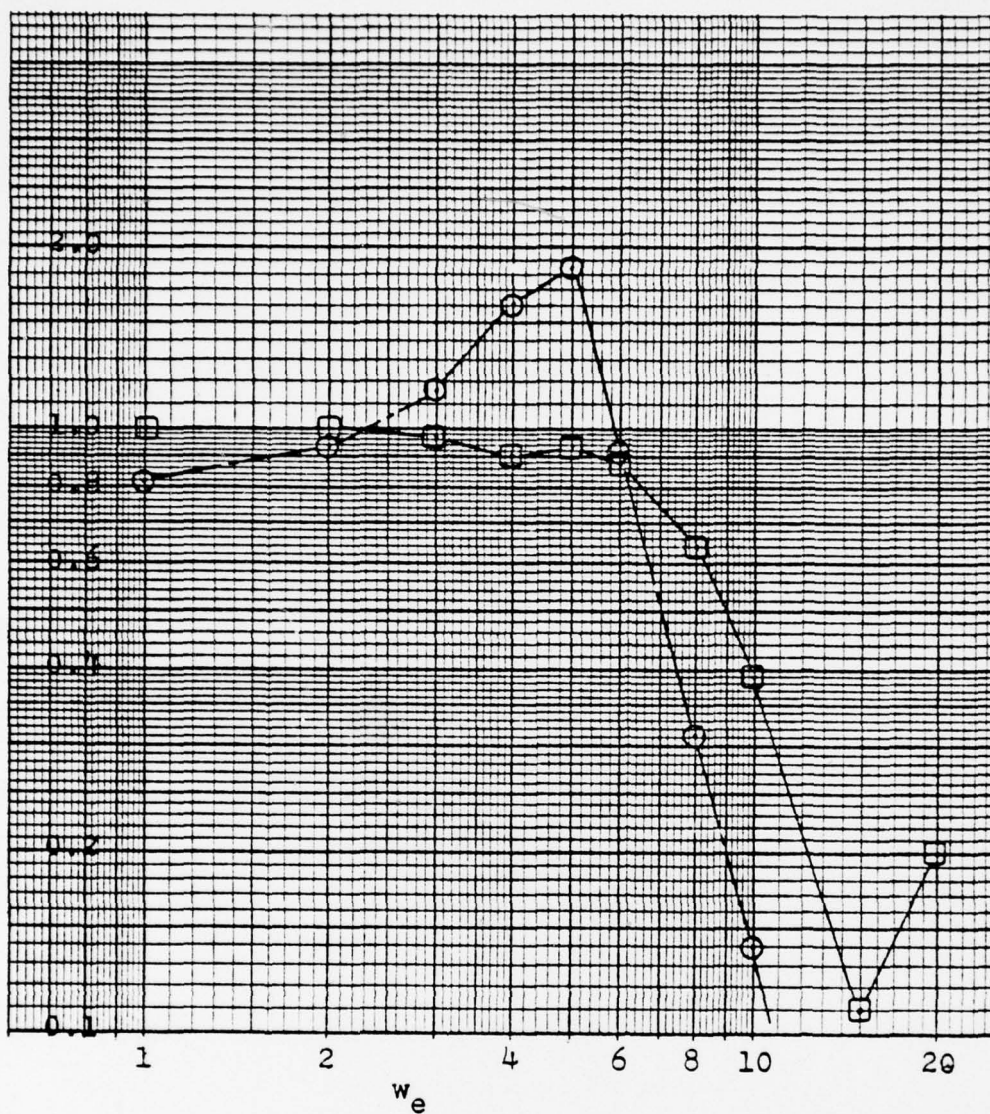
V=20 kts, A=0.1 ft,
Ahead Seas

⊡ = Heave Frequency Response

⊙ = Pitch Frequency Response

Figure 20 - LOADS AND MOTION FREQUENCY RESPONSE,
20 KTS, AHEAD SEAS

107
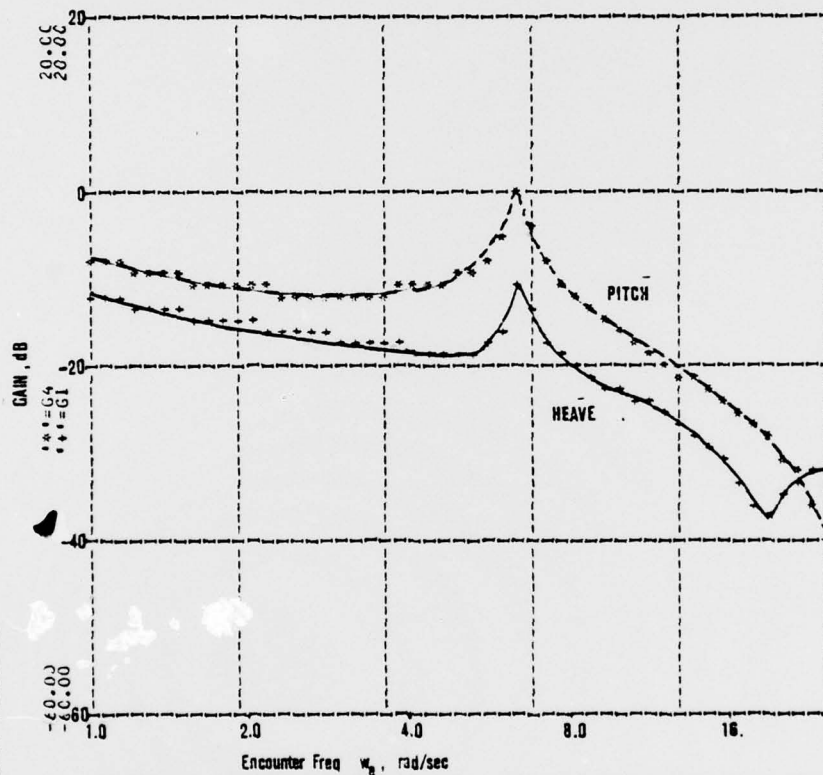
Figure 21 — LINEAR SYSTEM FREQUENCY RESPONSE, 30 KTS, AHEAD SEAS
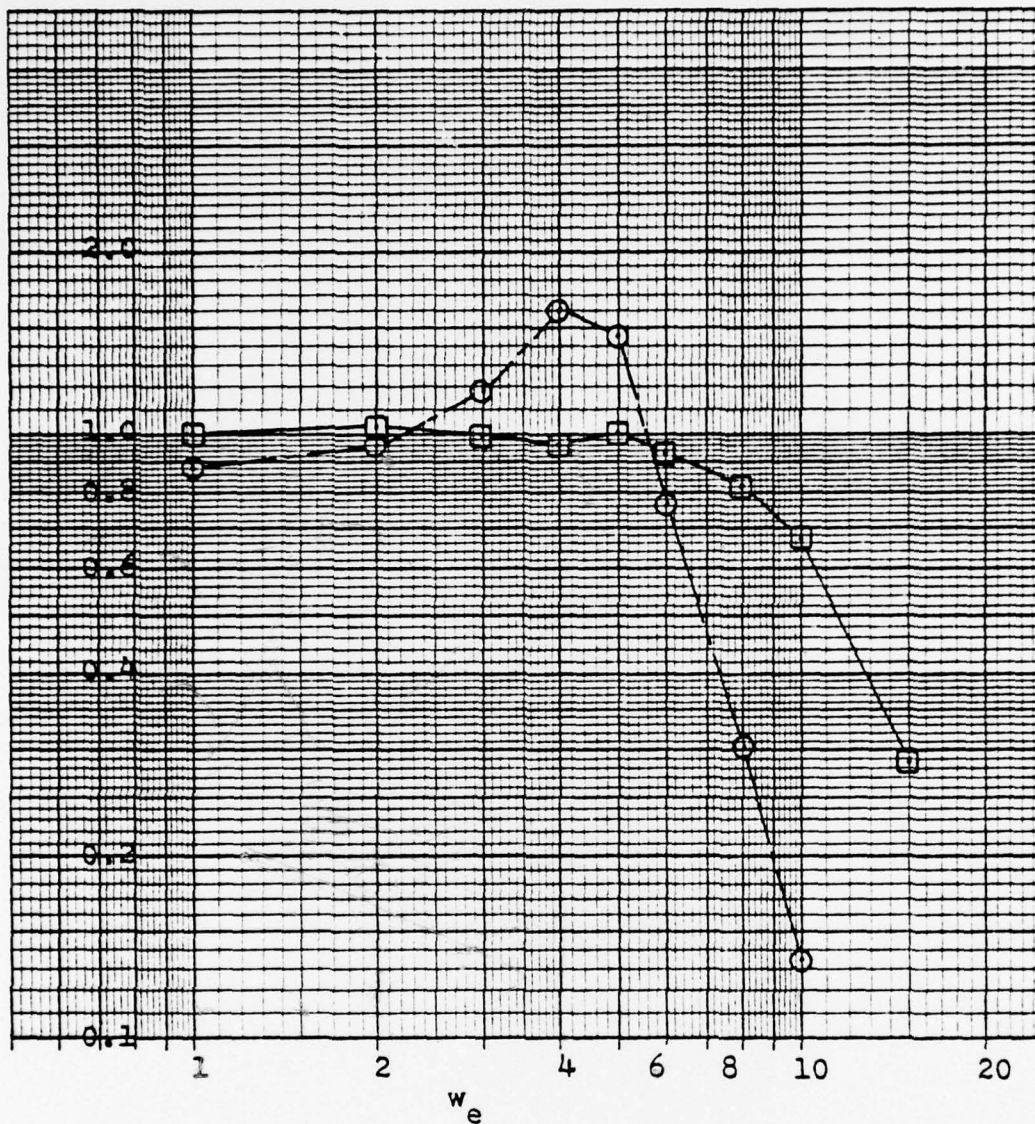
V=30 kts,  A=0.2 ft,

Ahead Seas

▢ = Heave Frequency Response

⊙ = Pitch Frequency Response

Figure 22 -  LOADS AND MOTION FREQUENCY RESPONSE,
30 KTS, AHEAD SEAS

109
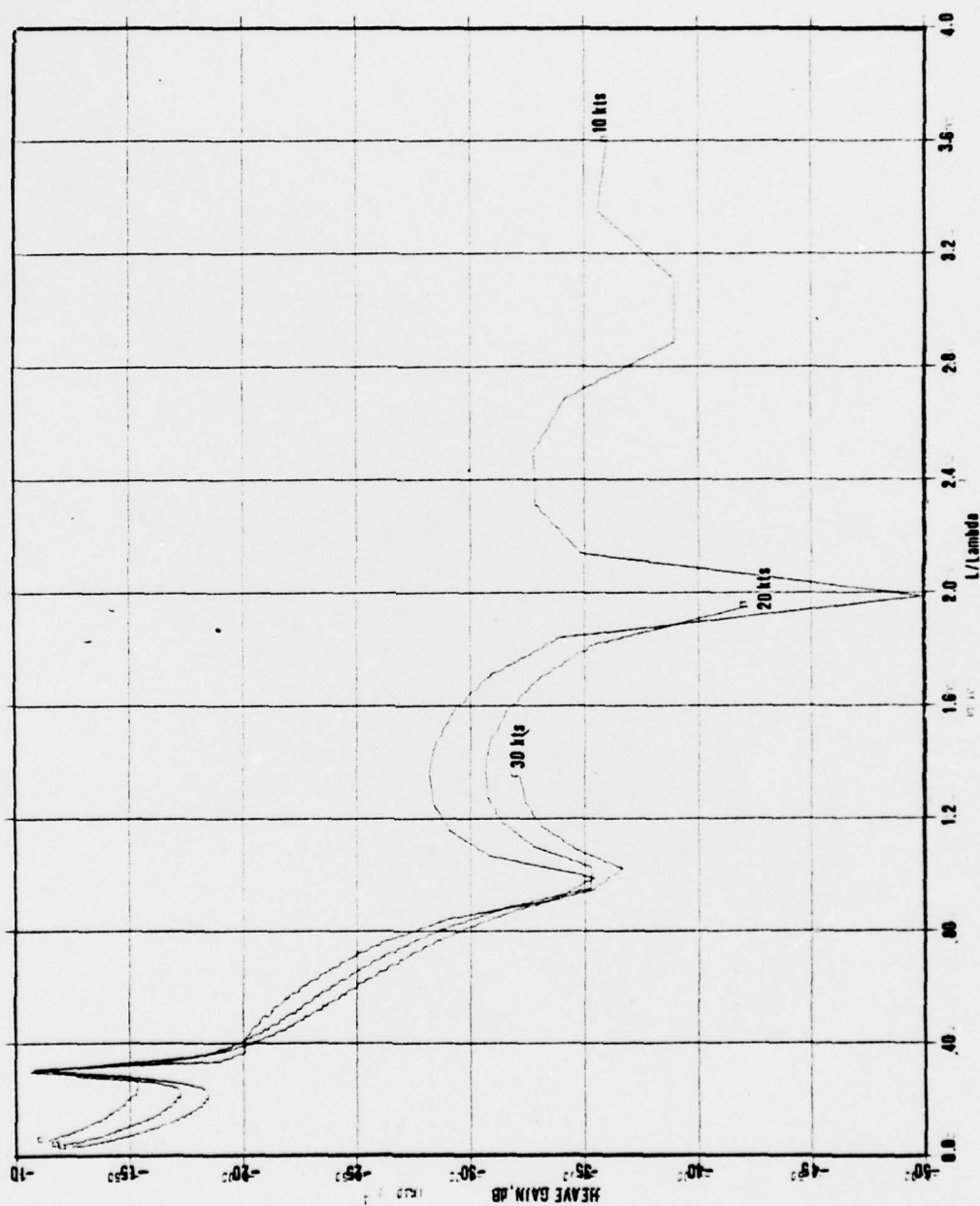
Figure 23 - LINEAR HEAVE FREQUENCY RESPONSE VS. L/LAMBDA

110
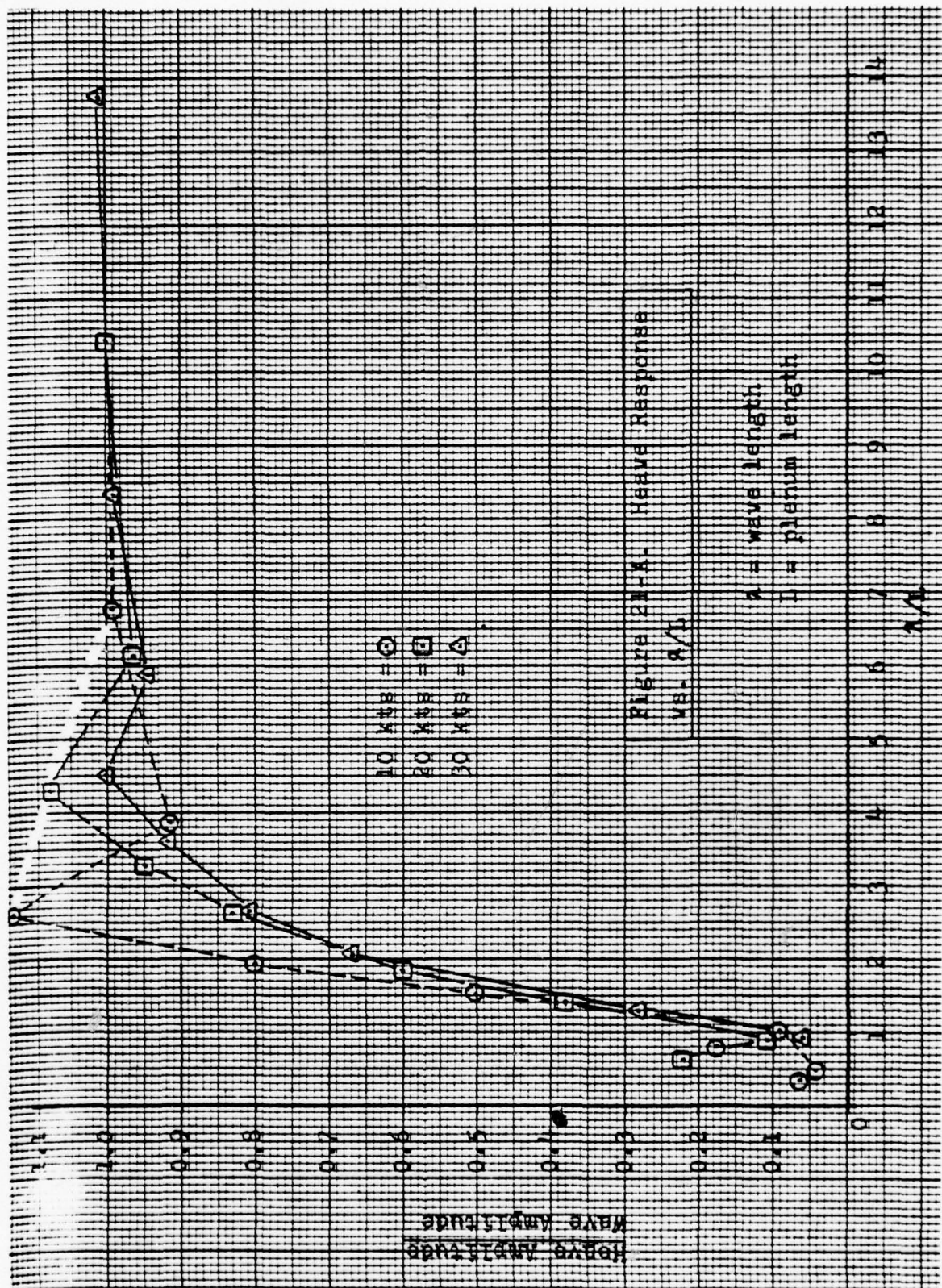
Figure 24 -  LOADS AND MOTION HEAVE RESPONSE VS. LAMBDA/L

111
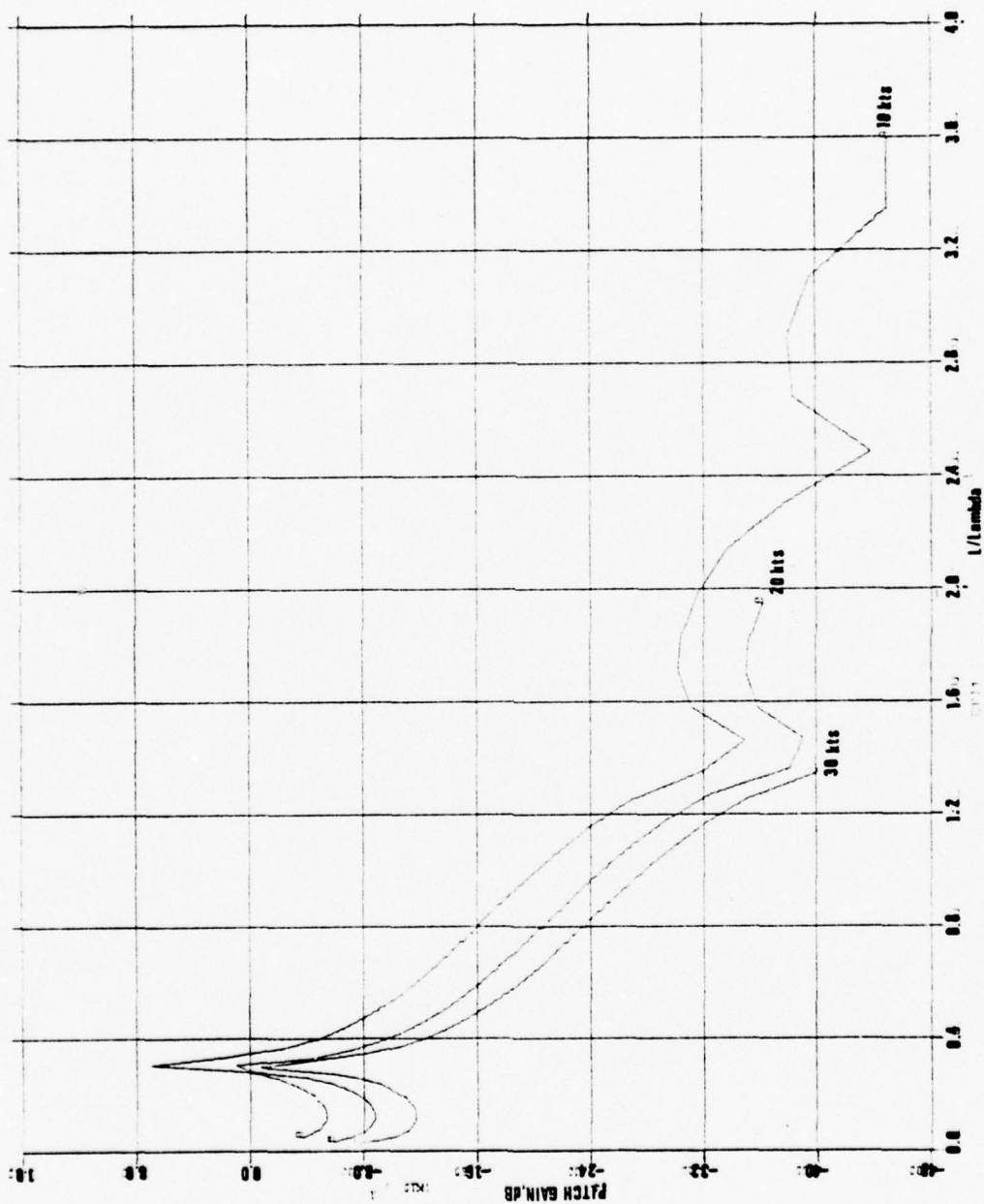
Figure 25 -  LINEAR PITCH FREQUENCY RESPONSE VS. L/LAMBDA
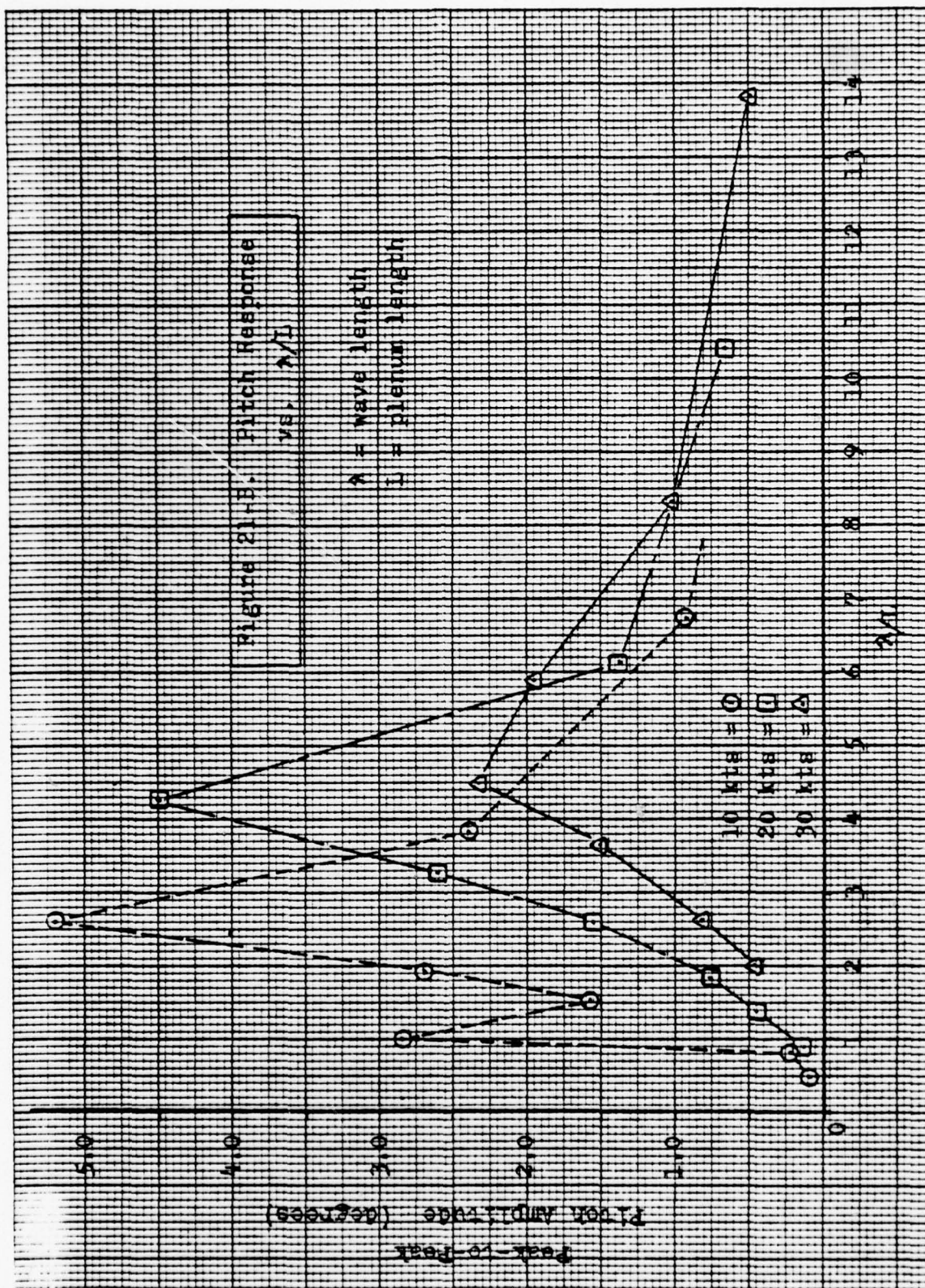
Figure 26 -  LOADS AND MOTION PITCH RESPONSE VS. LAMBDA/L
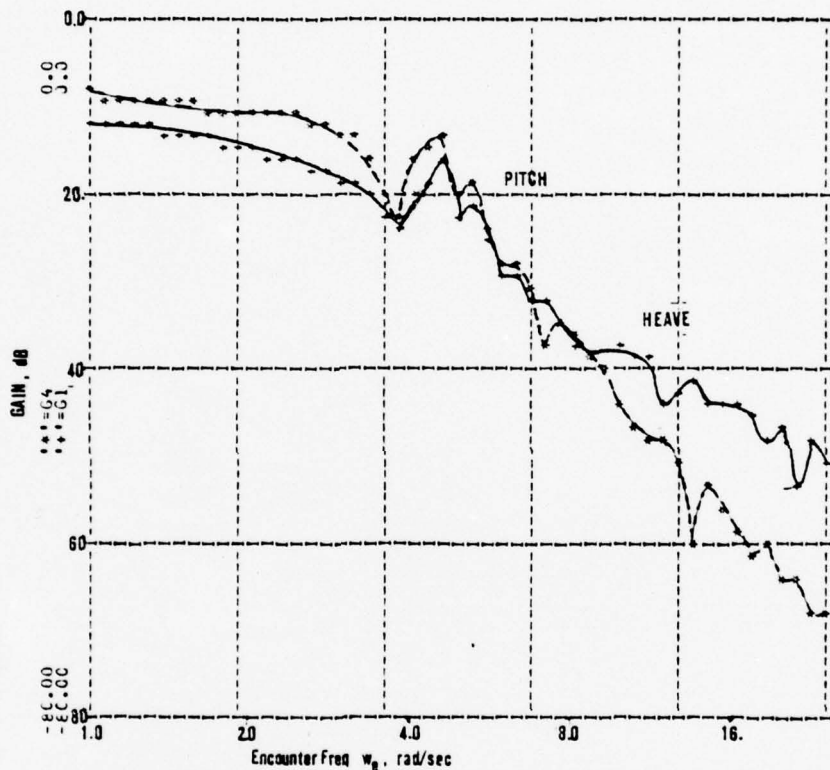
Figure 27 - LINEAR SYSTEM FREQUENCY RESPONSE, 20 KTS, CROSS SEAS
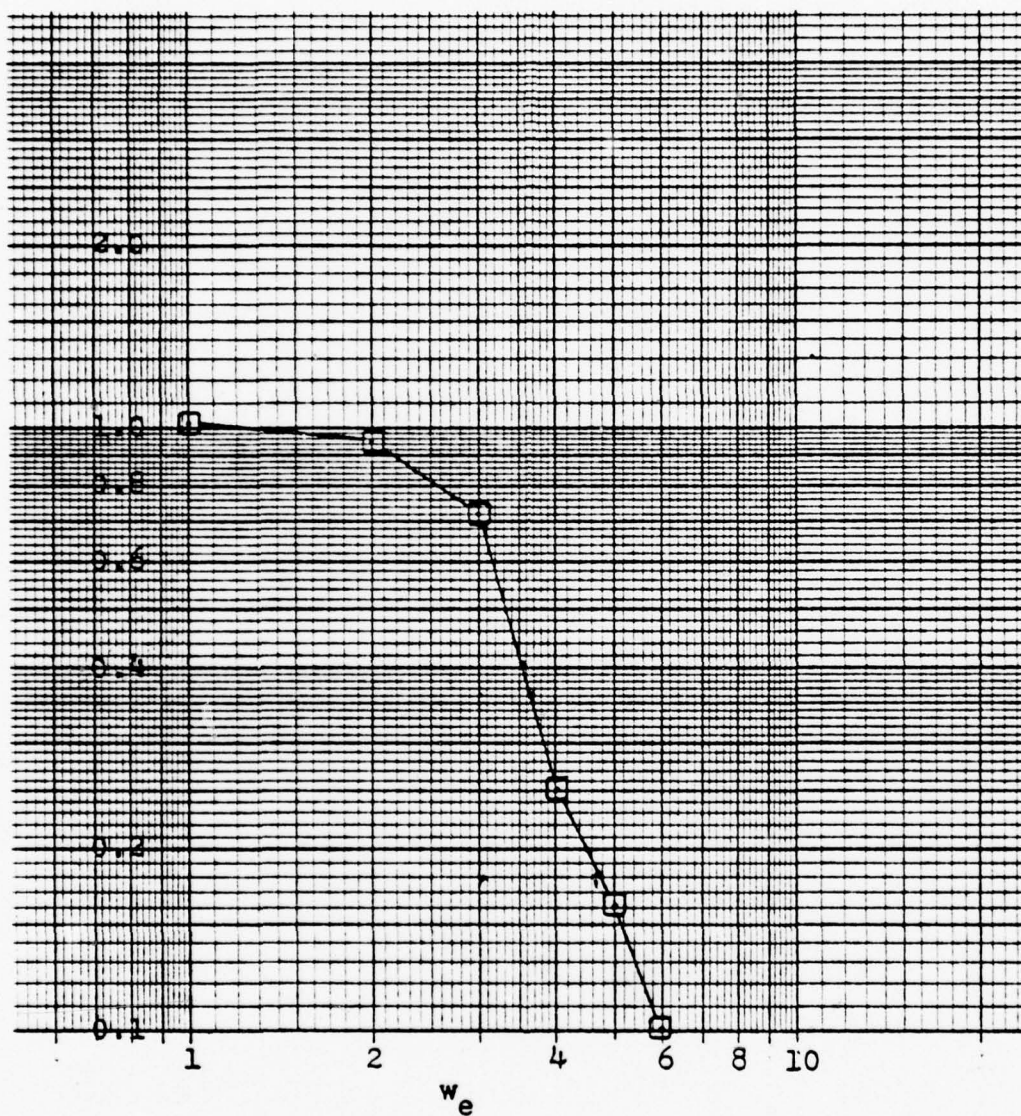
Figure 28 — LCADS AND MOTIONS HEAVE RESPONSE,
20 AND 30 KTS, CROSS SEAS

115
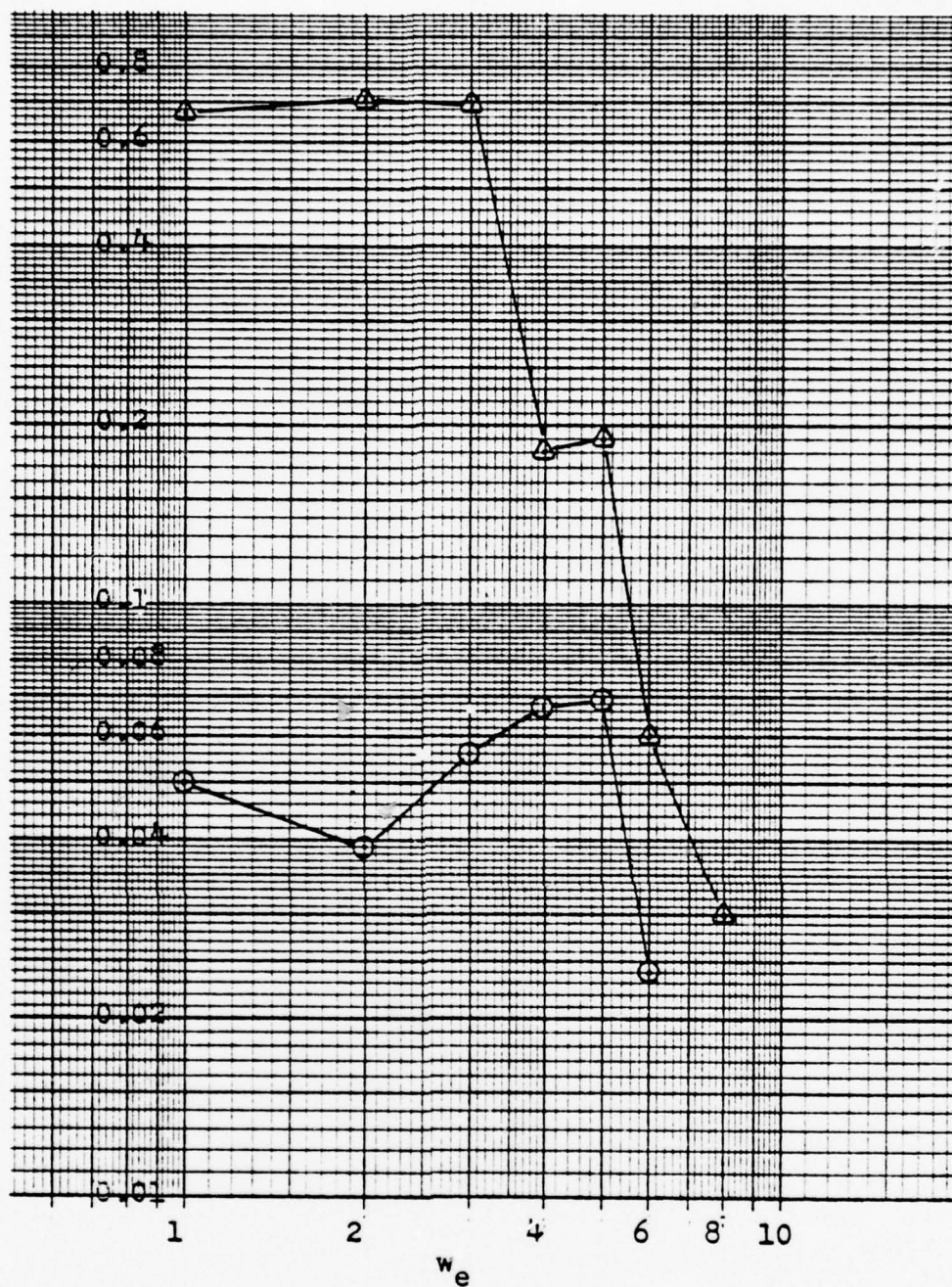
V=20 kts,  A=0.2 ft,

Abeam Seas

⊙ = Pitch Frequency Response

△ = Roll Frequency Response

Figure 29 -  LOADS AND MOTION PITCH RESPONSE,
20 KTS, CROSS SEAS

Figure 30 -   LINEAR SYSTEM FREQUENCY RESPONSE,
30 KTS, CROSS SEAS

117
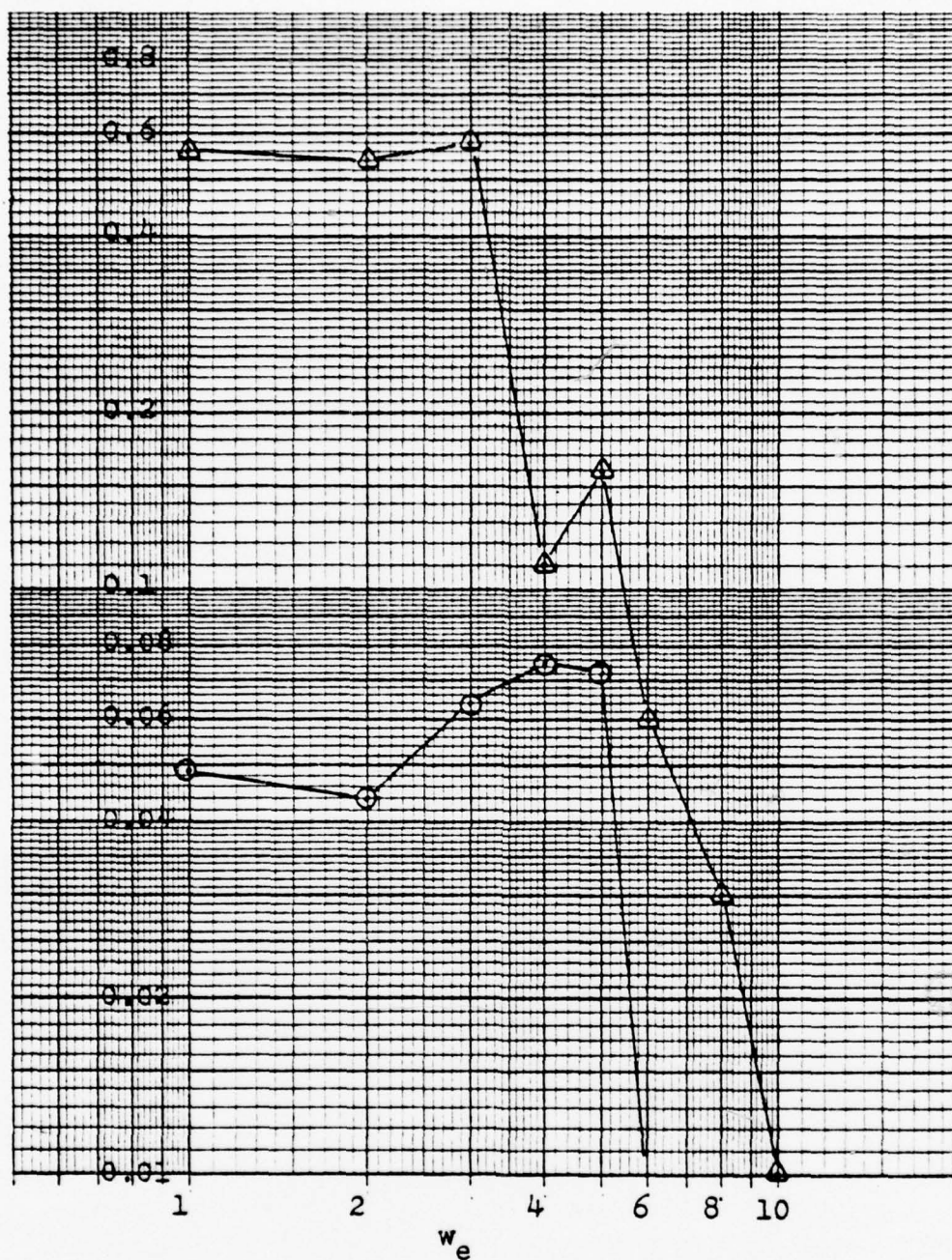
V=30 kts,  A=0.2 ft,
Abeam Seas

⊙ = Pitch Frequency Response

△ = Roll Frequency Response

Figure 31 -  LOADS AND MOTION PITCH RESPONSE,
30 KTS, CROSS SEAS

118

Figure 32 — LINEAR SYSTEM FREQUENCY RESPONSE, 20 KTS, FOLLOWING SEAS

119
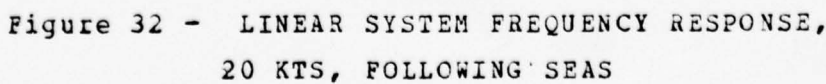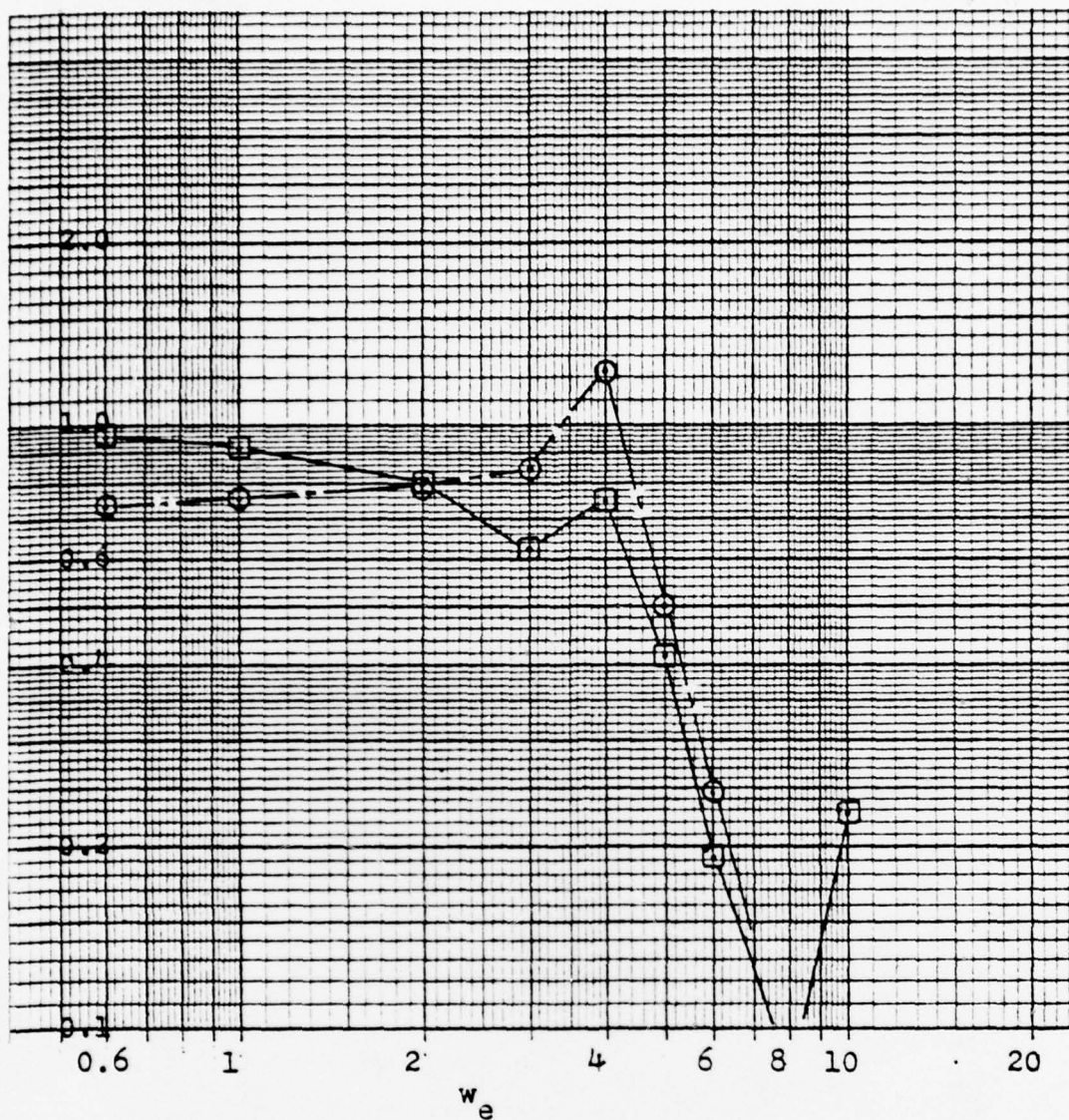
V=20 kts,    A=0.2 ft

Following Seas

⊡ = Heave Frequency Response

⊙ = Pitch Frequency Response

Figure 33 -  LOADS AND MOTION FREQUENCY RESPONSE,
20 KTS, FOLLOWING SEAS

## VI.  FREQUENCY DOMAIN REDUCTION OF XR-3 DATA


This chapter develops the techniques for fast efficient reduction of XR-3 testcraft data from the time domain to the frequency domain. Some more prominent noise sources are identified, and the mode of noise transmission is hypothesized. A very limited amount of pitch data is collected and closely examined using these techniques and compared with the theoretical development of the preceding chapters.


## A.  DATA ACQUISITION SYSTEM


The data acquisition system consists of the standard semi-permanently installed Pemco tape recorder. This is a 14-channel FM tape system, with output 0-1 volt positive. A 19-channel patch panel in the tape recorder compartment, located just aft of the cockpit, permits selection of the data to be recorded; voice edge track recording directly from the craft's radio/ICS system permits relatively simple documentation of experimental runs to be maintained.


## B.  FREQUENCY DOMAIN DATA REDUCTION SYSTEM


The Bio-Engineering Laboratory, Electrical Engineering Department, NPS, Monterey, CA, has a very powerful system for spectral analysis of analog data. This system, consisting of a PDP-11 Mini-computer and Time-Data

Corporation Superpanel-50 Spectrum Analyzer, was utilized for time-to-frequency domain data reduction of the analog tape data. This system is capable of performing a Fast Fourier Transform (FFT) on analog data of magnitudes of $\pm 5V$, from a maximum upper frequency of 10 Hz to 10 MHz, for up to 8094 discrete time samples. However, caution must be exercised to avoid memory overflow and/or program interrupt of the PDP-11 for samples in excess of 2048. In addition, this entire process may be repeated up to 2048 times, and the resultant Fourier coefficients averaged, for further reduction of transient frequency components. The resultant transformed data may be output as Fourier coefficients, power spectral coefficients, and as an amplitude histogram; output devices include a storage CRT and a Hewlett-Packard 7004-B X-Y plotter which will reproduce the display on the CRT on command from the panel. In addition the time domain data being analyzed may be observed on a time-base storage oscilloscope, and monitored throughout the transformation process. Processing times vary, of course, with upper frequency, number of samples, and number of averaging "windows", from less than a second to several minutes. For further information see ref [8], the operating instructions for the Superpanel-50. Fig 34 shows the details of the setup for data reduction to the frequency domain.


C.  FREQUENCY DOMAIN ANALYSIS


XR-3 data was collected on an experimental run conducted 20 January, 1977 at Lake San Antonio for the purpose of performing frequency domain analysis, using the previously-described FFT techniques. Two analyses were performed:

1.  a broad-band noise analysis, examining the frequency

122

spectra of all channels up to 200 Hz, as various suspected noise sources were brought up and shut down, or varied in power setting; the purpose of this experiment was to identify offending noise sources by their characteristic signature in the frequency domain;

2. a low-frequency analysis of craft characteristics in pitch and pitch rate, for 15 kt runs into, across, and with the prevailing wave directions. The frequency spectra of these channels were analyzed from .025 to 25 Hz, for the purpose of comparison with ref [1] and the work of the preceding chapters.

## 1. Wideband Noise Analysis

Noise data from the XR-3 was analyzed over a frequency range up to 200 Hz and 512 samples, averaged over 8 windows; this gave a total sample time of approximately 30 seconds. A Butterworth filter was used to reject signals above 200 Hz to prevent aliasing of higher frequency components into the lower range of interest due to discretization. In addition, a battery/rheostat combination was used to bias out the 1/2 volt offset of the FM tape, since , as previously noted, the FM tape output range is 0-1 volt positive, while the input to the Analog-to-Digital converter of the Superpanel-50 is ±5V; this considerably improves amplitude resolution of the transformed data.

A representative output of frequency spectra appears in Fig 35; the remainder may be examined in Appendix A. The data from all channels are basically identical in nature, and too repetitive to include in the main text. As may be expected, the craft main engines and the 60-Hz power supply contribute the major share of noise. As power is varied, the main engine noise may be observed to vary from 20 Hz to 100

123

Hz, while the power supply contributes significant noise at 55-60 Hz and its harmonics. Following these sources in order of magnitude are the lift fans, which may be observed in the vicinity of 40 Hz.

An attempt was made to ascertain the mode of transmission of this noise, specifically, whether by electrical means, or by mechanical vibration of the sensor package. Accordingly, the gyro package containing pitch, roll, and yaw, and pitch rate, roll rate, and yaw rate gyros was removed and placed on a Ling shaker table, and exposed to vibrations of 1/2 to 1 G, over a frequency range of 5-200 Hz. The RMS shaker table displacement was measured with a calibrated Bentley accelerometer, and compared with the RMS voltage output of the individual gyros. It was hoped to obtain frequency response curves of the gyro packages, but they seemed quite insensitive to vibrations in this frequency range, and the frequency curves showed significant scatter due to the low signal-to-noise ratio. They were not considered worthy of inclusion.

It was concluded, on the basis of this experiment, that mechanical vibration could not transmit such overwhelming amounts of noise as was observed being injected into the XR-3 data collection system. The medium of transmission is thus electrical; this conclusion is further supported by the observation that the eight engines installed aboard the XR-3 have no ignition noise suppressors; likewise, the 60 Hz power supply is unfiltered. Furthermore, while bonding straps run the length of the craft, the possibility of extensive AC ground loops is always present in a non-conducting hull, such as the XR-3. These areas should receive some close scrutiny in the future, for a tenfold reduction in noise injection into the data collection system should be possible, by means of ignition noise suppression, and the installation of .1 uF

capacitors at each AC outlet, at a relatively insignificant cost in time and money.


## 2. Low-Frequency Craft Dynamics

.

Three runs were made during the aforementioned data collection runs, in which pitch and pitch rate were recorded for 15 kt runs into, across, and with the prevailing seas. Qualitative sea conditions at the time of observation were noted as wave heights of 3 to 6 inches, with a wavelength of approximately 6 feet; this wavelength represents an incident wave frequency of approximately 2.2 rad/sec, corresponding to encounter frequencies of 6.2, 2.2, and -1.8 rad/sec, for ahead, cross, and following seas at 15 kts. Data was reduced in a manner similar to that used for wideband noise, with the exception that a maximum frequency of 25 Hz, 1024 samples with no averaging was utilized. A difficulty developed in that a Butterworth filter with cut-off below 100 Hz was not readily available at the time. However, when one is constrained from lowering the bridge, it may nevertheless be possible to raise the river. In this particular case, the tape was run at four times recorded speed, or 7 1/2 inches per second. The FFT was set for 100 Hz, as was the Butterworth filter, and the desired resolution of 1024 samples selected. This procedure had the beneficial side-effect of reducing the real elapsed processing time of the Superpanel-50/PDP-11 combination by a factor of four. The resultant transformed data was scale-expanded after computation, so that only the portion from 0-5 Hz (0-1.25 actual Hz) was plotted.

These admittedly unorthodox and awkward procedures were necessitated, not only by the lack of suitable filtering, but also by difficulties experienced in obtaining proper operation of the PDP-11 for very low frequencies at

that particular time. Long sample times combined with frequent inexplicable program interrupts rendered this particular session most frustrating. However, ventilation and overheating problems were apparently the major source of difficulties experienced with this particular exercise, and future data reductions in the frequency domain should require none of these awkward circumlocutions.

a. Pitch and Pitch Rate-Ahead Seas Run

Figs 36 and 37, the reduced FFT of pitch and pitch rate for the 15 kt ahead-seas run, may be compared with Figs 38 and 39, the linear system theoretical response in pitch and pitch rate. The linear system was plotted as dB with respect to waveslope logarithmically against encounter frequency, on a range of .1 to 7.85 rad/sec. The observed data are relative magnitudes plotted linearly vs. encounter frequency, on a range of 0 to 7.85 rad/sec. The unusual scale was necessitated for the observed data, to obtain the conversion to rad/sec; in Hz, the scale is .125 Hz/in. A qualitative comparison of the two plots shows a rather remarkable similarity; the FFT of pitch shows a falling off in response from the very low frequency end to a local minima at 2.0 rad/sec with the onset of resonance occurring in the vicinity of 2.75 rad/sec; resonance peaks at 3.9 rad/sec and is completed at approximately 5.0 rad/sec. Two small nodes may be observed at 2.36 and 6.28 rad/sec, the latter corresponding to the encounter frequency of the qualitatively-observed wavelength at the time of this run; this was, as previously noted, an incident wave frequency of 2.2 rad/sec.

The linear model replicates the observed data in pitch almost precisely, with the exception of the two nodes at 2.2 and 6.28 rad/sec, due to the dominant local wave

126

amplitudes in the observed data.

As may be expected, pitch rate data is somewhat more noisy than pitch data, although not excessively so. observed pitch rate shows an unusual double peak in resonance, which also occurs in the other two sea-conditions. The first peak occurs at 4.35 rad/sec, slightly higher in frequency than the observed pitch data, while the second peak occurs at 5.25 rad/sec and is of unexplained origin. This peak may be indicative of the onset of the non-linear behavior discussed in the preceding chapter, but that is only a speculative observation.

The linear system pitch rate data shows a sharper resonance than did linear pitch, the former being markedly peaked at 4.26 rad/sec, while the latter was relatively flat from 3.9 to 4.26 rad/sec. The agreement in the sharpness of pitch rate response between the observed data and the linear system is quite good. Resonant rise also occurs earlier in the linear model, at approximately 2.0 rad/sec; but there is no indication of the peak at 5.25 rad/sec which occurs in the observed data.

No significant nodes or nulls occur in this frequency range; the pitch node at n=1( $w_i$=3.15 rad/sec) does not occur until an encounter frequency of 9.75 rad/sec.

Overall, the observed and linear data compare remarkably well under these conditions.

b. Pitch and Pitch Rate-Cross Seas Run

Despite the fact that cross-seas runs induce modes of motion in roll and yaw that are unaccounted for in

127

this linear model, it was considered of interest to compare observed cross-seas data, Figs 40 and 41, with Figs 42 and 43, the linear data for $w_e = w_i$.

The observed pitch FFT, Fig 40, is more distinctly resonant at 4.0 rad/sec under these sea conditions than in the ahead-sea run;response decreases continuously from the very low frequency end until almost the onset of resonance at approximately 3.5 rad/sec. Resonance occurs at 4.0 rad/sec, and a distinct null occurs at 5.25 rad/sec. The observed predominant wavelength, which as noted previously corresponds to an incident wave frequency of 2.2 rad/sec, is distinctly visible at that frequency.

Comparison with the linear system pitch response curves of Fig 42 is as striking as the ahead-seas runs, the more so because of the modes of motion induced in the craft which are not in the linear model. As in the FFT data, linear pitch response decreases until almost the onset of resonance, with a pronounced null at 3.5 rad/sec. This null does not appear in the observed pitch data, but is distinctly visible in the observed pitch rate data. Linear system resonance is sharper under these sea conditions, as is the observed data, and occurs at 4.26 rad/sec. Two high-frequency nulls at 5.25 and 7.0 rad/sec, and a node at 6.0 rad/sec , are distinctly visible in the observed data, although less prominently.

The observed pitch rate data shows a sharper roll-off from the low frequency end of the spectrum, and a flatter response thereafter until the onset of resonance, than does pitch. The distinct double peak previously noted in the ahead-sea run, is distinctly visible in this run also.

128

Comparison of the pitch rate FFT, Fig 41, with the linear system pitch rate response of Fig 43 shows the same good agreement as did the pitch data; the low frequency roll-off characteristics are very much the same, and the null predicted at 3.5 rad/sec by the linear model is prominently visible in the FFT. However, the higher frequency nodes and nulls are much less distinct.

c.  Pitch and Pitch Rate-Following Seas

Due to the difficulties previously experienced in interpreting results of following seas runs with Booth's work, only a most general comparison of observed pitch and pitch rate FFT's, shown in Figs 44 and 45, and the linear system responses, shown in Figs 46 and 47, will be made. Note that due to the technique utilized in generating encounter frequencies in the linear model, the range of frequencies plotted in the linear model is much greater, (.3 rad/sec to -40 rad/sec), resulting in a much coarser frequency resolution in the range of interest. Negative encounter frequencies, as noted in the preceding chapter, represent a modified ahead-sea condition.

The linear system predicts a sharp roll-off in pitch response from the very low frequency end to about -.25 rad/sec, and a relatively flat response from there until the onset of resonance, at about -2.0 rad/sec. Resonance occurs quite sharply at -4.11 rad/sec. No nodes or nulls in this frequency range are predicted by the linear model. The observed pitch data is in general agreement with this; in addition the predominant wavelength, which occurs under these sea conditions at an encounter frequency of -1.8 rad/sec, may be observed in the FFT.

The linear system and observed data do not agree

129

well in pitch rate, the linear system predicting an increasing response from the low-frequency end until resonance, while observed data shows, as should be expected, a low-frequency roll-off to a relatively flat mid-range response. No plausible explanation may be advanced for this variance at this time; however, considerable difficulty has been observed by both Booth and this author in correctly interpreting following seas results.

The observed pitch rate FFT shows, as have the runs in the other two sea conditions, the mysterious double peak in pitch rate resonance.

D. SUMMARY OF FREQUENCY DOMAIN ANALYSIS

Comparison of measured and linear system theoretical frequency response shows significant correlation under small-sea conditions; nulls predicted by the linear system may be readily observed in test craft data, and the frequency domain is relatively uncluttered by noise. The bulk of noise in the system is not "white" noise, but tends to cluster about sharply-defined frequencies. The techniques developed in this chapter show the value of the frequency domain as an interesting alternative to the time domain as a means of model verification and validation.
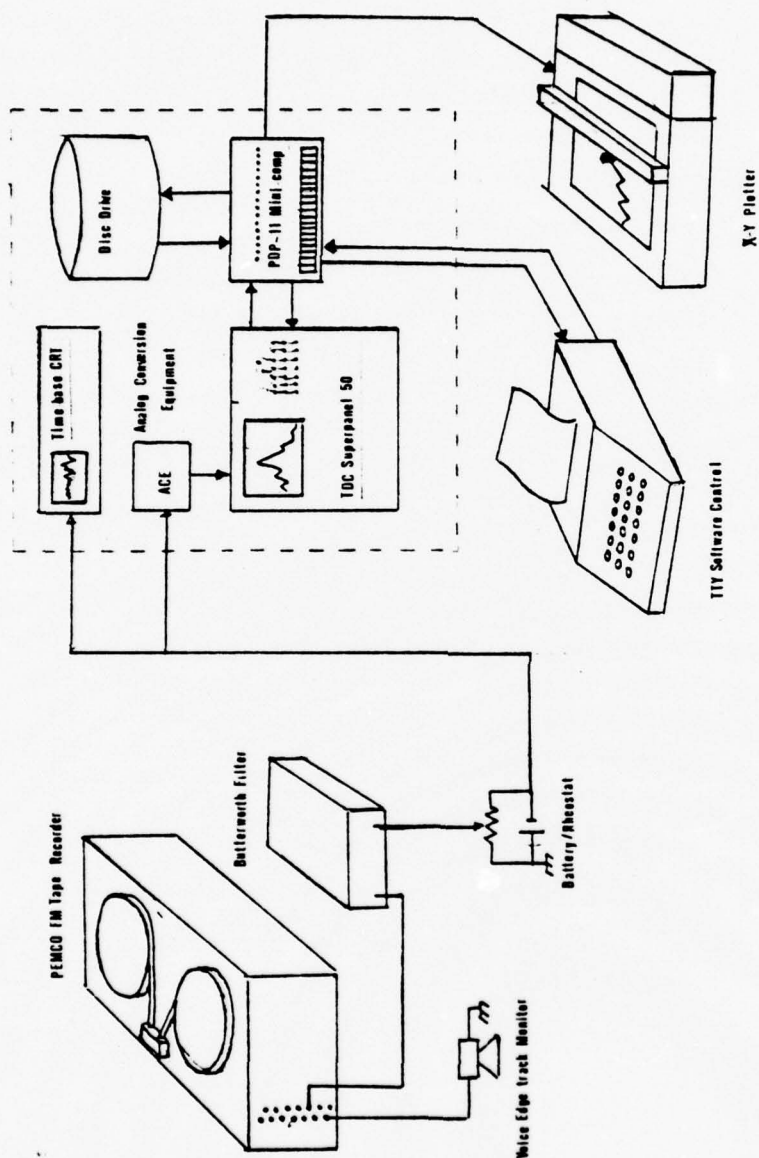
Figure 34 — SETUP FOR FREQUENCY DOMAIN DATA REDUCTION
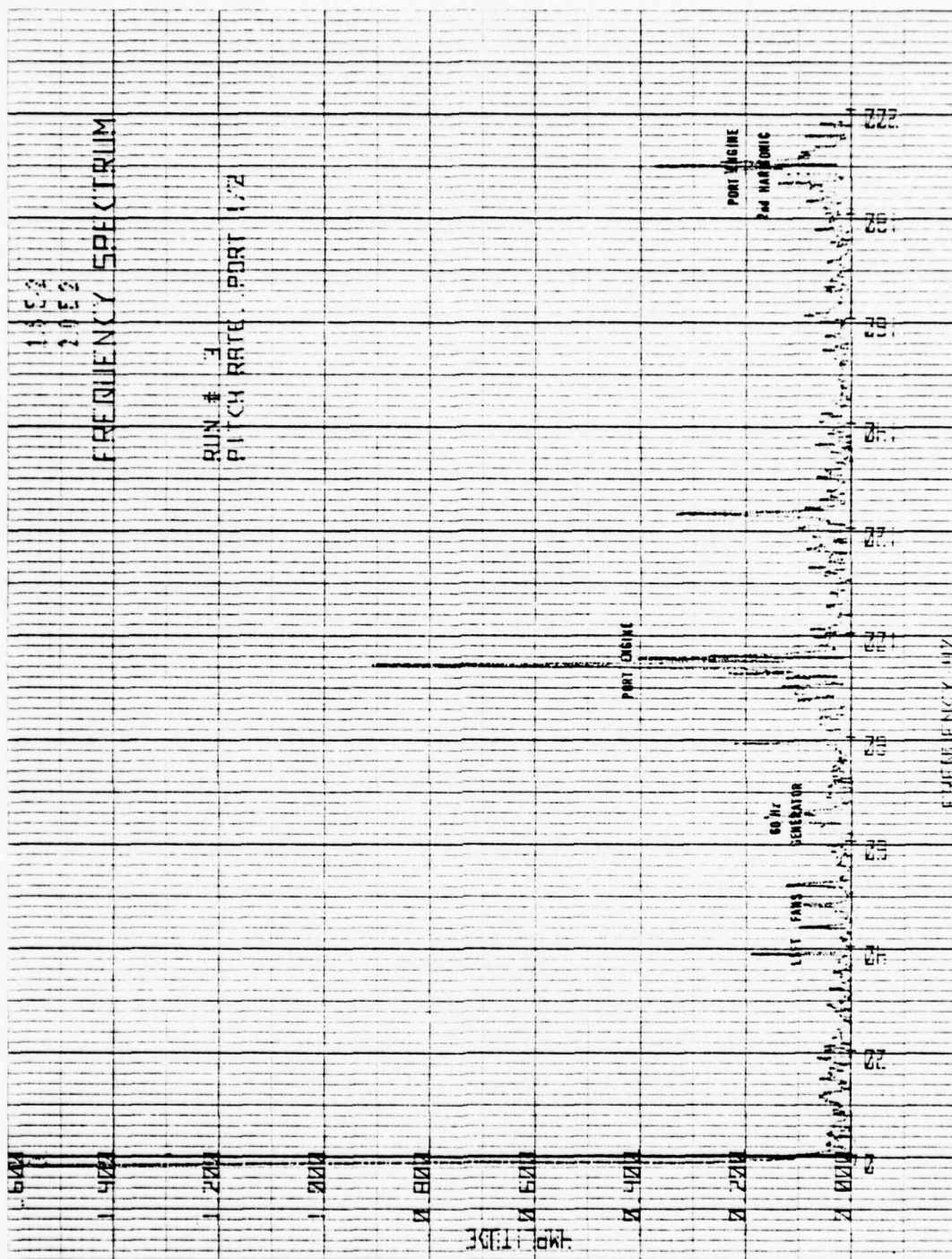
Figure 35 –   REPRESENTATIVE WIDE-BAND NOISE SPECTRUM OF THE
XR-3

132
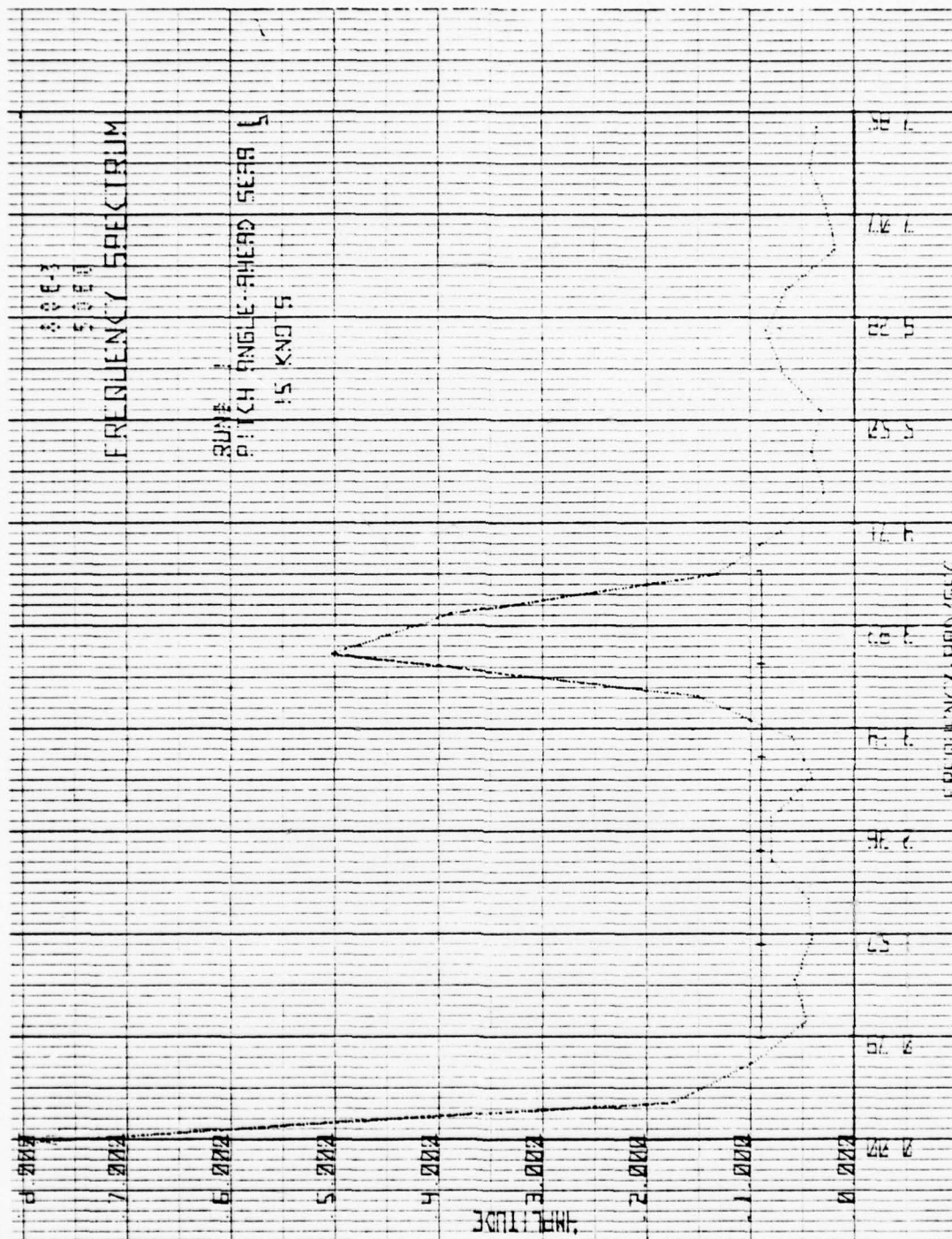
Figure 36 - OBSERVED PITCH FREQUENCY SPECTRUM,
15 KTS, AHEAD SEAS

133
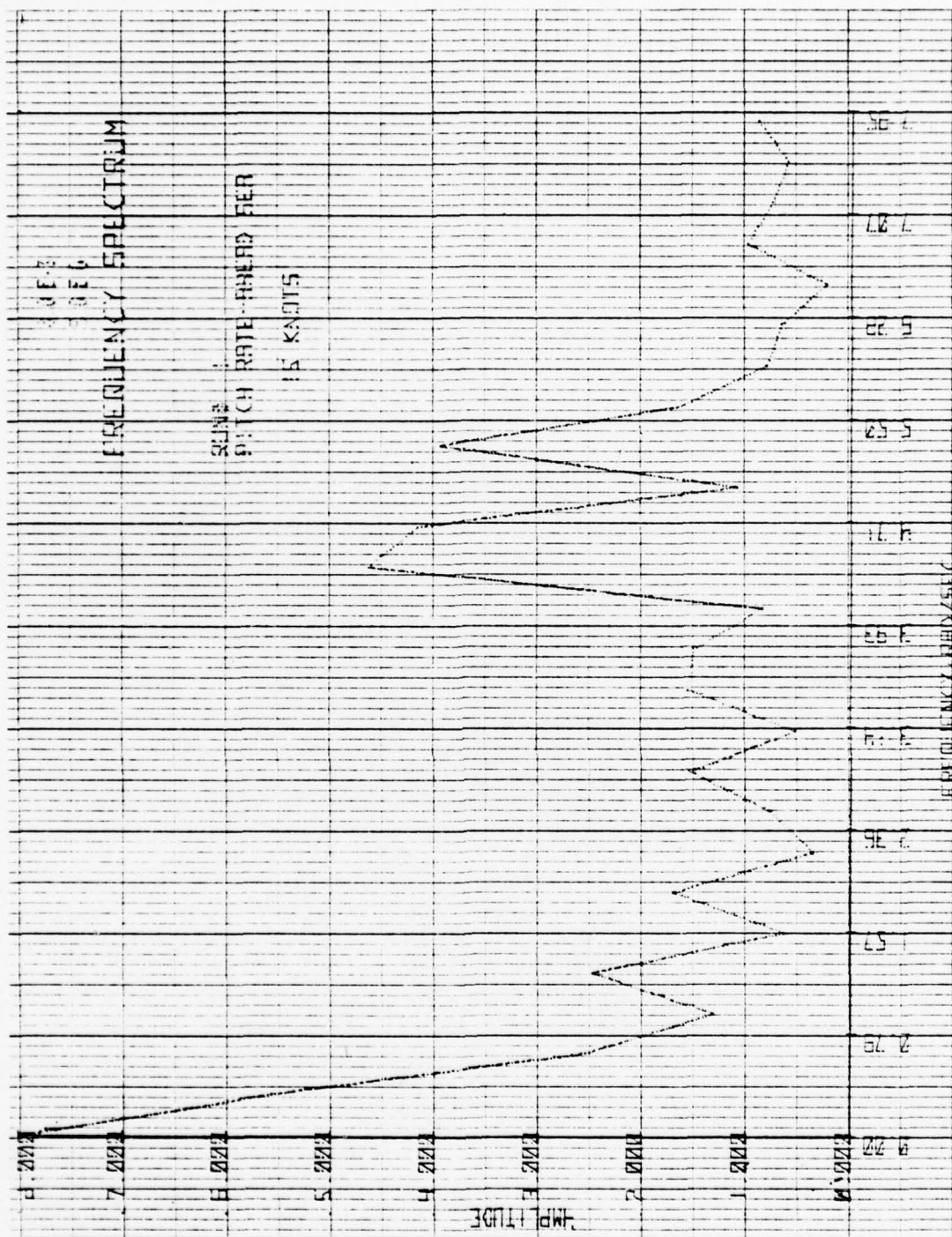
Figure 37 - OBSERVED PITCH RATE FREQUENCY SPECTRUM,
15 KTS, AHEAD SEAS

134

Gain, dB

PITCH

HEAVE

Encounter Freq $w_e$, rad/sec
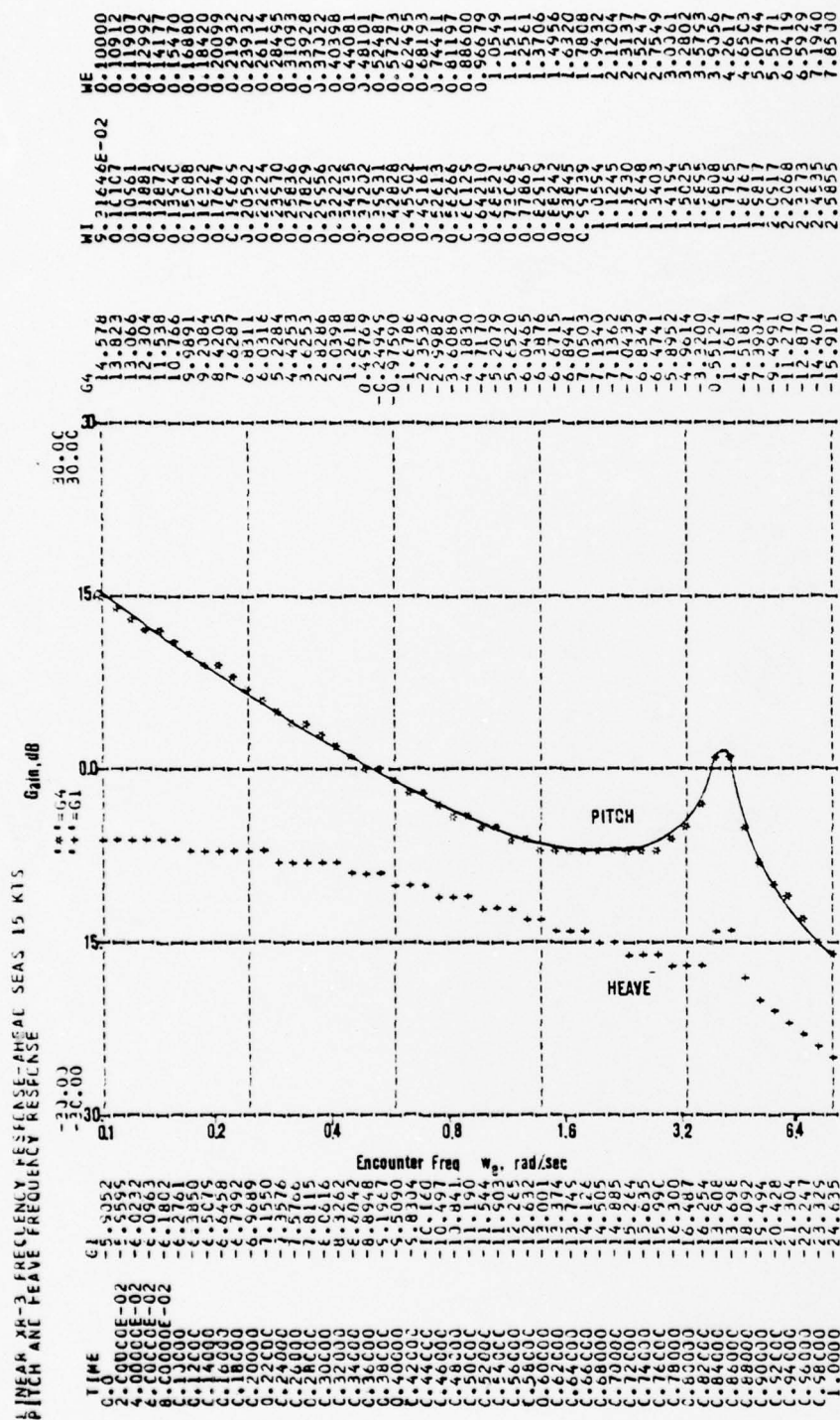
Figure 38 -   LINEAR SYSTEM PITCH FREQUENCY SPECTRUM,
15 KTS, AHEAD SEAS

Figure 39 — LINEAR SYSTEM PITCH RATE FREQUENCY SPECTRUM, 15 KTS, AHEAD SEAS
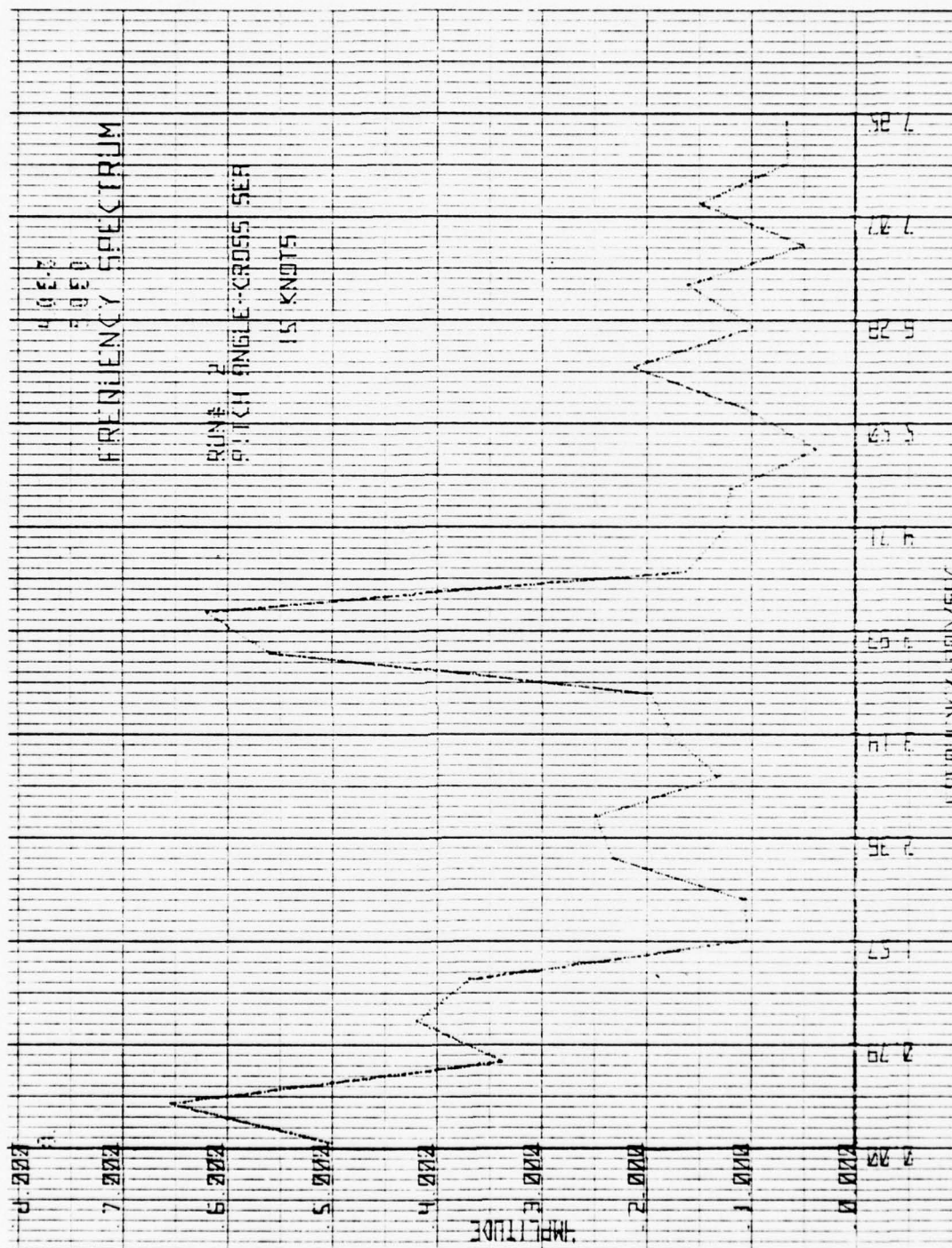
Figure 40 -    OBSERVED PITCH FREQUENCY SPECTRUM,
15 KTS, CROSS SEAS

137
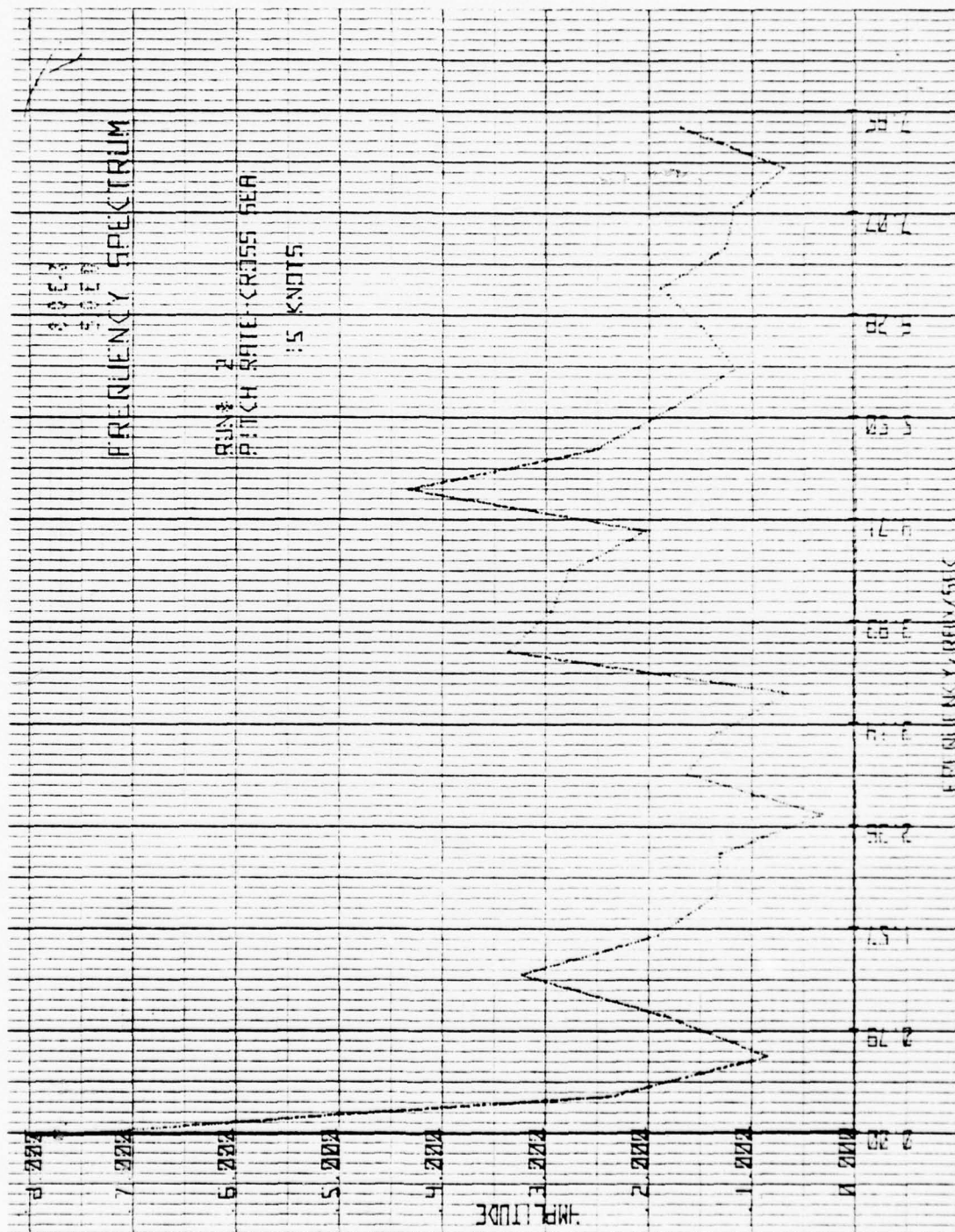
Figure 41 – OBSERVED PITCH RATE FREQUENCY SPECTRUM, 15 KTS, CROSS SEAS

138

Gain, dB

PITCH

HEAVE

15.00
0.0
-15
-30
-45

Encounter Freq $w_e$, rad/sec

0.1    0.2    0.4    0.8    1.6    3.2    6.4
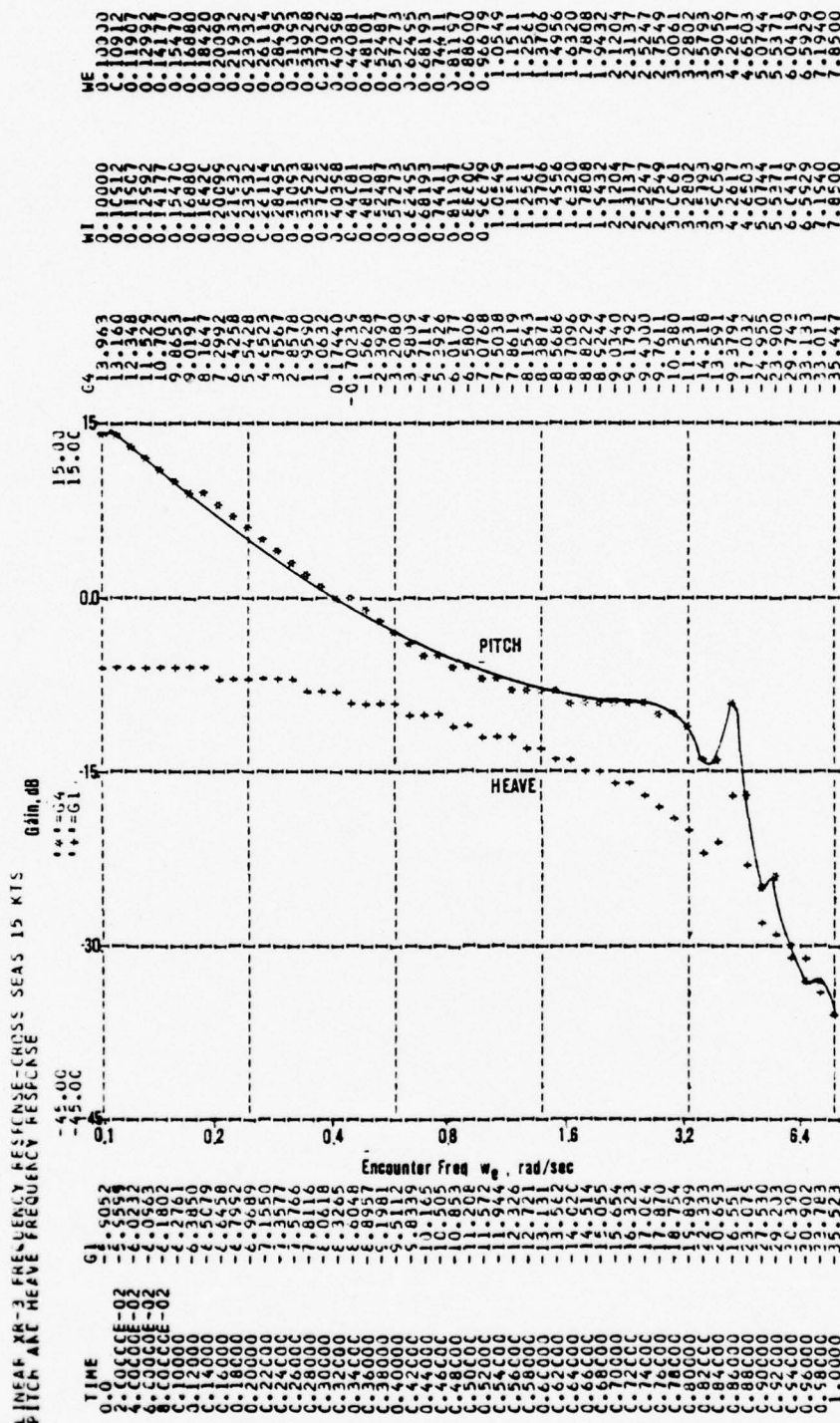
Figure 42 —  LINEAR SYSTEM PITCH FREQUENCY SPECTRUM,
15 KTS, CROSS SEAS

Figure 43 – LINEAR SYSTEM PITCH RATE FREQUENCY SPECTRUM,
15 KTS, CROSS SEAS
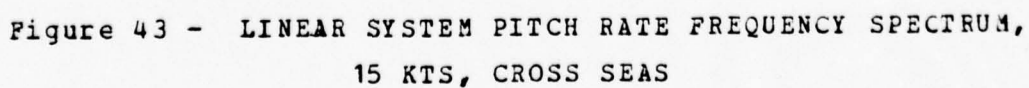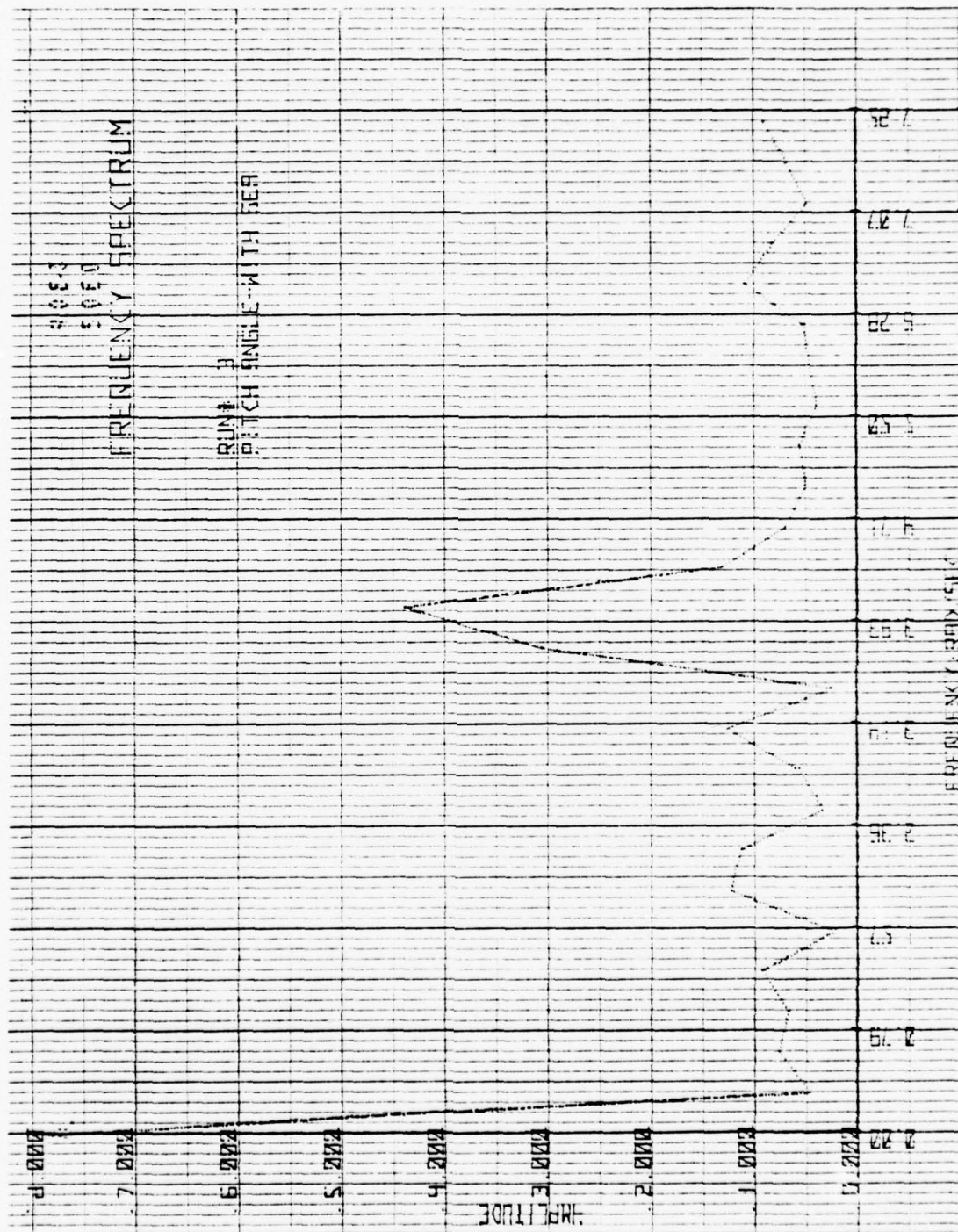
Figure 44 –   OBSERVED PITCH FREQUENCY SPECTRUM,
15 KTS, FOLLOWING SEAS

141
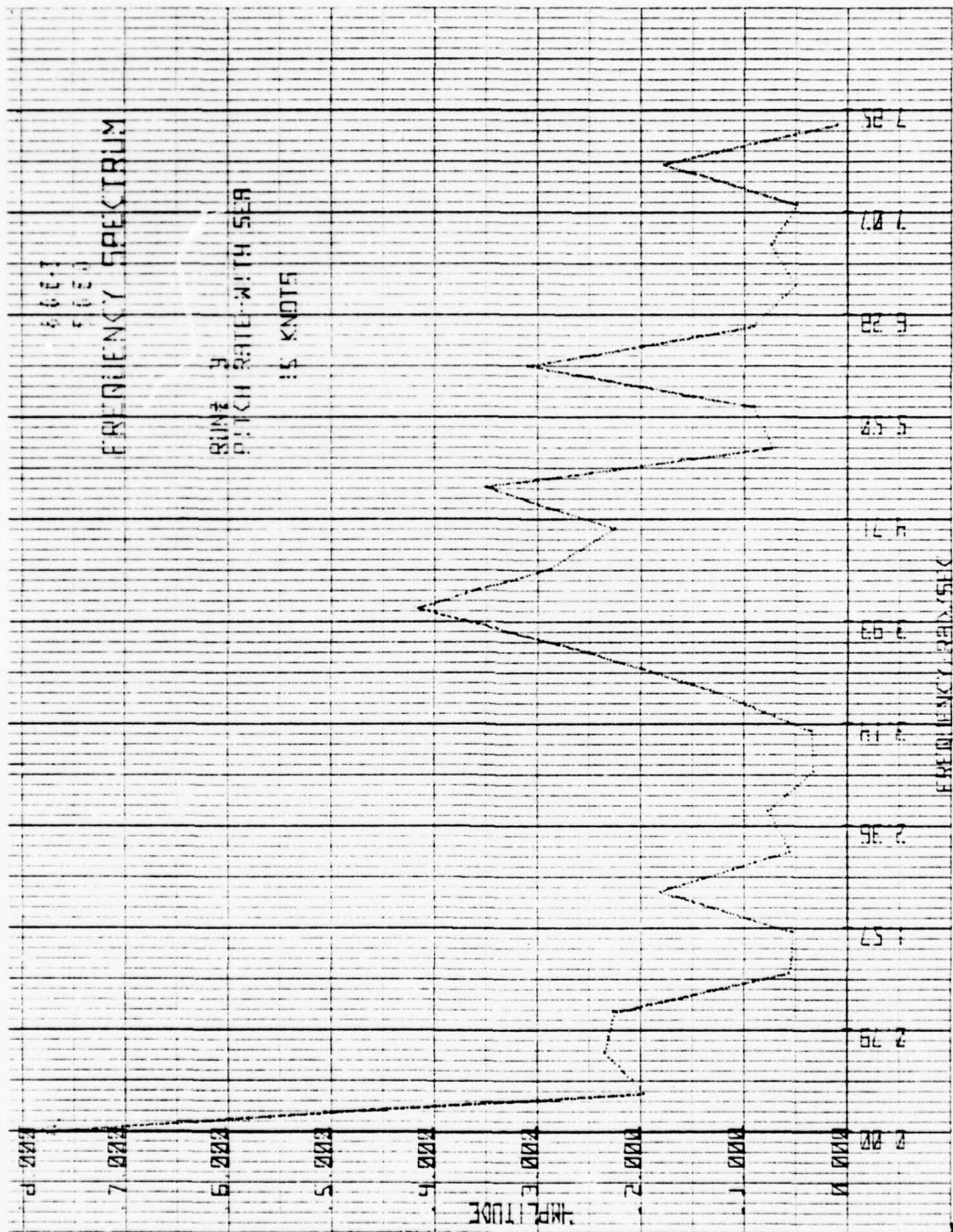
Figure 45 — OBSERVED PITCH RATE FREQUENCY SPECTRUM, 15 KTS, FOLLOWING SEAS

Figure 46 —   LINEAR SYSTEM PITCH FREQUENCY SPECTRUM,
15 KTS, FOLLOWING SEAS

143

Gain, dB

* = G5
+ = G2

15.00

0.0

PITCH RATE

-15

HEAVE RATE

-30

-45

| 0.1 | 0.2 | 0.4 | 0.8 | 1.6 | 3.2 | 6.4 |

Incident Wave Freq $w_1$, rad/sec

Figure 47 -  LINEAR SYSTEM PITCH RATE FREQUENCY SPECTRUM,
15 KTS, FOLLOWING SEAS
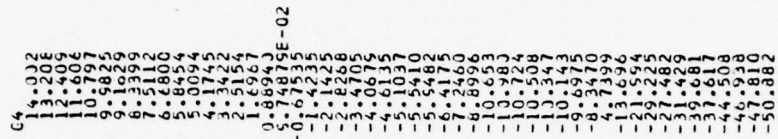
# VII.  SUMMARY

## A.  CONCLUSIONS AND OBSERVATIONS

The linear two-degree-of-freedom model developed in this work has been shown to be a reasonable approximation to both the  Loads  and Motions program and to actual observed craft behavior, in both the time and frequency domain; its relatively uncluttered simplicity has disclosed some interesting aspects of testcraft behavior, including the nulls and nodes that characterize the craft frequency response.  Furthermore, this simulation is extremely economical of CPU time, requiring less than three minutes of CPU time to generate the frequency response curves for up to 100 discrete frequencies.

The non-linear behavior described in Chapter V is somewhat supported by observations of testcraft data in the frequency domain in Chapter VI.  This interesting behavior is apparently akin to that of a relaxation oscillator.

Noise, which has interfered with varying degrees of severity in almost all transient analysis done with the recorded testcraft data at NPS, is reduced to little significance using the frequency domain method applied for testcraft data reduction in this work.  The major source of noise in the XR-3 has been identified as primarily ignition noise from the eight gasoline engines aboard the craft, transmitted electrically to the data acquisition system.

## B. RECOMMENDATIONS FOR FUTURE STUDY

The linear heave-pitch model developed in this work can readily be expanded to include roll, yaw and speed effects. Completion of this expansion would result in an analytical six-degree-of-freedom model, and lead to a more thorough understanding of CAB craft behavior. An example of the potential of this approach may be seen in ref [9], in which a rudimentary pitch control system, based upon this model and utilizing optimal Ricatti solutions, promises to reduce sea-state pitch accelerations to less than ten percent of the open loop response. The practical problems involved in the implementation of a test-bed ride control system for the XR-3 testcraft do not appear to be severe, aside from the physical installation of a suitable set of stern-plane control surfaces; an observer, based on a linear model, could be utilized as an optimal observer in a Kalman filtering scheme to generate some of the system states which may not otherwise be suitable for feedback. Since this system is only piecewise linear, the microprocessor appears as the most feasible means of implementing this control system, storing the optimal gains for several operating speeds in a table look-up or interpolation method. Most of the system development could be implemented on a slightly-modified version of the Loads and Motions program. This avenue has great future potential for expanding the sea-state envelope and improving the habitability of CAB craft.

The linear frequency domain response simulation should prove useful in the study of the non-linear behavior described in Chapter V. It is felt that this non-linearity can be modelled in the complex plane utilizing a describing function. Fortunately, the complex gains of the linear system are directly available from the linear system in the

program developed. This is an extremely interesting area of future study.

In the area of parametric analysis, such a linear model may be utilized with the technique of root locus analysis. An elementary program was developed for this purpose and is included at the end of the text with other programs developed for this investigation. However, time and space did not permit its inclusion into the main text. Furthermore, such parametric analysis was inconsistent with the main thrust of this effort. It is nevertheless hoped that the program will be of benefit in future studies.

The XR-3 testcraft was not available for data collection throughout the spring of 1977. The frequency domain data reduction techniques developed in this work could not, therefore, be utilized in anything approaching an in-depth study of craft behavior. One area in which these frequency domain techniques may prove most useful would be the investigation of actual testcraft gains in heave at various frequencies, to ascertain the significance of wave-plenum chamber interactions. The 15 dB discrepancy between the Loads and Motions program, which assumes a plenum wave, and this linear model, which does not, indicates this to be a vital factor in the accuracy of any model.

A serious effort at ignition filtering is certainly in order. Ignition suppression and power-line filtering is a relatively straightforward approach that can greatly enhance the quality of data collected from the XR-3.

An additional technique for data reduction to the frequency domain may become available in the very near future. The MDS-8 microprocessor-based data acquisition system, developed by Englehart in ref [10], will be capable of sampling sequentially and storing in mass memory up to 14

147

analog channels, with a sampling rate up to 7000 samples per second. Upon completion of the sampling and storage, the MDS-8 can perform a variety of data manipulations upon the data file, including an FFT; the data file, both in the raw form and after manipulation, is available to the NPS IBM 360/67 computer installation via the CP/CMS time-sharing link. The possibilities of this system as a data reduction system are, compared with techniques previously utilized for data reduction, impressive. However, much remains to be developed in this area.

APPENDIX A

WIDEBAND NOISE DATA

This appendix is a resume of the more significant wide-band noise spectra observed in the FFT's of XR-3 testcraft data collected at Lake San Antonio, 20 January 1977.

The following plots are FFT's of testcraft data, reduced as described in Chapter V, for a maximum upper frequency of 200 Hz, and a frequency resolution of 512 samples.

STARBOARD ENGINE 1/2 POWER, PORT IDLE

1. Pitch

2. Pitch Rate

3. Plenum Pressure

PORT ENGINE 1/2 POWER, STARBOARD IDLE

4. Pitch

5. Roll

6. Yaw Rate

BOTH ENGINES 1/2 POWER

7. Pitch

8. Pitch Rate

9.  Roll

10.  Roll Rate

11.  Plenum Pressure

    STARBOARD FULL, PORT 1/2 POWER

12.  Pitch
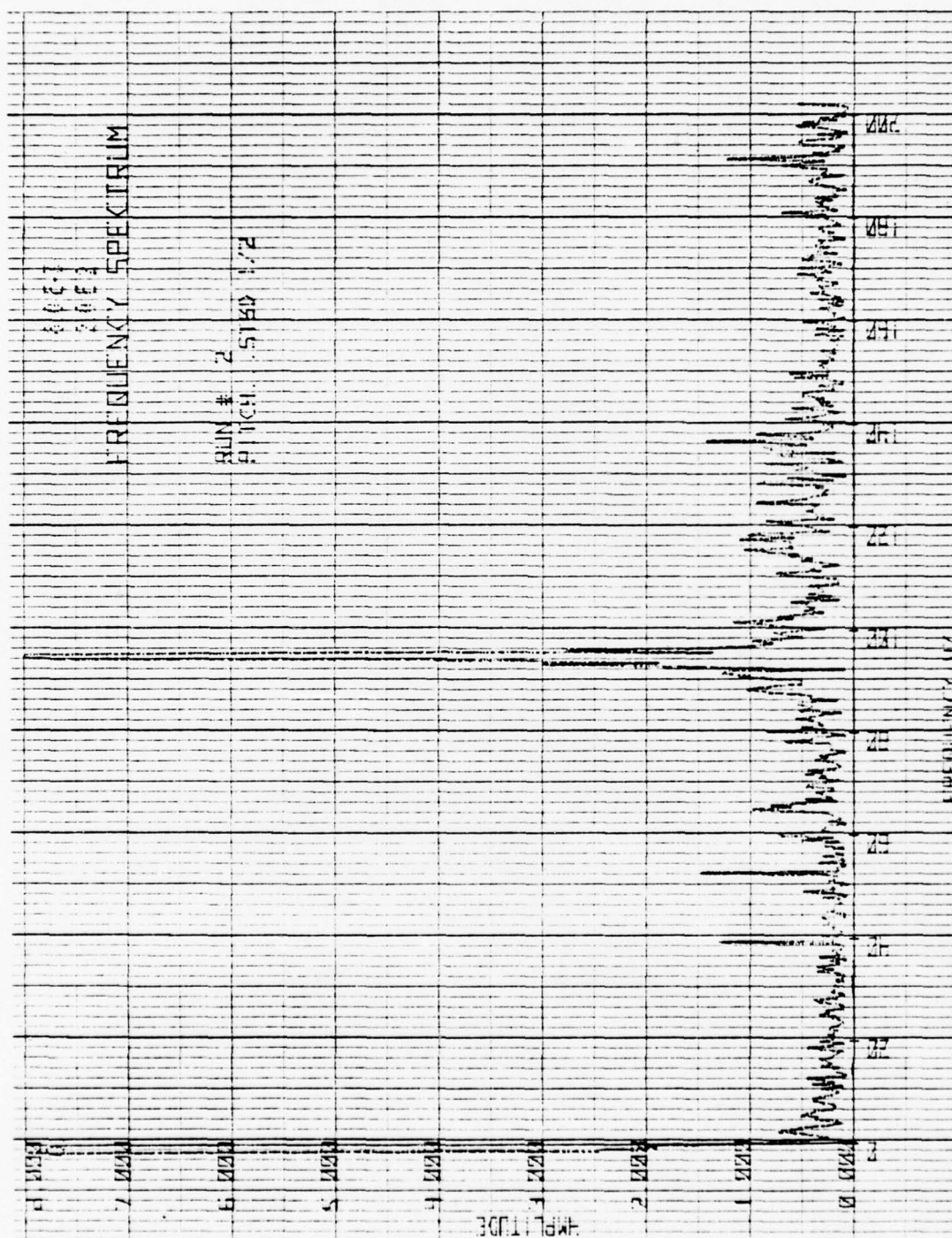
A 1 -  STARBOARD ENGINE 1/2 POWER, PORT IDLE

PITCH FREQUENCY SPECTRUM 0-200 Hz
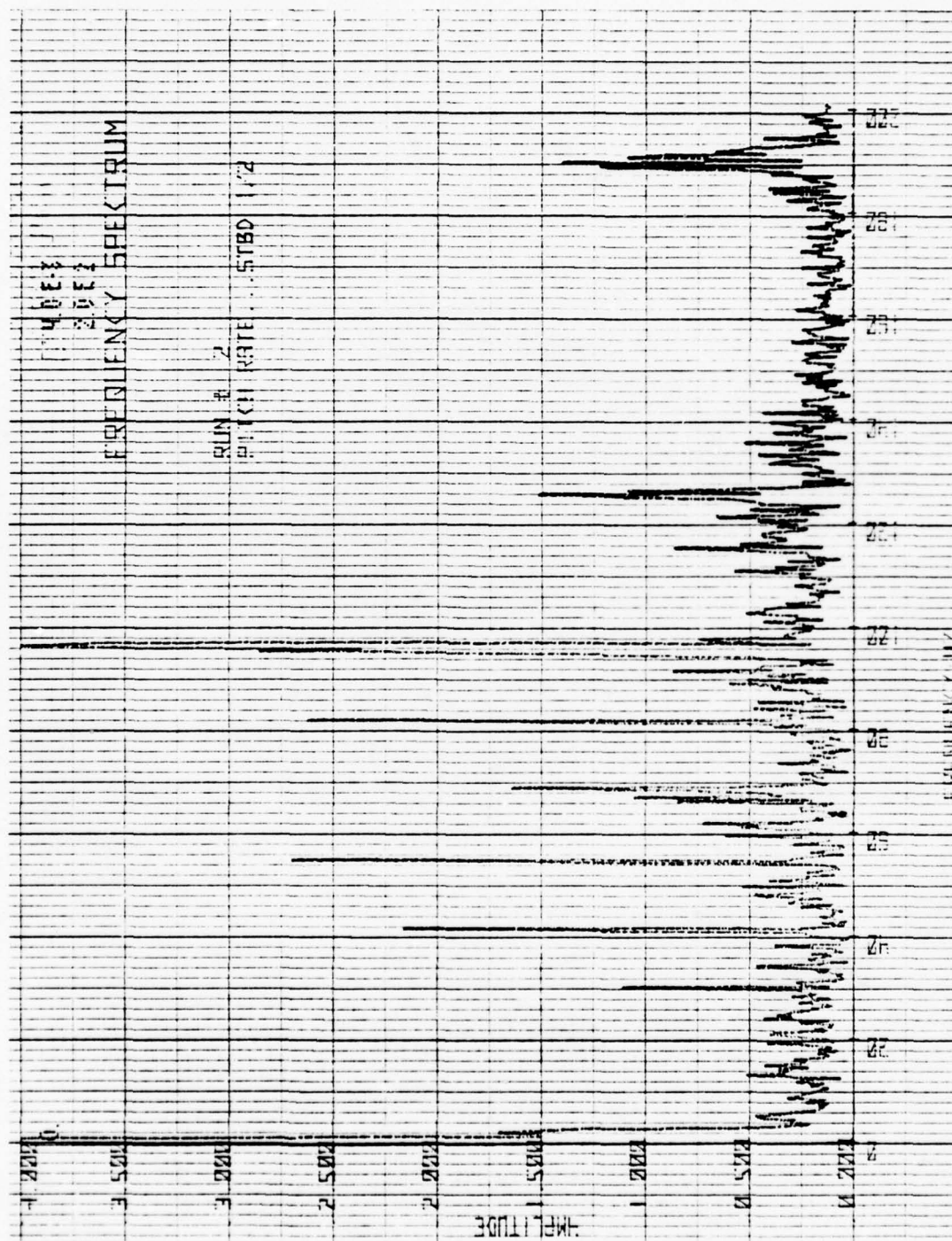
A 2 -    STARBOARD ENGINE 1/2 POWER, PORT IDLE

PITCH RATE FREQUENCY SPECTRUM 0-200 Hz
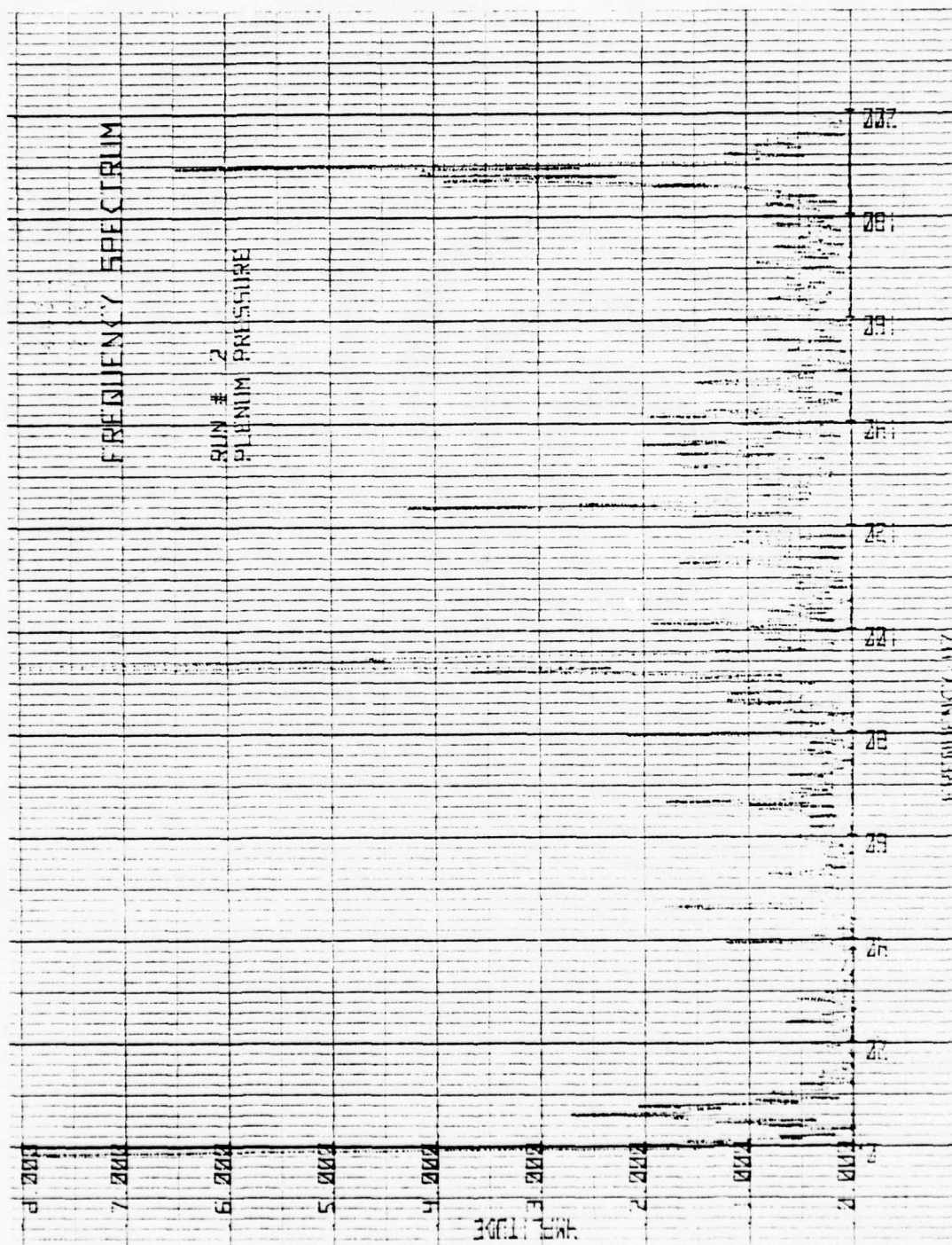
A 3 — STARBOARD ENGINE 1/2 POWER, PORT IDLE

PLENUM PRESSURE FREQUENCY SPECTRUM 0-200 Hz
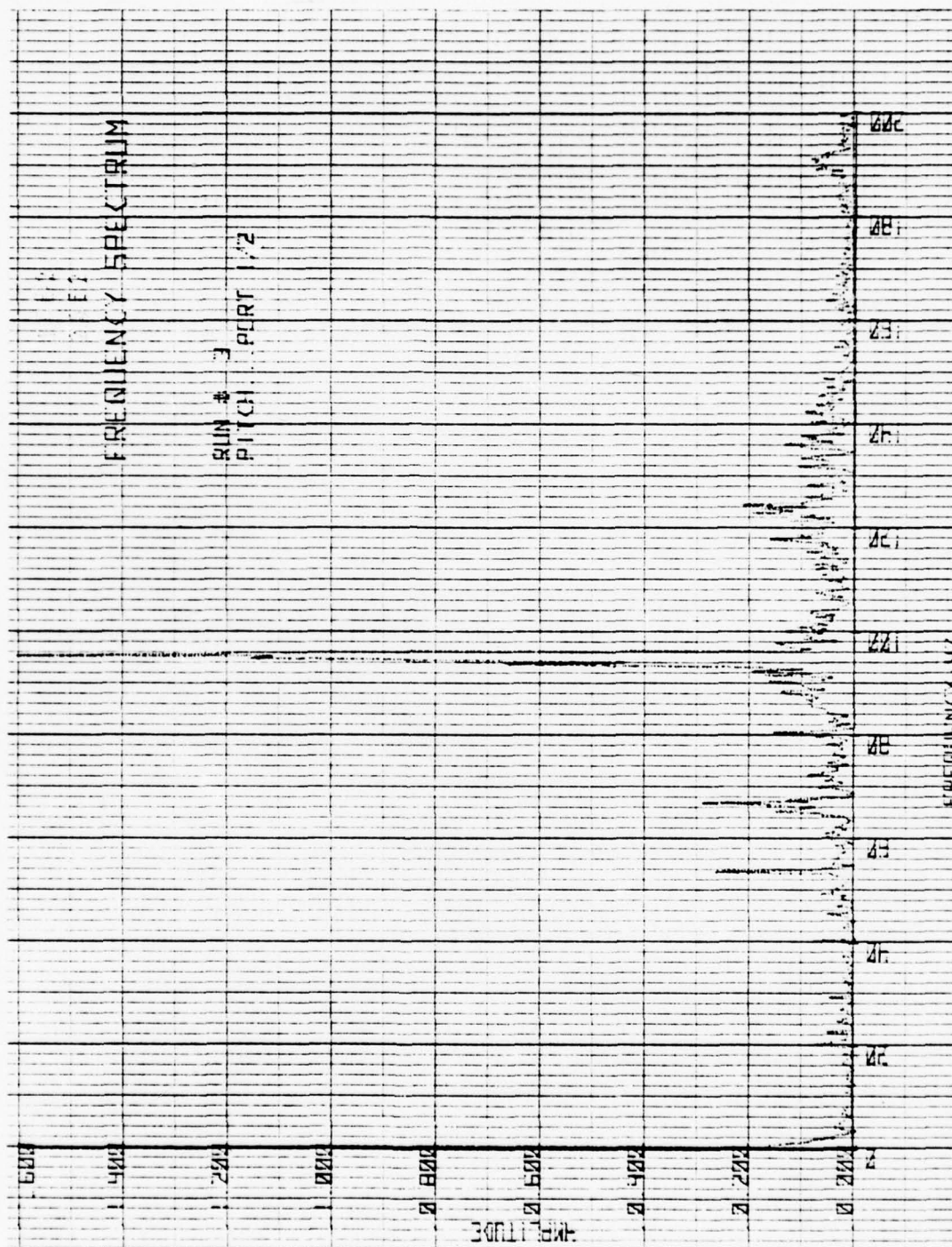
A 4 - PORT ENGINE 1/2 POWER, STARBOARD IDLE

PITCH FREQUENCY SPECTRUM 0-200 Hz

154
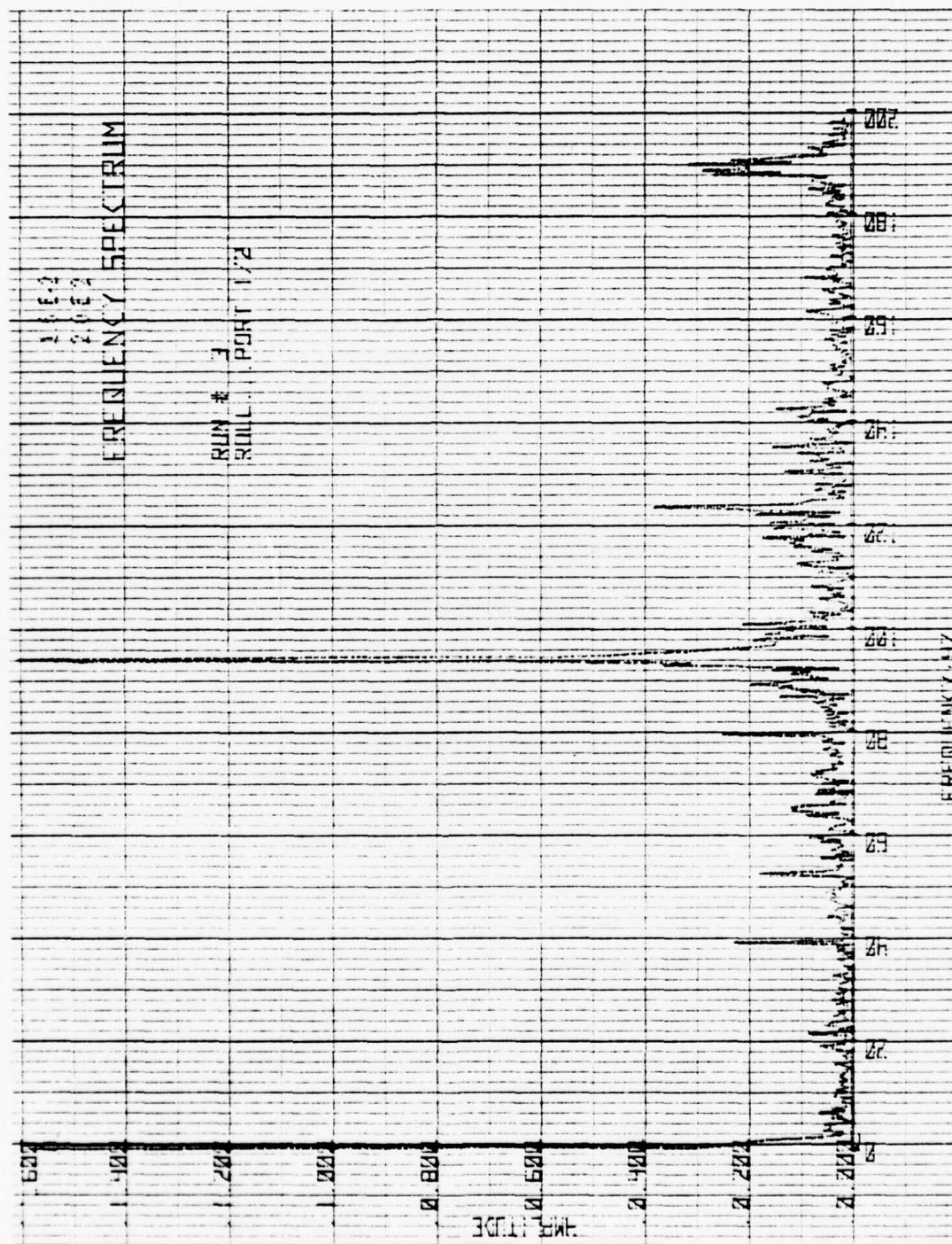
A 5 -  PORT ENGINE 1/2 POWER, STARBOARD IDLE

ROLL FREQUENCY SPECTRUM 0-200 Hz
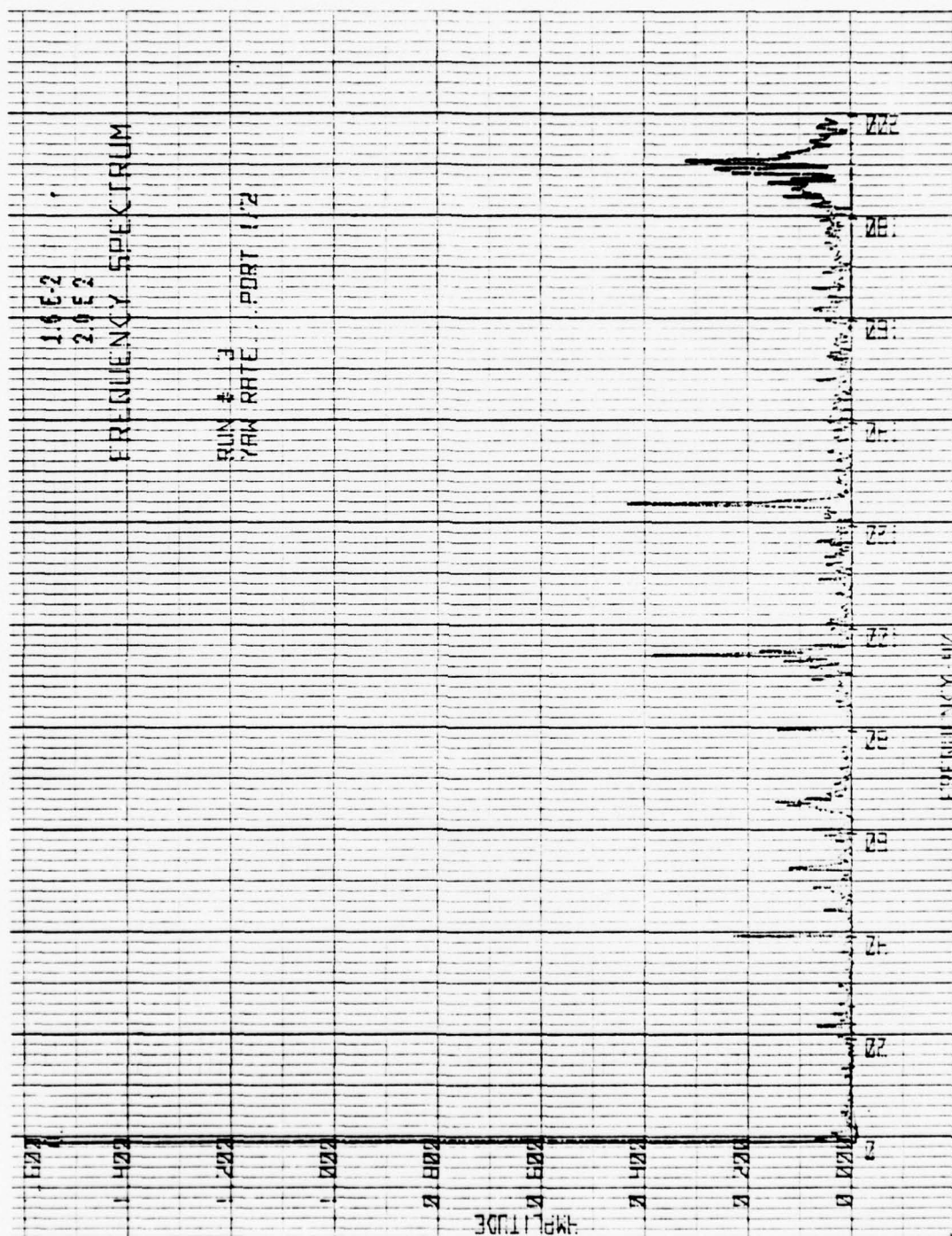
A 6 –    PORT ENGINE 1/2 POWER, STARBOARD IDLE

YAW RATE FREQUENCY SPECTRUM 0-200 Hz
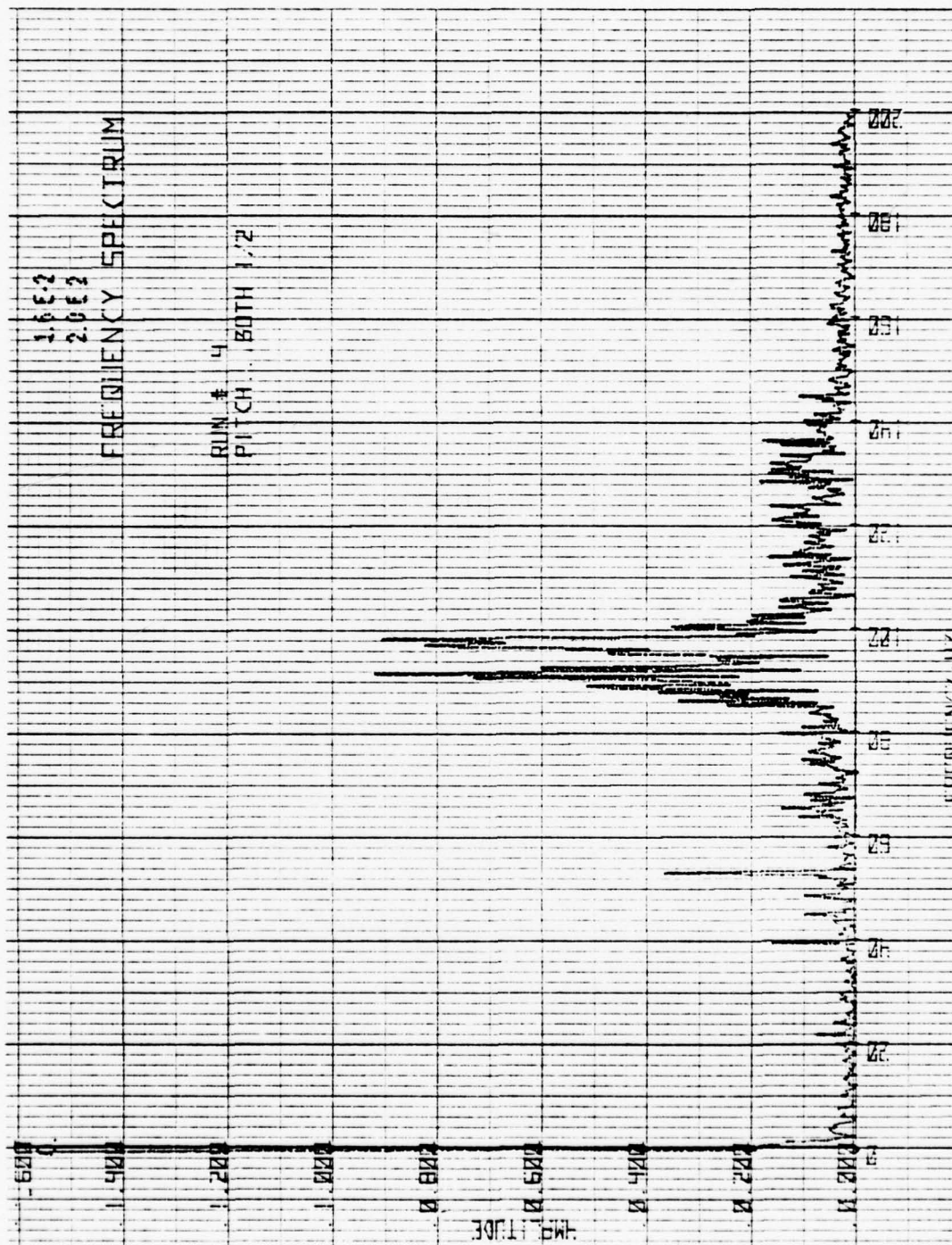
A 7 -    BOTH ENGINES 1/2 POWER

PITCH FREQUENCY SPECTRUM 0-200 Hz

157
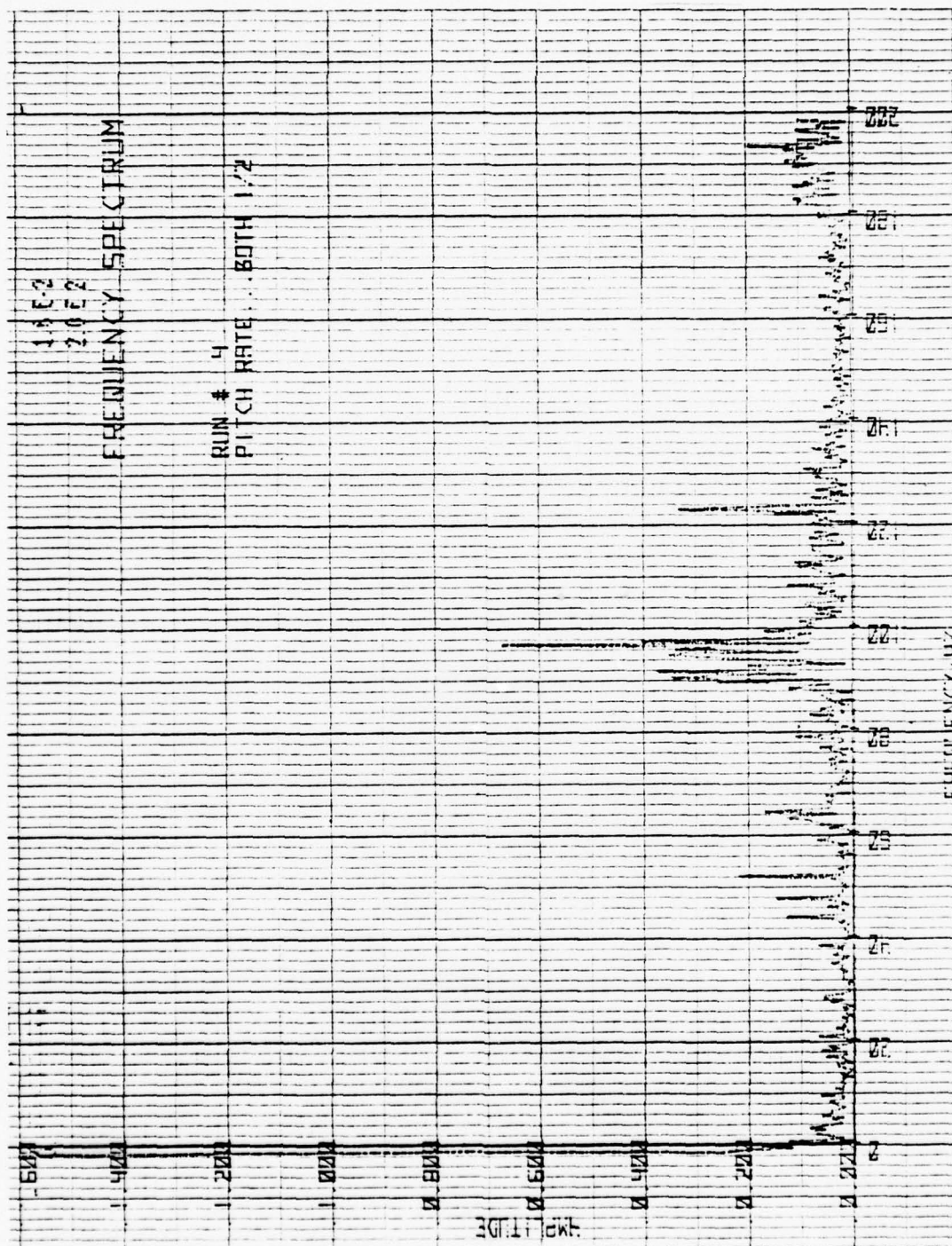
A 8 -    BOTH ENGINES 1/2 POWER

PITCH RATE FREQUENCY SPECTRUM 0-200 Hz

158
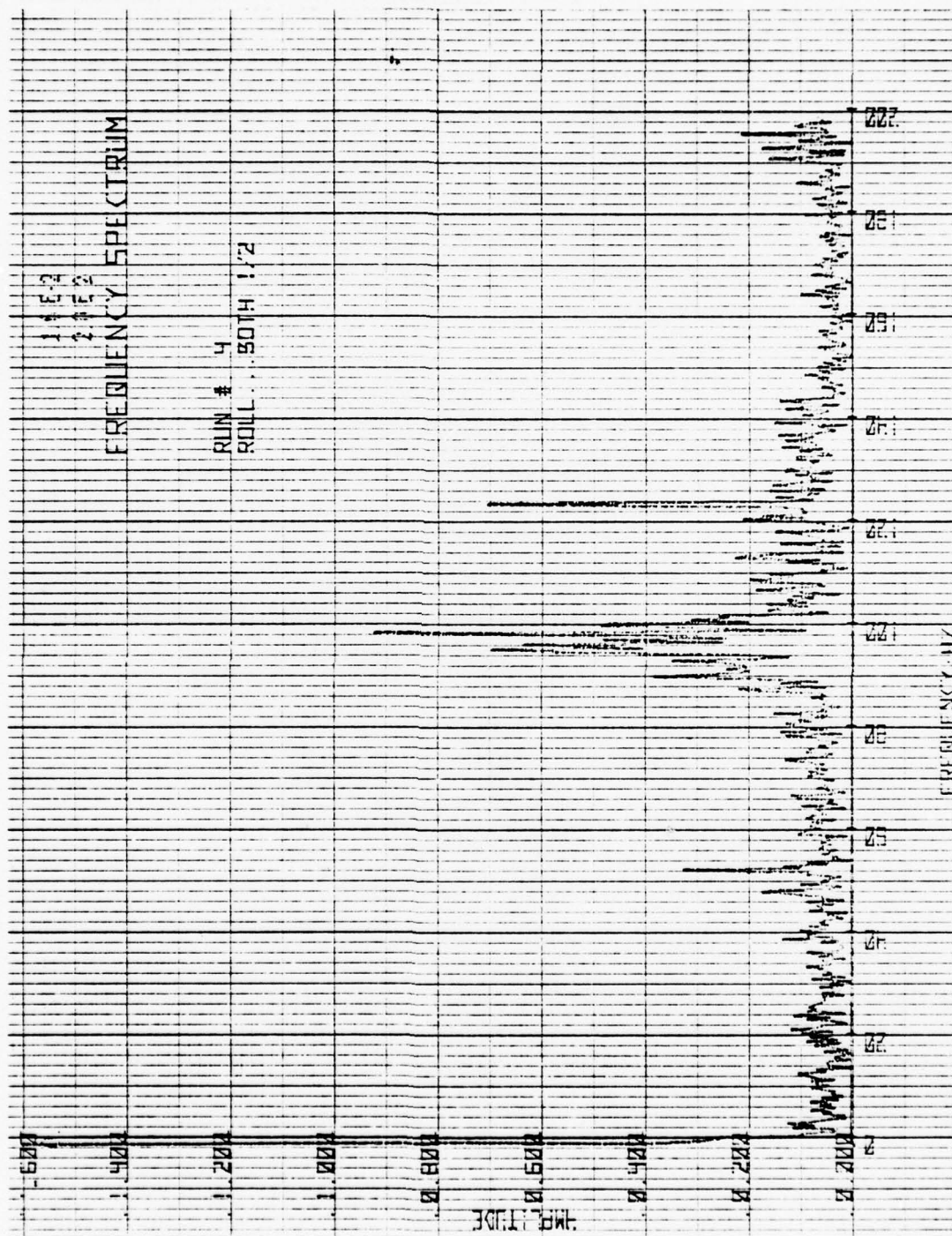
A 9 - BOTH ENGINES 1/2 POWER

ROLL FREQUENCY SPECTRUM 0-200 Hz
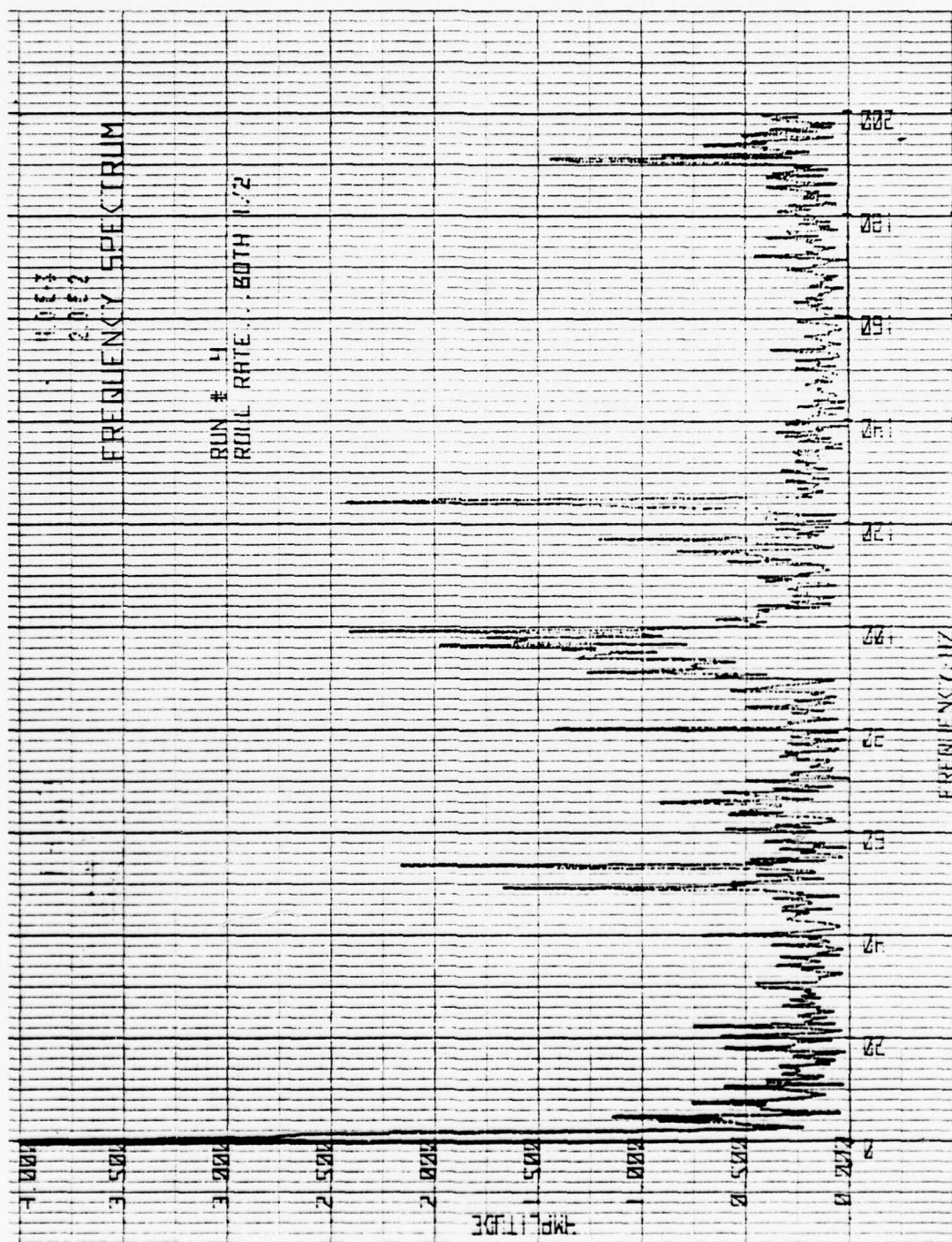
A10 -    BOTH ENGINES 1/2 POWER

ROLL RATE FREQUENCY SPECTRUM 0-200 Hz
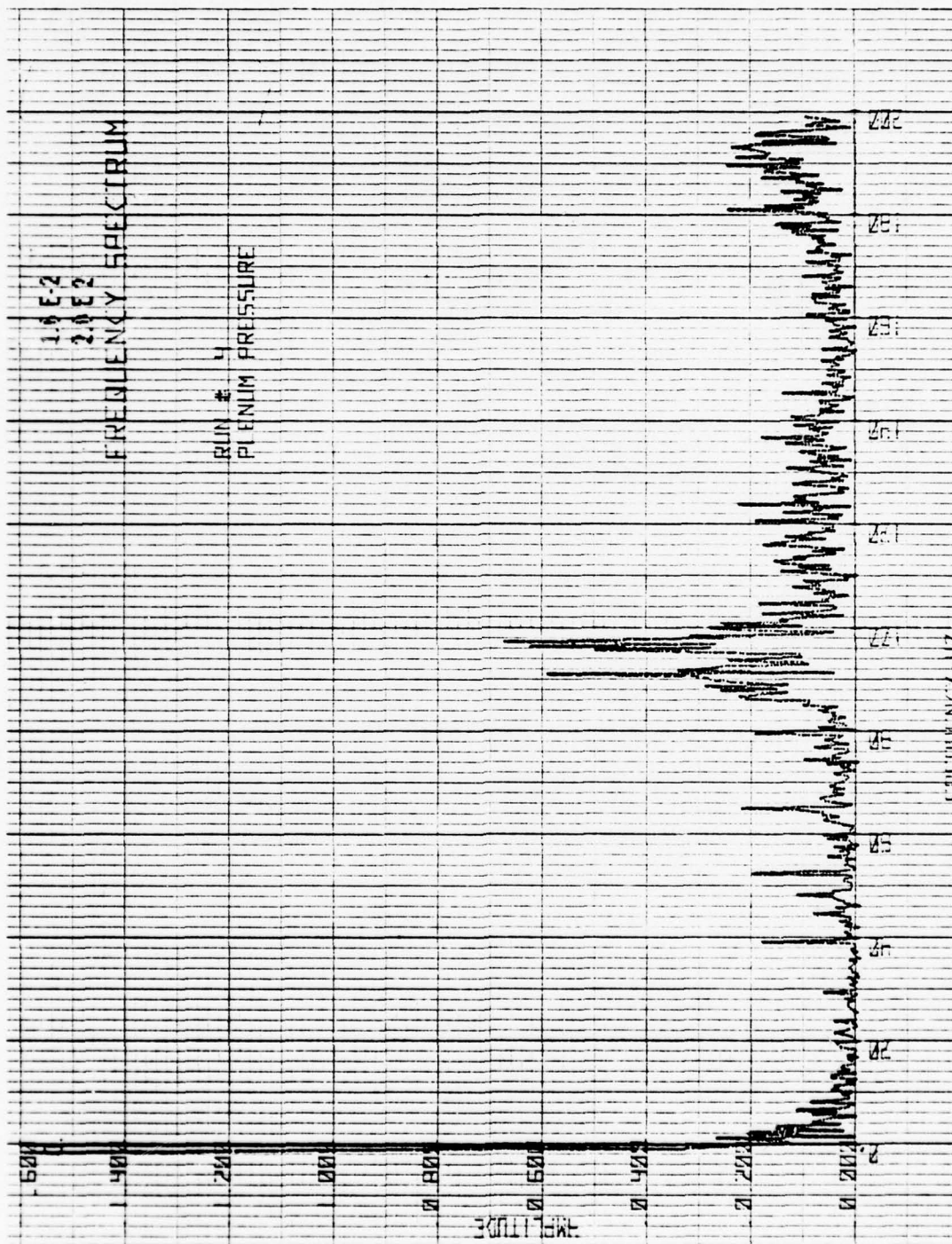
A11 —    BOTH ENGINES 1/2 POWER

PLENUM PRESSURE FREQUENCY SPECTRUM 0-200 Hz
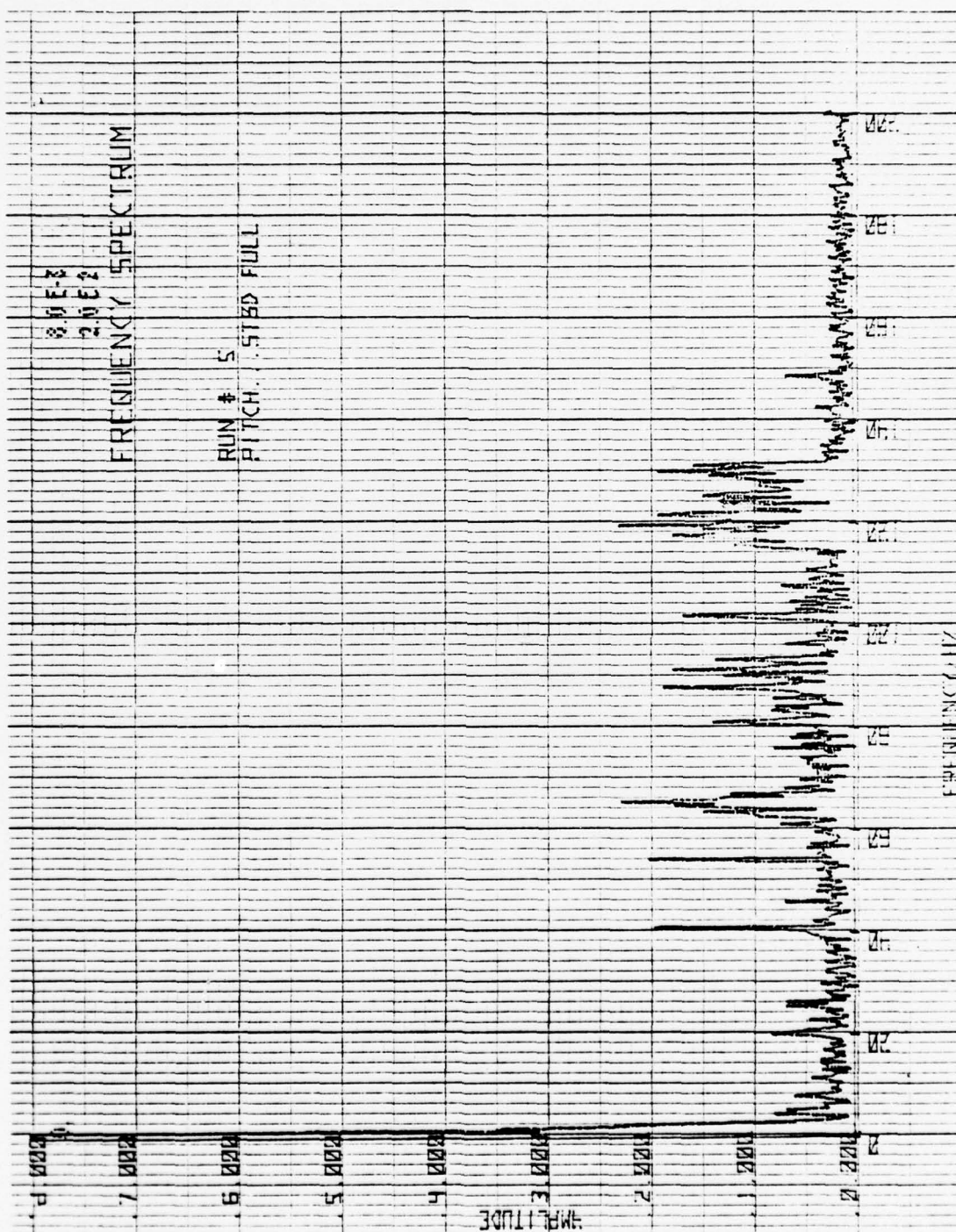
A12 —    STARBOARD FULL,PORT 1/2

PITCH FREQUENCY SPECTRUM 0-200 Hz

162

$$$CCNTINUOUS SYSTEM MCDELING PROGRAM  III   VIM3   TRANSLATOR OUTPLT$$$

FIXED I,K
INITIAL
*
*     CCNSTANTS USED IN THIS PROGRAM
CONSTANT G=32.0,GAMMA=1.4,PA=216.0,PI=3.141593,RHO=2.0,RHOA=.002378
*
*     NCN-VARIABLE CRAFT CCNSTANTS
CONSTANT WIDTH=10.0,L=20.0,N=5.0,QIO=35.,VN=383.,ZS=2.5,AB=200.,CN=.9
*
**  SIDEWALL GECMETRY
*
CCNSTANT CR1=60.0,CR2=80.,WS=.9375,WS0=.27
*
*     CRAFT PARAMETERS
*
PARAMETER W=65CC.,XCCC=-.125,XCP=.4,CV=1.5
PARAMETER AL=.350,IYY=562C.,MFO=-.1875.,SEALP=2.0
*
*     INITIAL CCNDITICNS
*
PARAMETER ZCCTC=0.0,OMECO=0.0,THETA=0.0,V=33.
*
**  STEP WEIGHT CHANGE AT TIME=0
*
PARAMETER WSTEF=100.
*
**  LOADS AND MOTICN DATA
*
**  CRAFT
FUNC LD1=(0.,8.55),(.C5,8.545),(.10,8.5348),(.15,8.5249),(.2,8.5155),...
(.25,8.5065),(.3,8.4976),(.35,8.4891),(.4,8.4809),(.45,8.4728),...
(.5,8.4648),(.55,8.4571),(.6,8.4495),(.65,8.4421),(.7,8.4348),...
(.75,8.4276),(.8,8.42C7),(.85,8.4139),(.9,8.4075),(.95,8.4011),...
(1.,8.3951),(1.C5,8.3894),(1.1,8.3839),(1.15,8.3786),(1.2,8.3735),...
(1.25,8.3687),(1.3,8.3639),(1.35,8.3594),(1.4,8.3549),(1.45,8.3505),...
(1.5,8.3462),(1.55,8.3420),(1.6,8.3378),(1.65,8.3336),(1.7,8.3295),...
(1.75,8.3253),(1.8,8.3213),(1.85,8.3172),(1.9,8.3133),(1.95,8.3020),...
(2.,8.3057),(2.C5,8.3020),(2.1,8.2979),(2.15,8.2918),(2.2,8.2886),...
(2.3,8.28715),(2.35,8.2826),(2.4,8.2797),(2.45,8.2769),(2.5,8.2742),...
(2.55,8.2715),(2.6,8.2688),(2.65,8.2662),(2.7,8.2636),(2.75,8.2606),...
(2.8,8.2583),(2.85,8.2557),(2.9,8.2531),(2.95,8.2505),(3.0,8.2479),...
*
*  PITCH ANGLE:
FUNC TH1=(0.,1.199),(.C5,1.1991),(.1,1.1984),(.15,1.1970),(.2,1.195),...
(.25,1.1919),(.3,1.1882),(.35,1.1835),(.4,1.1793),(.45,1.1745),...
(.5,1.16945),(.55,1.1655),(.6,1.1617),(.65,1.1585),(.7,1.1561),...
(.75,1.15443),(.8,1.15365),(.85,1.1573),(.9,1.15403),(.95,1.1549),...
(1.,1.15611),(1.C5,1.1573),(1.1,1.1584),(1.15,1.1592),(1.2,1.1595),...
(1.25,1.1593),(1.3,1.1585),(1.35,1.1571),(1.4,1.1552),(1.45,1.1528),...
(1.5,1.151),(1.55,1.1471),(1.6,1.1442),(1.65,1.1414),(1.7,1.1389),...
(1.75,1.1367),(1.8,1.1351),(1.85,1.1339),(1.9,1.1334),(1.95,1.1333),...
(2.,1.1361),(2.C5,1.1343),(2.1,1.1352),(2.15,1.1362),(2.2,1.1371),...
(2.25,1.13715),(2.3,1.1384),(2.35,1.1385),(2.4,1.1382),(2.45,1.1375),...
(2.55,1.1369),(2.55,1.1357),(2.6,1.1330),(2.65,1.1314),(2.7,1.1295),...
(2.75,1.1274),(2.8,1.1258),(2.85,1.1242),(2.9,1.1230),(2.95,1.1221),...

(3.C.1.1216)
* PLENUM GAUGE PRESSURE
FUNC PB1=(0.0,24.8372),(.05,24.5083),(1.24.4558),(.15,24.4153),...
...
* C.G. ACCELERATION Z2CT
FUNC Z21=(0.,-.0014),(.05,-.0004),(.1,-.0018),(.15,-.0001),...
...
* ANGULAR VELOCITY
FUNC CM1=(0.,.0001),(.05,.0047),(.1,.0186),(.15,.035),(.2,-.035),...
...

RADEG=360./(2.0*PI)
DEGRAD=1.0/RADEG
* AVERAGE SIDEWALL WIDTH AND AREAS
AS=WS*L
M=W/G
XCC=XCCO
ZCCT=ZCCTO
OMEGA=OMEGO
**
*       SELECT A VALUE OF PBBAR SUCH THAT MBDOT=0.0 AT TIME=0.0

164

```
B=-2.C*(QIO+((CN*AL/N)**2)/RHOA)
PEBARC=PEBAR
PEBAR=(-E-SQRT(E**2-4.C*QIO**2))/2.0
PEPAC=1.0+PEBAR/PA
* CCMPUTE PRESSURE FORCES AND MCMENTS
HPRES=-AB*PEBAR
FPRES=HPRES*(XCG-XCP)
NCSORT SELECT A VALUE CF CRAFT AND THETA SUCH THAT MCMENTS AND FORCES ARE ZERC

THETA=C.0
LC=(W+FPRES+HPLAN)/(2.C*RHO*G*WS*L)
**       ITERATE TC A SOLUTICN FOR DRAFT AND THETA
*
DC 10 I=1,250
K=1
1 CCNTINUE
*
** CCMPUTE FORCES AND MCMENTS DUE TO BOWSEAL AND STERNSEAL
FCR ECWSEAL:
XSEAL1=2.0*(LC-(L/2.-XCG)*TAN(THETA))
ASEAL1=WIDTH*XSEAL1
HSEAL1=-PEBAR*ASEAL1
PSEAL1=-HSEAL1*(L/2.-XSEAL1/2.-XCG)
FCR STERN SEAL:
XSEAL2=2.C*(LC+(L/2.+XCG)*TAN(THETA))
ASEAL2=WIDTH*ASEAL2
HSEAL2=-SEALF*ASEAL2
HSEAL2=HSEAL1+HSEAL2
PSEAL=PSEAL1+PSEAL2
*
** SIDEWALL GECMETRY CCRRECTED FCR DRAFT AND DEADRISE
** BOW:
LCBAR1=LD-(L/2-XCG)*THETA/2.
WS1=LCBAR1/(2.0*TAN(CR1*CEGRAD))+WSO
IF(WS1.LT.0.C)WS1=C.0
IF(WS1.GT.WS)WS1=WS-WS**2*TAN(CR1*CEGRAD)/(2.0*LDBAR1)
** STEFN:
LCBAR2=LD+(L/2+XCG)*THETA/2.
WS2=LCBAR2/(2.C*TAN(CR2*CEGRAD))+WSO
IF(WS2.LT.C.C)WS2=0.0
IF(WS2.GT.WS)WS2=WS-WS**2*TAN(CR2*DEGRAD)/(2.0*LDBAR2)
** BUCYANT FCRCES AND MCMENTS:
HEUCY1=-2.0*RHC*G*WS1*(L/2.-XCG)*(LC-(L/2.-XCG)*TAN(THETA)/2.)
HEUCY2=-2.0*RHC*G*WS2*(L/2.+XCG)*(LD+(L/2.+XCG)*TAN(THETA)/2.)
PBUCY1=-.5*(L/2.-XCG)*HBUCY1
PBUCY2=.5*(L/2.+XCG)*HBUCY2
*
```

```
*  PLANING FORCES AND MOMENTS:
** FFLAN=-(CV/2.0)*RHO*V**2*(WS1+WS2)*L*THETA
   PFLAN= 5.0*FFLAN
*  RESIDUAL FORCES AND MOMENTS:
** RES1=FPRES+FSEAL+HBUOY1+FBUOY2+HPLAN+W
   RES2=PPRES+PSEAL+PBUOY1+PBUCY2+PPLAN +MFO
** COMPUTE THE PARTIAL DERIVATIVES OF RESIDUAL FORCES AND MOMENTS
** AND THE NEW VALUES CF CRAFT AND THETA TO DRIVE
** RESIDUALS TC ZERO
   GC TO(2,3,4),K
** PARTIAL DERIVATIVES WITH RESPECT TO DRAFT:
 2 DLD=.C1*LD
   IF(CLC.EC.0.0)CLC=.001
   LC=LC+DLD
   RESIC=RES1
   RES2C=RES2
   K=2
   GC TO 1
** PARTIAL DERIVATIVES WITH RESPECT TO THETA:
 3 DRICL=(RES1-RESIO)/CLD
   DR2DL=(RES2-RES2O)/DLC
   IF(CTHET.EC.0.0)CTHET=.001
   THETA=THETA+CTHET
   RES1O=RES1
   RES2O=RES2
   K=3
   GC TO 1
** BAIRSTCW'S METHOD FOR NEW VALUES CF DRAFT AND THETA TO REDUCE
** THE RESIDUALS.
 4 DR1CTH=(RES1-RESIO)/CTHET
   CR2DTH=(RES2-RES2O)/DTHET
   CET=DR1DL*CF2CTH-DR1DTH*CR2DL
   DLD=(-RES1*DR2CTH+DRICTH*RES2)/CET
   DTHET=(-RES2*CRICL+DR2CL*RES1)/DET
   THETA=THETA+1.E5*DTHET
   LC=LD+1.85*CLD
 1C CCNTINUE
** ADD ANY REMAINING RESICLALS TC ACCELERATION TERMS
*  Z2DCTC=RES1/W
   ALFO=RES2/IYY
   ZC=LC-ZS
   Z=ZO
   THETO=THETA
*
```

```
*     CCMPUTE THE INITIAL MASS OF AIR IN THE PLENUM AT THESE CONDITIONS
*
      VB=VN-AB*(LC+XCG*TAN(THETA))
      MBO=FHCA**VB*(PEPAO**(1.0/GAMMA))
      MB=MBC
*
**    THIS CCMPLETES THE DEFINITION OF THE OPERATING POINT.
**    FOR THIS STATIC EQUILIBRIUM CONDITICN,COMPUTE THE PARTIALS
**    WITH RESPECT TC THE STATE VARIABLES,Z,ZDOT,THETA,OMEGA AND MB
**    FOR THE NON-LINEAR RELATICNSHIPS IN PBBAR,Z2DOT,ALFA, AND MBDOT
*
**    FOR PBBAR
*
*     PBBAR=PA*(((MB/RHA )**GAMMA*(VN-AB*(Z+ZS+XCG*THETA))*(-GAMMA)-1.0)
*
      DPBZ=GAMMA*AE*(PBBAR+FA)/VB
      DPBTH=GAMMA*AB*XCC*(PBBAR+PA)/VB
      CFBMB=GAMMA*(PBBAR+PA)/MB
*
**    FOR Z2DOT
*             +PRES TERM
*
      DPPZ=-AB*CPBZ
      DPPTH=-AE*CFBTH
      DPPME=-AE*CFBMB
*             +BUCY TERM
*
      DPBZ=-2.0*RHC*G*(WS1*(L/2.-XCG)+WS2*(L/2.+XCG))
      DPBTH=RHC*G*(WS1*(L/2.-XCG)**2-WS2*(L/2.+XCG)**2)
*             +SEAL TERM
*
**    BOW AND STERN SEALS
*
**    BCWSEAL:
      XSEAL1=2.0*(Z+ZS-(L/2.C-XCG)*THETA)
      DXCZ1=2.-0
      CXDTH1=-2.C*(L/2.-XCG)
      DHSZ1=-WICTH*XSEAL1*DPEZ-WIDTH*CXDZ1*PBBAR
      DHSTH1=-WICTH*XSEAL1*CFBTH-WICTH*DXCTH1*PBBAR
*     STERN SEAL:
      XSEAL2=2.0*(Z+ZS+(L/2.+XCG)*THETA)
      DXDZ2=2.C
      DXDTH2=2.0*(L/2.+XCG)
      DHSZ2=-WICTH*DXCZ2*SEALP
      DHSTH2=-WIDTH*CXDTH2*SEALP
*
      DHSZ=CHSZ1+DHSZ2
      DHSTH=DHSTH1+DHSTH2
      DHSMB=-WICTH*XSEAL1*DPEMB
*
**    PLANING FORCES:
```

167

```
* DFPLTH=-(CV/2.C)*RHO*(WS1+WS2)*L*V**2
*FOR ALFA TERM
CFPZ=(XCG-XCF)*CHPZ
DFPTH=(XCG-XCP)*CFPTH
DPPME=(XCG-XCP)*CFPME
*
* PBUOY TERM
DPBYZ=RHO*G*(WS1*(L/2.-XCG)**2-WS2*(L/2.+XCG)**2)
DFBYTH=-RHO*G*(WS1*(L/2.-XCG)**3+WS2*(L/2.+XCG)**3)/2.
*
* FSEAL TERM
*BOWSEAL:
*
DFSZ1=-CHSZ1*(L/2.-XSEAL1/2.-XCG)+HSEAL1*DXDZ1/2.0
DPSTH1=-DHSTH1*(L/2.-XSEAL1/2.-XCG)+HSEAL1*DXDTH1/2.
* STERNSEAL
*
DPSZ2=DHSZ2*(L/2.+XSEAL2/2.+XCG)+HSEAL2*DXDZ2/2.
DFSTH2=DHSTH2*(L/2.+XSEAL2/2.+XCG)+HSEAL2*DXDTH2/2.
DPSZ=CPSZ1+CFSZ2
CFSTH=CPSTH1+CPSTH2
DFSMB=-CHSMB*(L/2.C-XSEAL1/2.0-XCG)
*
* PLANING MOMENTS
CPPLTH=(L/4.)*CFPLTH
*
*FOR MBDOT
*
CMBTH=-DFBTH+(N*RHOA+CN*AL/SQRT(2.0*PBBAR/RHOA))
DMBMB=-DPBME+(N*RHOA+CN*AL/SQRT(2.0*PBBAR/RHOA))
CMBZ=-DPBZ+(N*RHOA+CN*AL/SQRT(2.0*PBBAR/RHOA))
Z2DOTO=Z2CCTO-G*STEP/(W-WSTEP)
*
* BEGIN THE TIME DOMAIN SOLUTION AT THIS POINT
* WITH A STEP WEIGHT CHANGE AND INITIAL C.G. ACCELERATION
*
M=(W-WSTEP)/G
Z2DOT=Z2CCTO
SCRT
DYNAMIC
PBDOT=(CPBZ*ZCCT+CPBTH*CMEGA+CPBMB*MBDOT)
CZZ=(CFPZ+CHEZ+CHSZ)/2
CZZTH=(CCFPTH+CHSTH+DFPLTH)/M
DZZMB=(CC+PME+CHS+ME)/M
Z3DOT=(CPZZ*ZDCT+CZTH*CMEGA+CZMB*MBDOT
DTHZ=(CPPZZ*ZDCT+CPSZ)/IYY
DTHTH=(CDPPTH+DPEYTH+DFSTH+CPPLTH)/IYY
CTHMB=(CPPME+DFSMB)/IYY
ALFCOT=DTHZ*ZDCT+CTHTH*OMEGA+DTHMB*MBDOT
MB2DCT=CMBZ*ZDCT+DMBTH*CMEGA+DMBMB*MBDOT
MBDCT=INTGRL(0.C,MB2DCT)
WE=INTGRL(WEC,WEDOT)
PEBAR=INTGRL(PEBARO,PEDOT)
Z2DCT=INTGRL(Z2CCTO,Z2DCT)
ZCOT=INTGRL(0.0,Z2DCT)
```

168

```
Z=INTGRL(ZO,ZCCT)
LC=Z+ZS
ALFA=INTGRL(ALFC,ALFCCT)
CMEGA=INTGRL(O-C,ALFA)
THETA=INTGRL(THETO,CMEGA)
LCIN=LO*12.C
THDEG=THETA*36C./(2.C*FI)
CMDEG=QMEGA*36C./(2.O*FI)
LCLM=AFGEN(LCI,TIME)
ERR1=2.*(LCIN-LCLM)/(LCIN+LCLM)
THLM=AFGEN(TI,TIME)
ERR2=2.*(THDEG-THLM)/(TH-DEG+THLM)
PBLM=AFGEN(PBI,TIME)
ERR3=2.*(PBBAR-PBLM)/(FEBAR+PBLM)
Z2LM=AFGEN(Z21,TIME)
ERR4=2.*(Z2CCT-Z2LM)/(Z2CCT+Z2LM)
CMLM=AFGEN(CMI,TIME)
ERR5=2.*(CMDEG-CMLM)/(CMDEG+CMLM)
TIMER FINTIM=3.C,CUTDEL=.C5
LABEL SMALL-SIGNAL XR-3 MODEL 600 LB WT STEP,5500 LB WT
OUTPUT PEBAR,PELM
PAGE GRCUP
LABEL FLENUM GAGE PRESSURE
CLTPLT ERR3
LABEL PLENUM PRESSURE ERRCR
OLTPUT Z2CCT,Z2LM
PAGE GRCUP
LABEL CC VERT ACCEL, FT/SEC**2 VS TIME
CLTPUT ERR4
LABEL PERCENT ACCELERATION ERRCR VS. TIME
CLTPLT LDIN,LDLM
PAGE GRCUP
LABEL DRAFT, INCHES VS. TIME
CLTPLT ERR1
LABEL DRAFT ERRCR,LDACS AND MOTION AND LINEAR
OUTPUT COMDEG,CMLM
PAGE GRCUP
LABEL PITCH RATE, DEG/SEC VS. TIME
CLTPUT ERR5
LACEL ANG VELCCITY PCT ERRCR VS TIME
OUTPUT THDEG,THLM
PAGE GRCUP
LABEL PITCH ANGLE, CEGREES VS. TIME
CLTPLT ERR2
LABEL PITCH ANGLE ERRCR, LCADS AND MOTION AND LINEAR
END
STCP
```

169

FREQUENCY DOMAIN LINEAR SYSTEM CSMP III COMPUTER SIMULATION

This is a listing of the CSMP-III computer simulation used, with minor variations in details such as frequency range, tc generate all frequency response curves cf the linear system used throughout this work.

The CSMP III program is not linked automatically to the IMSL Subroutine Library at the W.R. Church Computer Center, NPS, Monterey. To acheive this linkage and access the subroutine LEQT2C, the following Job Control Language (JCL) must be inserted at the beginning of the program deck:

```
//SYSLIB DD UNIT=3330,VOL=SER=DISKC1,DISP=SHR,DSN=SYS3.CSMP3.LOADMOD
// CC DISP=SHR,DSN=SYS1.FCRTLIB
// DD DISP=SHR,DSN=SYS1.MFSLIB
// CD DISP=SHR,DSN=SYS3.IMSL.SP
```

```
$$$CCNTINUCLS SYSTEM MCDELING PROGRAM III   V1M3   TRANSLATOR OLTPLT$$$

FIXED I,J,K
     CIMENSICN A(10,10)
    / CCMPLEX AJW(1C,1C),BI(10),WA(10,13)
INITIAL
*
*      CCNSTANTS LSEC IN THIS PRCGRAM
CCNSTANT G=32.0,GAMMA=1.4,FA=2116.0,PI=3.141593,RHO=2.0,RHCA=.002378
*
*      NCN-VARIABLE CRAFT CCNSTANTS
CCNSTANT WICTF=10.0,L=20.C,N=5.C,QIO=35.,VN=383.,ZS=2.5,AB=200.,CN=.9
*  SICEWALL GECMETRY
*
CCNSTANT CR1=6C.C,DR2=80.,WS=.9375,WSO=.27
*      CRAFT PARAMETERS
*
PARAMETER W=65CC.,XCGC=-.125,XCF=.4,CV=1.5
PARAMETER AL=.350,IYY=S62C.,MFJ=-1875.,SEALP=2.0
*
*      INITIAL CCNDITICNS
*
PARAMETER V=(1C.,20.,30.),EETA=180.
*
*  FOURIER PARAMETERS
*
PARAMETER WC=1.,WMAX=25.
*  INITIALIZATION
NCSORT
EELW=ALCG(WMAX/WC)
DC S I=1,10
BI(I)=(0.0,0.0)
DC S J=1,10
S  A(I,J)=0.C
*  INITIALIZATION
RADEC=360./(2.C*PI)
DEGRAC=1.0/RADEC
V=1.E8*V
*  AVERAGE SICEWALL WICTH AND AREAS
AS=WS*L
W=WS/C
YCC=XCGC
*
*      SELECT A VALUE CF PEBAR SUCH THAT MBDCT=0.0 AT TIME=0.0
B=-2.C*(QIO+((CN*AL/N)**2)/RHOA)
PEBARO=PEBAR
PEBAR=(-E-SCRT(B**2-4.C*GIC**2))/2.C
PEPAC=1.0+PEEAR/PA
*  CCMPUTE PRESSURE FORCES AND MCMENTS
*
```

171

```
FFRES=-AB*PEEAR
PFRES=FFRES*(XCC-XCP)
NCSCRT   SELECT A VALUE CF CRAFT AND THETA SUCH THAT MCMENTS AND FORCES ARE ZI
**
THETA=C.O
LC=(W+FFRES+FLAN)/(2.C*R+C*G*W*S*L)
**     ITERATE TC A SCLTICN FGR DRAFT AND THETA
**
DC 10 I=1,250
K=1
1 CCNTINUE
**
**   CCMPUTE FORCES AND MCMENTS DUE TC BGWSEAL AND STERNSEAL
*    FCR BCWSEAL:
XSEALI=2.C*(LC-(L/2.-XCG)*TAN(TI-ETA))
ASEALI=MICTH*XSEALI
HSEALI=-FBBAR*ASEALI
PEEALI=+SEALI*(L/2.-XSEALI/2.-XCG)
*    FCR STERN SEAL:
XSEAL2=2.C*(LC+(L/2.+XCG)*TAN(THETA))
ASEAL2=WIDTH*XSEAL2
HSEAL2=-SEALF*ASEAL2
PSEAL2=+SEALI+FSEAL2
HSEAL=+SEALI+HSEAL2
PSEAL=PSEALI+FSEAL2
**
**    SIDEWALL GECMETRY CCRRECTED FCR DRAFT AND DEADRISE
**
*    BCW:
LCBARI=LC-(L/2-XCG)*THETA/2.
WSI=LCBARI/(2.O*TAN(CRI*CEGRAC))+WSO
IF(WSI.LT.O.C)WSI=0.0
IF(WSI.GT.WS)WSI=WS-WS**2*TAN(CRI*DEGRAD)/(2.3*LDBARI)
*    STEFN:
LCBOR2=LC+(L/2+XCG)*THETA/2.
WS2=LCBAR2/(2.C*TAN(CR2*DEGRAD))+WSC
IF(WS2.LT.O.C)WS2=0.0
IF(WS2.GT.WS)WS2=WS-WS**2*TAN(CR2*DEGRAD)/(2.0*LDBAR2)
*    BUCYANT FORCES AND MCMENTS:
HEUCYI=-2.C*RHC*G*WSI*(L/2.-XCG)*(LC-(L/2.-XCG)*TAN(THETA)/2.)
HEUCY2=-2.O*RHC*G*WS2*(L/2.+XCG)*(LC+(L/2.+XCG)*TAN(THETA)/2.)
PBUCYI=-.5*(L/2.-XCG)*HBUCYI
PBUCY2=-.5*(L/2.+XCG)*HBUCY2
*    PLANING FORCES AND MCMENTS:
**
HFLAN=-(CV/2.O)*RFO*V**2*(WSI+WS2)*L*THETA
PFLAN=5.C*FFLAN
**    RESICUAL FCRCES ANC MCMENTS:
**
```

172

```
RES1=FPRES+FPSEAL+FBUOY1+FELCY2+FPLAN+W
RES2=PPRES+PPSEAL+PBUOY1+PELCY2+PPLAN+MFO
*
** COMPUTE THE PARTIAL DERIVATIVES OF RESIDUAL FORCES AND MOMENTS
** AND THE NEW VALUES OF DRAFT AND THETA TO DRIVE
** RESIDUALS TO ZERO
*
GO TO (2,3,4),K
*
** PARTIAL DERIVATIVES WITH RESPECT TO DRAFT:
*
2 DLD=.01*LD
IF(DLD.EQ.0.0)DLD=.001
LD=LD+DLD
RES10=RES1
RES20=RES2
K=2
GO TO 1
*
** PARTIAL DERIVATIVES WITH RESPECT TO THETA:
*
3 DRIDL=(RES1-RES10)/DLD
DR2DL=(RES2-RES20)/DLD
DTHET=.01*THETA
IF(DTHET.EQ.0.0)DTHET=.001
THETA=THETA+DTHET
RES10=RES1
RES20=RES2
K=3
GO TO 1
*
** BAIRSTOW'S METHOD FOR NEW VALUES OF DRAFT AND THETA TO REDUCE
** THE RESIDUALS.
*
4 DRIDTH=(RES1-RES10)/DTHET
DR2DTH=(RES2-RES20)/DTHET
DET=DRIDL*DR2DTH-DR1DTH*DR2DL
DLD=(-RES1*DR2DTH+DR1DTH*RES2)/DET
DTHET=(-RES2*DR1DL+DR2DL*RES1)/DET
THETA=THETA+1.85*DTHET
LD=LD+1.85*DLD
1 CONTINUE
*
**
** COMPUTE THE INITIAL MASS OF AIR IN THE PLENUM AT THESE CONDITIONS
*
VB=VN-AB*(LD+XCG*TAN(THETA))
MBO=RTCA*VE*(PEFAO**(1.O/GAMMA))
ME=MBO
*
** THIS COMPLETES THE DEFINITION OF THE OPERATING POINT.
** FOR THIS STATIC EQUILIBRIUM CONDITION, COMPUTE THE PARTIALS
** WITH RESPECT TO THE STATE VARIABLES,Z,ZDOT,THETA,OMEGA AND MB
** FOR THE NON-LINEAR RELATIONSHIPS IN PBBAR,ZZDOT,ALFA, AND MBDOT
*
** FOR FEEAR
*
```

173

```
*     PBBAR=PA*(((MB/RFA )**GAMMA*(VN-AB*(LC+XCG*THETA))*(-GAMMA)-1.0)
      DPBZ=GAMMA*AE*(PBBAR+FA)/VB
      DPBTH=GAMMA*AB*XCG*(PBBAR+FA)/VB
      DFBMB=GAMMA*(PBBAR+PA)/MB
*
*FOR 22GCT
*       HPRES TERM
*
      DFPZ=-AE*DPBZ
      DFPTH=-AE*DPBTH
      DFPMB=-AE*CFBMB
*
*       HBUCY TERM
*
      DFBZ=-2.0*RFC*G*(WS1*(L/2.-XCG)+WS2*(L/2.+XCG))
      DFBTH=RFC*G*(WS1*(L/2.-XCG)**2-WS2*(L/2.+XCG)**2)
*       +SEAL TERM
*
*       BOW AND STERN SEALS
*
*       BOWSEAL:
*
      XSEAL1=2.C*(LC-(L/2.0-XCG)*THETA)
      DXDZ1=2.C
      CXDTH1=-2.0*(L/2.-XCG)
      DFSZ1=-WIDTH*XSEAL1*DFBZ-WICTH*CXCZ1*PBBAR
      CFSTH1=-WIDTH*XSEAL1*CFBTH-WIDTH*DXDTH1*PBBAR
*
*       STERN SEAL:
*
      XSEAL2=2.C*(LC+(L/2.+XCG)*THETA)
      DXDZ2=2.0
      CXDTH2=2.C*(L/2.+XCG)
      DFSZ2=-WIDTH*DXCZ2*SEALP
      DFSTH2=-WIDTH*CXDTH2*SEALF
*
      DFSZ=DFSZ1+DFSZ2
      DFSTH=DFSTH1+DFSTH2
      DFSMB=-WIDTH*XSEAL1*DPBMB
*
*       PLANING FORCES:
*
      DFPLTH=-(CV/2.C)*RHO*(WS1+WS2)*L*V**2
*       FOR ALFA TERM
*       PRES TERM
*
      DFPZ=(XCG-XCF)*DFPZ
      DFPTH=(XCG-XCF)*DFPTH
      DFPMB=(XCG-XCF)*DFPME
*
*       FBUCY TERM
*
      DFBYZ=RFC*G*(WS1*(L/2.-XCG)**2-WS2*(L/2.+XCG)**2)
      DFBYTH=-RFC*G*(WS1*(L/2.-XCG)**3+WS2*(L/2.+XCG)**3)/2.
*
*       FSEAL TERM
*       BCWSEAL TERM
```

174

```
*     DFSZ1=-CHSZ1*(L/2.-XSEAL1/2.-XCG)+HSEAL1*(2.-XCG)+HSEAL1*CXDZ1/2.0
      DFSTH1=-DHSTH1*(L/2.-XSEAL1/2.-XCG)+HSEAL1*CXDTH1/2.
**    STERNSEAL
**
      DFSZ2=DFSZ2*(L/2.+XSEAL2/2.+XCG)+HSEAL2*DXDZ2/2.
      DFSTH2=CHSTH2*(L/2.+XSEAL2/2.+XCG)+HSEAL2*DXDTH2/2.
      CFSZH=CPSZ1+CFSZ2
      DFSMB=-CHSMB*(L/2.0-XSEAL1/2.0-XCG)
**    PLANING MOMENTS
**
      DFPLTH=(L/4.)*CFPLTH
**    FOR MECCT
**
      CMBTH=-CPBTH*(N*RHOA+CN*AL/SQRT(2.0*PBBAR/RHOA))
      DDBMB=-DPBWE*(N*RHOA+CN*AL/SQRT(2.0*PBBAR/RHOA))
      CMEZ=-CPBZ*(N*RHOA+CN*AL/SQRT(2.0*PBBAR/RHOA))
**
      A(1,2)=1.0
      A(2,3)=1.0
      A(3,2)=(DFPZ+CHEZ+CHSZ2)/M
      A(3,5)=(DFPTH+CFSTH+CFPLTH)/M
      A(4,5)=(DFSMB+CFFMB)/M
      A(5,6)=1.C
      A(5,10)=1.0
      A(6,2)=(DFPZ+CFEYZ+CPSZ)/IYY
      A(6,5)=(DPPTH+CFEYTH+CFSTH+DPPLTH)/IYY
      A(6,9)=(CCPMB+DFSMB)/IYY
      A(7,2)=CPBZ
      A(7,5)=CPBTH
      A(7,9)=CFBMB
      A(8,9)=1.0C
      A(9,2)=CMBZ
      A(9,5)=CMBTH
      A(9,9)=CMBMB
      DYNAMIC
      NCSCRT
      WE=WO*EXF(CELH*TIME)
      WI=(G-SQRT(G**2-4.*G*WE*V*CCS(BETA*DEGRAD)))/(2.0*V*COS(BETA*DEGRAC))
      C=(C/WI)
      LAMELA=2.C*PI*C/WI
      RATIC=L/LAMBCA
      INT1=(WSI+WS2)*RFO*G*(C/WI)*SIN(WI*L/(2.0*C))
      INT2=(C/WI)*2*SIN(WI*L/2.C*C))-(C/WI)*(L/2.0)*COS(WI*L/(2.0*C))
      INT2=RFC*C*(WSI+WS2)*INT2
      DO 45 IC=1,21J
      BI(1)=(C.C,0.0)
      BI(2)=CMPLX(INT1/M,0.C)
      BI(5)=CMPLX(XCG*INT1/IYY,C.C)
      BI(10)=CMPLX(-WE*INT2/IYY,C.C)
      DO 45 J=1,1J
      AJW(I,J)=CMPLX(-A(I,J),0.C)
      IF(I.EQ.J)AJW(I,I)=CMPLX(-A(I,I),WE)
   45 CCNTINLE
```

175

```
CALL JECT2C(AJW,10,10,B1,1,10,0,WA,IER)
G1=CAABS(BII(1))
G2=CAABS(BII(2))
G3=CAABS(BII(3))
G4=CAABS(BII(4))
G5=CAABS(BII(5))
G6=CAABS(BII(6))
G7=CAABS(BII(7))
G11C=CO**ALUG1O(G1)
G21C=CO**ALUG1O(G2)
G31C=CO**ALUG1O(G3)
G41C=OO**ALUG1O(G4**G/WI**2)
G51C=OO**ALUG1O(G5*G/WI**2)
G61C=OO**ALUG1O(G6*G/WI**2)
TIMER FINTIM=1.0,OUTDEL=.C2,DELT=.02
LABEL LINEAR XR-3 FREQUENCY RESPONSE-AHEAD SEAS
OUTPUT G1,G4 ,WI,WE
PAGE GROUF, NFLCT=2
LABEL PITCH AND HEAVE FREQUENCY RESPONSE
OUTPUT G2,G5 ,WI,WE
PAGE GROUF,NFLCT=2
LABEL HEAVE AND PITCH RATE FREQ RESPONSE
OUTPUT G3,G6,WI,WE
PAGE GROUP,NFLCT=2
LABEL HEAVE AND PITCH ACCELERATION FREQ RESPONSE
OUTPUT G1
PAGE MERGE
LABEL HEAVE FREQUENCY RESPONSE AS A FUNCTION OF VELOCITY
OUTPUT G4
PAGE MERGE
LABEL PITCH FREQUENCY RESPONSE AS A FUNCTION OF VELOCITY
OUTPUT XYPLOT,G1
LABEL HEAVE FREQUENCY RESPONSE AS A FUNCTION OF WAVELENGTH
OUTPUT XYPLOT ,G4
PAGE XYPLOT
LABEL PITCH FREQUENCY RESPONSE AS A FUNCTION OF WAVELENGTH
END
STOP
```

| $$$ TRANSLATION TABLE CONTENTS $$$ | CURRENT | MAXIMUM |
|---|---|---|
| MACRO AND STATEMENT OUTPUTS | 134 | 600 |
| STATEMENT+WORK AREA OUTPUTS | 385 | 1900 |
| INTEGRATORS+MEMORY BLOCK OUTPUTS | 30 ++ 0 | 3000 |
| PARAMETERS+FUNCTION GENERATORS | 30 ++ 3 | 4000 |
| STORAGE VARIABLES+INTEGRATOR ARRAYS | 21 ++ 0/2 | 500 |
| HISTORY AND MEMORY BLOCK NAMES | 6 | 50 |
| MACRO DEFINITIONS AND NESTED MACROS | 13 | 125 |
| MACRO STATEMENT STORAGE | 0 | 1000 |
| LITERAL CONSTANT STORAGE | 0 | 1200 |
| SORT SECTIONS | | |
| MAXIMUM STATEMENTS IN SECTION | 0 | 600 |

## PARAMETRIC EIGENVALUE CSMP III SOLUTION


This program provides a root locus solution to the two-degree-of-freedom linear model. The reserved CSMP variable TIME is redesignated as the parameter of interest with the RENAME statement, with the range of variation specified on the FINTIM card. One additional variable may be stepped, using the PARAMETER statement.

The parametric eigenvalue program also must access the IMSL Subroutine Library; see the Frequency Domain computer program listing for the appropriate JCL to acheive this linkage at the W.R. Church Computer Facility.

```
FIXED I,J,K
      DIMENSION A(9,9),B(9,9),BET1(9),WK(9)
(     COMPLEX EIGVAL(9),ALF1(9),EIGVEC(9)
INITIAL
*     CONSTANTS USED IN THIS PROGRAM
CONSTANT G=32.0,GAMMA=1.4,PA=2116.0,PI=3.14159,RHC=2.0,RHOA=.002378
*
*     NON-VARIABLE CRAFT CONSTANTS
CONSTANT WIDTH=10.0,L=20.0,D=5.0,QIC=35.,VN=3E3.,ZS=2.5,AB=200.,CN=.5
*
* SIDEWALL GEOMETRY
*
CONSTANT CR1=60.0,CR2=80.,WS=.9375,WL=1.25
*
*     CRAFT PARAMETERS
*
PARAMETER W=6500.,XCP=(-.25,0.0,.25),CV=1.5,XCG=0.0
PARAMETER AL=.390,IY=5020.,NFO=-1875.,SEALP=2.0
*
** CONTROL FIN PARAMETERS
PARAMETER CLF=6.28, S=5.0
*
*
*          INITIALIZATION
INITIAL
NOSORT
*
RADEG=360./(2.0*PI)
DEGRAD=1.0/RADEG
WS10=WS-WL/TAN(DR1*DEGRAD)
WS20=WS-WL/TAN(DR2*DEGRAD)
* AVERAGE SIDEWALL WIDTH AND AREAS
*
AS=WS*L
M=W/G
*
DYNAMIC
V=1.6d*TIME
NOSORT
DO 9 I=1,9
DO 5 J=1,9
A(I,J)=0.0
5 B(I,J)=0.0
9 B(I,I)=1.0
*
*     SELECT A VALUE OF PBBAR SUCH THAT MECDT=0.0 AT TIME=0.0
B=-2.0*(QIC+((CN*AL/N)*(2)/RHOA)
PBBARO=PBBAR
PBBAR=(-B-SQRT(B**2-4.0*(CT0**2))/2.0
PBPAD=1.0+PBBAR/PA
* COMPUTE PRESSURE FORCES AND MOMENTS
*
HPRES=-AB*PBBAR
```

```
      PPRES=HPRES*(XCG-XCP)
**    SELECT A VALUE OF CRAFT AND THETA SUCH THAT MOMENTS AND FORCES ARE ZERO

      THETA=C.0
      LD=(W+PPRES*HPLAN)/(2.C*RHO*G*WS*L)
**    ITERATE TO A SOLUTION FOR CRAFT AND THETA

      DO 10 I=1,250
      K=1
    1 CONTINUE
**
**    COMPUTE FORCES AND MOMENTS DUE TO BOWSEAL AND STERNSEAL
**    FOR BOWSEAL:
      XSEAL1=2.0*(LD-(L/2.-XCG)*TAN(THETA))
      ASEAL1=WIDTH*XSEAL1
      HSEAL1=-PBBAR*ASEAL1
      PSEAL1=HSEAL1*(L/2.-XSEAL1/2.-XCG)
**    FOR STERN SEAL:
      XSEAL2=2.0*(LD+(L/2.+XCG)*TAN(THETA))
      ASEAL2=WIDTH*XSEAL2
      HSEAL2=-SEALP*ASEAL2
      PSEAL2=HSEAL2*(L/2.+XSEAL2/2.+XCG)
      HSEAL=HSEAL1+HSEAL2
      PSEAL=PSEAL1+PSEAL2
**
**    SIDEWALL GEOMETRY CORRECTED FOR CRAFT AND DEADRISE
**
**    BOW:
      LDBAR1=LD-(L/2+XCG)*THETA/2.
      WS1=LDBAR1/(2.C*TAN(DRI*DEGRAD))+WS1O
      IF(WS1.LT.0.0)WS1=0.0
      IF(WS1.GT.WS)WS1=WS-WS**2*TAN(CRI*CEGRAD)/(2.0*LDBAR1)
**    STERN:
      LDBAR2=LD+(L/2+XCG)*THETA/2.
      WS2=LDBAR2/(2.0*TAN(CR2*DEGRAD))+WS2C
      IF(WS2.LT.0.0)WS2=0.0
      IF(WS2.GT.WS)WS2=WS-WS**2*TAN(LR2*DEGRAD)/(2.0*LDBAR2)
**    BUOYANT FORCES AND MOMENTS:
      HBUGY1=-2.0*RHO*G*WS1*(L/2.-XCG)*(LD-(L/2.-XCG)*TAN(THETA)/2.)
      HBUGY2=-2.0*RHO*G*WS2*(L/2.+XCG)*(LD+(L/2.+XCG)*TAN(THETA)/2.)
      PBUGY1=-.5*(L/2.-XCG)*HBUGY1
      PBUGY2=.5*(L/2.+XCG)*HBUGY2
**    PLANING FORCES AND MOMENTS:
      HPLAN=-(CV/2.0)+RHO*V**2*(WS1+WS2)*L*THETA
      PPLAN=5.0*FPLAN
**
**    CONTROL FIN FORCES AND MOMENTS
      HFIN=-CLF*RHO*V**2*S/2*THETA
```

```
      PFIN=(L/2-1.C+XCG)*dFIN
C *** RESIDUAL FORCES AND MOMENTS:
C
      RES1=HPRES+HSEAL+HBUOY1+HBUOY2+HPLAN+HFIN+W
      RES2=PPRES+PSEAL+PBUOY1+PBUOY2+PFLAN+PFIN+MFO
C
C *** COMPUTE THE PARTIAL DERIVATIVES OF RESIDUAL FORCES AND MOMENTS
C *** AND THE NEW VALUES OF DRAFT AND THETA TO DRIVE
C *** RESIDUALS TO ZERO
C
      GO TO(2,3,4),K
C *** PARTIAL DERIVATIVES WITH RESPECT TO DRAFT:
C
    2 CLD=.01*LD
      IF(CLD.EQ.0.)CLD=.001
      LD=LD+CLD
      RES1D=RES1
      RES2D=RES2
      K=2
      GO TC 1
C ***
C *** PARTIAL DERIVATIVES WITH RESPECT TO THETA:
C ***
    3 DR1DL=(RES1-RES1D)/CLD
      DR2DL=(RES2-RES2D)/DLD
      DTHET=.01*THETA
      IF(DTHET.EQ.0.)DTHET=.001
      THETA=THETA+DTHET
      RES1D=RES1
      RES2D=RES2
      K=3
      GO TO 1
C *** BAIRSTOW'S METHOD FOR NEW VALUES OF DRAFT AND THETA TO REDUCE
C *** THE RESIDUALS.
C
    4 DR1DTH=(RES1-RES1D)/DTHET
      DR2DTH=(RES2-RES2D)/DTHET
      DET=DR1DL*DR2DTH-DR1DTH*DR2DL
      DLD=(-RES1*DR2DTH+DR1DTH*RES2)/DET
      DTHET=(-RES2*DR1DL+DR2DL*RES1)/DET
      THETA=THETA(1.05*DTHET
      LD=LD+1.85*CLD
   10 CONTINUE
C ***
C *** COMPUTE THE INITIAL MASS OF AIR IN THE PLENUM AT THESE CONDITIONS
C ***
      VB=VN-AB*(LC+XCG*TAN(THETA))
      MBO=RHCA*VB*(PEPS)**(1.0/GAMMA))
      MB=MBO
C ***
C *** THIS COMPLETES THE DEFINITION OF THE OPERATING POINT.
C *** FOR THIS STATIC EQUILIBRIUM CONDITION,COMPUTE THE PARTIALS
C *** WITH RESPECT TO THE STATE VARIABLES,Z,ZDOT,THETA,OMEGA AND MB
```

```
*FOR THE NON-LINEAR RELATIONSHIPS IN PBBAR,Z2CLJ,ALFA, AND MBDOT

**FOR PBBAR

**      FBBAR=PA*(((MB/RHA )**GAMMA*(VN-AB*(LD+XCG*THETA))*(-GAMMA)-1.C)

DPBZ=GAMMA*AB*(PBBAR+FA)/VB
DPBTH=GAMMA*AB*XCG*(FBBAR+PA)/VB
CPBMB=GAMMA*(PBBAR+PA)/AB

**FOR Z2DDT
**      FPRES TERM

DHPBZ=-AB*DPBZ
DHFTH=-AB*DPBTH
DHFMB=-AE*CFBME

**      FBUDY TERM

DHBZ=-2.0*RHO*G*(WSL*(L/2.-XCG)+WS2*(L/2.+XCG))
DHBTH=RHO*G*(WSL*(L/2.-XCG)**2-WS2*(L/2.+XCG)**2)
**      FSEAL TERM

**
** BOW AND STERN SEALS
**
** BCWSEAL:
**
XSEALL=2.0*(LD-(L/2.0-XCG)+THETA)
DXDZ1=2.0
CXCTH1=-2.0*(L/2.-XCG)
DHSZ1=-WIDTH*XSEALL*CPEZ-WICTH*CXCZ1*PBBAR
DHSTH1=-WIDTH*XSEALL*DPBTH-WIDIH*CXCTH1*PBBAF
**
** STERN SEAL:
XSEAL2=2.C*(LD+(L/2.+XCG)*THETA)
DXCZ2=2.0
DXDTH2=2.0*(L/2.+XCG)
DHSZ2=-WICTH*DXDZ2*SEALP
DHSTH2=-WIDTH*CXCTH2*SEALP
**
DHSZ=DHSZ1+DHSZ2
DHSTH=DHSTH1+DHSTH2
DHSMB=-WIDTH*XSEALL*DPEAB
**
** PLANING FORCES:
**
DHPLTH=-(CV/2.0)*RHJ*(WSL+WS2)*L*V**2
**
** CCNTROL FIN FORCES:
**
DHFTH=-CLF*RHO*V**2*S/2
DHFA=-CLF*RHO*V*S/2
CHFP=-CLF*RHO*V*(L/2-1.3*XCG)*S/2.C
**
*FOR ALFA TERM
```

```
*     PPRES TERM
CPPZ=(XCG-XCP)*DPPZ
DPPTH=(XCG-XCP)*DHPTH
CPPMB=(XCG-XCP)*DHPMB
*
*     PBODY TERM
DPBYZ=RHO*G*(WSL*(L/2.-XCG)**2-WS2*(L/2.+XCG)**2)
DPBYTH=-RHO*G*(WSL*(L/2.-XCG)**3+WS2*(L/2.+XCG)**3)/2.
*
*     PSEAL TERM
*BCWSEAL:

DPSZ1=-DHSZ1*(L/2.-XSEAL1/2.-XCG)+FSEAL*DXDZ1/2.0
DPSTH1=-DHSTH1*(L/2.-XSEAL1/2.-XCG)+FSEAL1*DXDTH1/2.
*
*     STERNSEAL
*
DPSZ2=DHSZ2*(L/2.+XSEAL2/2.+XCG)+HSEAL2*DXDZ2/2.
DPSTH2=DHSTH2*(L/2.+XSEAL2/2.+XCG)+HSEAL2*DXDZ2/2./2.
DPSZ=DPSZ1+DPSZ2
DPSTH=DPSTH1+DPSTH2
DPSMB=-DHSME*(L/2.0-XSEAL1/2.0-XCG)
*
*     PLANING MOMENTS

DPPLTH=(L/4.)*DHPLTH
*
*     CONTROL FIN MOMENTS:
*
DPFTH=(L/2.0-1.0+XCG)*CHFTH
CPFW=(L/2.0-1.0+XCG)*DHFW
DPFP=(L/2.0-1.0+XCG)*CHFW
*
*FOR MBDOT
*
DMBTH=-DPBTH*(N*RHDA+CA*AL/SQRT(2.0+FBBAR/RHOA))
DMBMB=-DPBMB*(N*RHDA+CA*AL/SQRT(2.C*PBBAR/RHOA))
DMBZ=-DPBZ*(N*RHCA+CA*AL/SQRT(2.0*PBBAR/RHOA))
WRITE(6,101) DHFTH,DPFTH,(2F15.5)
101 FORMAT(2F15.5)
A(1,2)=1.0
A(2,3)=1.0
A(3,2)=(DHPZ+DHEZ+DHSZ)/M
A(3,3)=DHFW/M
A(3,5)=(CHFTH+CHFTH+CHFST+DFPLIH+CFFTH)/M
A(3,6)=DHFP/M
A(3,9)=(DHSM3+DHPMB)/M
A(4,5)=1.0
A(5,6)=1.0
A(6,2)=(DPPZ+DPBYZ+DPSZ)/IYY
A(6,3)=DPFW/IYY
A(6,5)=(DPSTH+DPBYTH+DFSTH+DPFLTH+CFFTH)/IYY
A(6,6)=DPFP/IYY
A(6,9)=(DPPMB+DPSVB)/IYY
A(7,2)=DPEZ
A(7,5)=DPBTH
A(7,9)=DPBMB
```

```
A(8,9)=1.0
A(9,2)=DMBZ
A(9,5)=DMBTH
A(9,9)=DMBMB
NDSORT
WRITE(6, )
40 FORMAT(//,'THE A MATRIX:')
DO 41 I=1,9
WRITE(6,42)(A(I,J),J=1,9)
42 FORMAT(9F13.5)
41 CONTINUE
CALL EIGZF(A,9,B1,9,0,ALF1,BET1,EIGVEC,9,WK,IER)
WRITE(6,44)
44 FORMAT(//,1X,'THE EIGENVALUES ARE:')
DO 50 I=1,9
EIGVAL(I)=ALF1(I)/BET1(I)
WRITE(6,45)EIGVAL(I)
45 FORMAT(2F15.5,/,J)
50 CONTINUE
SORT
WN1=CABS(EIGVAL(2))
ZETA1=-REAL(EIGVAL(2))/WN1
WN2=CABS(EIGVAL(5))
ZETA2=-REAL(EIGVAL(5))/WN2
ZETA3=-REAL(EIGVAL(4))
SORT
TIMER FINTIM=30.0, TIME=8.0, CLIDEL=1.0,DELT=1.0
LABEL MCINTYRE VELOCITY SENSITIVITY
OUTPUT ZETA1
PAGE MERGE
LABEL SHORT PERIOD DAMPING
OUTPUT WN1
PAGE MERGE
LABEL SHORT PERIOD NATURAL FREQUENCY
OUTPUT ZETA2
PAGE MERGE
LABEL PITCH DAMPING
OUTPUT WN2
PAGE MERGE
LABEL PITCH NATURAL FREQUENCY
OUTPUT ZETA3
PAGE MERGE
LABEL CRAFT EXPONENTIAL
OUTPUT LO
PAGE MERGE
LABEL STEADY-STATE CRAFT
OUTPUT THETA
PAGE MERGE
LABEL STEADY STATE PITCH
END
STOP
```

# LIST OF REFERENCES

1.  Booth, F.B., *The Frequency Response and Operating Characteristics of the XR-3 Loads and Motions Program*, M.S. Thesis, U.S. Naval Postgraduate School, Monterey, California, 1976.

2.  Leo,D.G., and Boncal, R., *XR-3 Surface Effects Ship Test Craft: A Mathematical Model and Simulation Program with Verification*, M.S. Thesis, U.S.Naval Postgraduate School,Monterey, California, December 1973.

3.  Menzel, Reinhard Fritz, *Study of the Roll and Pitch Transients in Calm Water Using the Simulated Performance of the XR-3 Surface Effects Ship Loads and Motion Program*, M.S. Thesis, U.S.Naval Postgraduate School,Monterey, California, December 1975.

4.  Mitchell, W. R., *Investigations of Methods to Optimize Captured Air Bubble Surface Effect Ship Digital Simulation for Irregular Sea Conditions*, M.S. Thesis, U.S.Naval Postgraduate School,Monterey, California, September 1974.

5.  Gerba, A., Jr., and Thaler, G.J., *Pressure Ratio Effects on the Heave Motion Characteristics and Pressure Dynamics of the XR-3 Loads and Motion Program for Step Weight Transients*, Progress Report to SESPO, U.S. Naval Postgraduate School, Monterey, California, January 1977.

6.  Speckhart, F.H. and Green, J.L., *A Guide to Using CSMP-the Continuous System Modeling Program*, pp.

220-335, Prentice-Hall, 1976.

7.  Gerald, C.F., _Applied Numerical Analysis_, p. 16, California State Polytechnic College, San Luis Obispo, California, November 1973.

8.  (No Author Listed), _Installation and Operating Instructions for the TDC SuperPanel-50 Spectrum Analyzer_, Instruction Manual, Time Data Corporation, 1976.

9.  McIntyre, L.F., _Optimal Pitch Control of the XR-3 Captured Air Bubble (CAB) Testcraft_, Private Correspondence with Dr. D.H.Collins,PhD., U.S. Naval Postgraduate School, Monterey, California, June 1977.

10.  Englehart, C.D., _Data Acquisition System for Unsteady Aerodynamic Investigations_, M.S. Thesis, U.S. Naval Postgraduate School, Monterey, California, June 1977.

INITIAL DISTRIBUTION LIST

No. Copies

1. Defense Documentation Center 2
   Cameron Station
   Alexandria, Virginia 22314

2. Library, Code 0142 2
   Naval Postgraduate School
   Monterey,California 93940

3. Department Chairman, Code 67 1
   Department of Aeronautics
   Naval Postgraduate School
   Monterey, California 93940

4. Department Chairman, Code 62 1
   Department of Electrical Engineering
   Naval Postgraduate School
   Monterey, California 93940

5. Professor Alex Gerba, Jr., Code 52Gz 5
   Department of Electrical Engineering
   Naval Postgraduate School
   Monterey, California 93940

6. Professor George J. Thaler, Code 52Tr 1
   Department of Electrical Engineering
   Naval Postgraduate School
   Monterey, California 93940

7.  Asst Professor D.M. Layton, Code 67Ln                    1
    Department of Aeronautics
    Naval Postgraduate School
    Monterey, California 93940

8.  Mr. A.W. Anderson                                        6
    PMS 304-31A-1
    Surface Effects Ships Project Office
    PO Box 34401
    Bethesda, Maryland 20034

9.  LT Lewis F. McIntyre, USN                                1
    21 Rumbough Place
    West Asheville, North Carolina 28806